

Immune System Involvement in Cerebral Amyloid Angiopathy  
by

Danielle Munsterman

A thesis submitted in partial fulfillment of the requirements for the degree of

Master of Science

Department of Medicine  
University of Alberta

## ***Abstract***

### **Background:**

Cerebral amyloid angiopathy (CAA) is a cerebral small vessel disease featuring beta-amyloid deposits within the cerebral vasculature. It is a major cause of cognitive decline and intracerebral hemorrhage in the elderly. A gap in knowledge surrounding mechanisms underlying CAA pathogenesis has contributed to a lack of treatments and early diagnostic biomarkers for CAA. Expanding understanding of the mechanisms contributing to CAA pathophysiology may aid in diagnostic and risk stratification biomarker discovery and potential identification of novel therapeutic targets. This is of clinical interest, given the high prevalence of CAA amongst the elderly and a globally aging population. This thesis evaluated differences in blood gene expression in CAA and the relationship to CAA severity. Insight to changes in immune system that occur in CAA are identified which may have relevance to cerebrovascular disease in CAA and as biomarkers to aid in the diagnosis and severity assessment of CAA.

### **Methods:**

In 27 patients with CAA blood cell gene expression was compared to 55 controls. RNA was isolated from PAXgene tubes and measured by RNA sequencing. Differentially expressed genes between CAA and controls were identified by ANOVA adjusting for age and sex. Functional pathway analysis identified pathways associated with CAA. A prediction model to distinguish CAA from controls was developed and evaluated. Differentially expressed genes based on CAA small vessel disease (CAA-SVD) score as a marker of CAA severity were identified using ANOVA and functional pathway analysis in patients with CAA.

## **Results:**

In patients with CAA compared to controls 686 differentially expressed genes were identified ( $p < 0.05$ , fold change  $> |1.2|$ ), of interest *ADAM15*, *CAMK1D*, *CAP1* and *TGFBI*. In CAA canonical pathway analysis identified cell movement of phagocytes, activation of phagocytes, CREB, degranulation of leukocytes, immune response of cells, inflammatory response, and IL-23 signaling. A 24 gene panel differentiated patients with CAA from controls with  $>95\%$  sensitivity and specificity. The identified genes reveal differences in immune system regulation in patients with CAA compared to controls. Differences identified include a potential shift in beta-amyloid uptake by phagocytes (*TGFBI*, *CREB*, *CAMK1D*), an increase in vascular extracellular matrix disruption (*ADAM15*, *CAP1*), and a possible alteration in amyloid precursor processing (*BRI3BP*, *SORCS3*). ANOVA was used to identify genes associated with CAA-SVD score ( $p \leq 0.05$ , partial correlation coefficient  $\geq |0.5|$ ). *HDAC11*, *IL23A*, *TRAIL*, *TRAILR1*, *TRAILR2*, and *ICAM-1* were associated with CAA severity (CAA-SVD score). Canonical pathways analysis identified induction of T lymphocytes, binding of antigen presentation cells, IL-12 signaling in macrophages/monocytes, activation of phagocytes, and activation of antigen presenting cells to be associated with CAA severity ( $p \leq 0.05$ ).

## **Conclusions:**

Differences in blood gene expression are present in patients with CAA compared to control patients. These relate to differences in immune activation and signaling associated with CAA. The differences in blood cell gene expression shows promise to distinguish CAA from controls, though further evaluation in larger cohorts is required. An association between the peripheral immune system and CAA severity was also identified. Changes in neutrophil, monocyte, and Th17 cell gene expression in peripheral blood was associated with CAA severity.

Such gene expression changes were associated with cognitive measures including decreases in memory, executive functioning, and processing speed. This supports greater specificity of immune system changes contributing to CAA pathogenesis and cognitive decline, which may be of clinical value as future therapeutic targets or risk stratification markers in CAA. Although this data is preliminary and further evaluation in larger cohorts is required, differences in peripheral immune system responses were identified in CAA revealing gene targets with potential for providing diagnostic and risk stratification information.

## Preface

This thesis is an original work by Danielle Munsterman. No part of this thesis has been previously published. This research was conducted at the University of Alberta under the supervision of Dr. Glen Jickling, Dr. Eric Smith, and Dr. Richard Camicioli. Ethics approval for this study was obtained by the University of Alberta Research Ethics Board (Pro00067006, Pro00066577), and the University of Calgary Research Ethics Board (REB15-0601). Enrollment of study participants, neuroimaging, cognitive assessments, and collection of peripheral blood samples were done so as part of the Functional Assessment of Vascular Reactivity (FAVR) study conducted at both the University of Alberta and University of Calgary sites. Clinical data was generously provided by Dr. Richard Camicioli and Dr. Eric Smith. RNA extraction and cDNA library preparation were conducted at the University of Alberta by myself and Twinkle Joy. RNA sequencing was carried out by Novogene. My contributions to this project included writing the literature review in chapter 1, performing the RNA extractions, and cDNA library preparations. Dr. Glen Jickling assisted with gene expression analysis, while I conceptualized and explored gene expression and pathway level changes. I also wrote the manuscripts for chapters 2 and 3. Throughout this process, I received incredible support from my supervisor Dr. Glen Jickling and committee members Dr. Eric Smith, and Dr. Richard Camicioli. Funds from the FAVR study were from Canadian Health Research (Grant #MOP-142175 and FDN-154317), Brain Canada, Canadian Stroke Network (Grant #MIRI2015-3994), Heart and Stroke Foundation of Alberta, and the Alzheimer Society of Canada.

## Acknowledgements

Firstly, I would like to express my gratitude to my mentor and supervisor Dr. Glen Jickling. I could not have completed this degree without your unwavering support, guidance, and encouragement. I appreciate the mentorship and insights you have provided to me over the years, as this helped me to grow as an individual while working towards my long-term career goals and vision – you have contributed to inspiring my passion for science, learning, and hopes to use research as a form of patient advocacy as a future physician myself. Thank you to my fellow lab mates and colleagues, getting to work alongside and getting to know each one of you has truly enriched my time with the lab over the past four years. Of course, I would like to thank the “ladies of the lab” for the moral support, laughter, and enjoyment as we worked alongside one another while exploring our own interests in research and medicine. You all contributed to making the Jickling lab a special place to be. Thank you Twinkle for all the support in processing RNA samples, the many lab lunches and daily positivity. Next, I would like to express my sincere thanks to my committee members Dr. Eric Smith, Dr. Richard Camicioli and Dr. Roger Dixon. Thank you for the invaluable guidance, resources, and feedback on my project. I appreciate each of you sharing your unique expertise and knowledge, it has been central to my development throughout my program. I would also like to sincerely thank the FAVR research team members from both the UofA and UofC for their contributions in sample collection, patient recruitment, imaging, and cognitive assessments. Thank you to my friends and family for your constant support in my academic pursuits, I would not be where I am today without you all. Lastly, I would like to thank Sean for being my biggest supporter over all these years – I am incredibly grateful for everything you have done for me and continue to do.

## Table of Contents

	Page
Abstract	ii
Preface	v
Acknowledgements	vi
Chapter 1: Current Understandings of Cerebral Amyloid Angiopathy and the Immune System	1
1.1 General Introduction	1
1.2 Clearance of beta-amyloid	2
1.2.1 <i>Beta-amyloid accumulation and removal</i>	2
1.2.2 <i>Efflux receptors and immune cells</i>	3
1.2.3 <i>Perivascular clearance of beta-amyloid</i>	5
1.2.4 <i>Clearance of beta-amyloid in the peripheral blood</i>	5
1.3 Neutrophils and BBB disruption in cerebral amyloid angiopathy	7
1.3.1 <i>Introduction to neutrophils</i>	7
1.3.2 <i>Neutrophil infiltration into brain</i>	8
1.3.3 <i>Tissue repair by neutrophils</i>	9
1.4 Monocytes in cerebral amyloid angiopathy	10
1.4.1 <i>Monocyte origins and function</i>	10
1.4.2 <i>Monocytes and beta-amyloid in peripheral blood</i>	11
1.4.3 <i>Receptor mediated endocytosis in monocytes</i>	11
1.5 Perivascular macrophages	12
1.5.1 <i>Origin of perivascular macrophages</i>	12
1.5.2 <i>Functional roles of perivascular macrophages</i>	13
1.5.3 <i>Perivascular macrophages and beta-amyloid</i>	14
1.6 CAA related inflammation	15
1.6.1 <i>An introduction to CAA related inflammation and ABRA</i>	15
1.6.2 <i>Immune system involvement in CAA-ri</i>	16
1.7 Summary of immune system in CAA	18
Chapter 2: Cerebral amyloid angiopathy blood gene expression	19

2.1 Abstract	19
2.2 Introduction	21
2.3 Methods	22
2.4 Results	24
2.5 Discussions	27
2.6 Figures and Tables	32
Chapter 3: Transcriptomic changes in peripheral blood leukocytes associated with cerebral amyloid angiopathy severity	38
3.1 Abstract	38
3.2 Introduction	40
3.3 Methods	41
3.4 Results	44
3.5 Discussion	46
3.6 Figures and Tables	51
Chapter 4: Conclusions and Future Directions	54
4.1 Summary of Findings	54
4.2 Limitations	54
4.3 Future Directions	55
4.4 Conclusions	56
<i>References</i>	57
<i>Appendices</i>	74



## List of Tables

<b>Table 1.1</b> Patient Demographics in patients with cerebral amyloid angiopathy compared to controls	32
<b>Table 1.2</b> Differentially expressed gene list comparing patients with cerebral amyloid angiopathy (CAA) and controls (CTL)	33
<b>Table 1.3</b> Canonical pathways determined from differentially expressed genes in patients with cerebral amyloid angiopathy compared to controls	33
<b>Table 2. 1</b> Table 2.1: Patient demographics in patients with cerebral amyloid angiopathy	51
<b>Table 2.2</b> Biologically significant genes associated with CAA-severity (CAA-SVD Score)	51
<b>Table 2.3</b> Biological pathways determined by ingenuity pathway analysis associated with CAA severity (CAA-SVD Score)	51
<b>Table S1.1</b> Differentially expressed genes in patients with cerebral amyloid angiopathy compared to controls	74
<b>Table S2.1</b> Genes associated with cerebral amyloid angiopathy severity	79

## List of Figures

<b>Figure 1.1</b> Principal components analysis of the 24 genes found to differentiate patients with cerebral amyloid angiopathy from control patients	35
<b>Figure 1.2</b> Hierarchical cluster plot of the 24 genes differentially expressed in patients with cerebral amyloid angiopathy compared to control patients	36
<b>Figure 1.3</b> Box Plots of select differentially expressed genes comparing patients with cerebral amyloid angiopathy in orange and controls in blue ( $p < 0.05$ , fold change $>  1.2 $ ).	37
<b>Figure 2.1</b> Dot plots of select differentially expressed genes based on CAA-severity (CAA-SVD Score)	53

## *Chapter 1: Current Understandings of Cerebral Amyloid Angiopathy and the Immune System*

### **1.1 General Introduction**

Cerebral amyloid angiopathy (CAA) is a cerebral small vessel disease characterized by beta-amyloid deposition within small and medium sized cortical vessels and the leptomeninges of the brain [1]. CAA is prevalent in the elderly and is a major cause of intracerebral hemorrhage (ICH), dementia and cognitive decline [2]. The prevalence of CAA increases with age and is estimated between 10-50% in elderly populations [3]. Given the aging global population and the lack of current treatments for CAA, early diagnosis, and development of therapeutics to slow the progression of CAA will be of tremendous value. The mechanisms contributing to CAA development and severity remains to be determined [1, 4]. Enhancing this understanding could contribute to biomarkers to improve diagnosis and risk stratification, as well as the development of novel treatments to improve the health of patients with CAA.

Common presentations of CAA include lobar ICH, transient focal neurological episodes, convexity subarachnoid hemorrhage, cognitive decline, inflammatory leukoencephalopathy, or incidental cerebral microbleeds or cortical superficial siderosis on neuroimaging [5, 6]. Incidence of CAA is strongly linked to age, with prevalence higher amongst populations with dementia [7-9]. Based on a systematic review by Jakel et al prevalence of mild to severe CAA in patients with AD and a mean age of 79.8 years was between 72.5 and 85.3%, while the prevalence of mild to severe CAA in the general population with a mean age of 84.9 was between 17.3 and 29.1% [10]. In cognitively normal elderly populations with a mean age of 80.5 years the prevalence of mild to severe CAA was between 22.8 and 35.5%, in patients with intracerebral hemorrhage and a mean age of 56.8 the prevalence of mild to severe CAA was between 3.8 and 54.1%, and in patients with lobar hemorrhage and a mean age of 72.7 years the prevalence of

mild to severe CAA ranged from 41.7 to 71.0%. Sporadic aetiologies of CAA comprise most cases, with a smaller portion having genetic or familial origin [11-13]. Carriers of the *APOE\** $\epsilon$ 2 or *APOE\** $\epsilon$ 4 alleles are at greater risk of CAA related hemorrhage, earlier age of disease onset, and recurrent hemorrhage [14-18]. Sporadic CAA has a dose dependent association with *APOE\** $\epsilon$ 4 [19]. Variants of the complement receptor type 1 (*CRI*) gene have also been associated with ICH in CAA [20]. However, the presence of a genetic variant only is neither sensitive nor specific for CAA diagnosis. Thus, the diagnosis of CAA is made using the modified Boston criteria, relying on brain imaging and clinical features. However, a definitive diagnosis of CAA requires neuropathology [2, 21-23].

The role immune system changes in CAA pathophysiology are not well understood [24-30]. Investigation of leukocytes gene expression signatures could offer diagnostic information, and risk stratification of CAA. Evaluation of immune involvement in CAA may also provide novel targets for therapeutics to potentially aid in beta-amyloid clearance, reducing risk of cerebral hemorrhage, or possibly slowing progression of CAA.

In chapter 1 immune system involvement in CAA is presented. In chapter 2, differences in blood cell gene expression in patients with CAA compared to controls is described and identification of CAA patients using a prediction model is evaluated. In chapter 3, differences in blood cell gene expression in relation to severity of CAA using the CAA small vessel disease score are presented.

## **1.2 Clearance of beta-amyloid**

### *1.2.1 Beta-amyloid accumulation and removal*

Cleavage of amyloid precursor protein (APP) by beta and gamma secretases produce  $A\beta_{40}$  and  $A\beta_{42}$ , with  $A\beta_{40}$  being the predominant beta-amyloid isoform present in CAA [31].  $A\beta_{40}$  has a propensity to accumulate in the cerebral blood vessels, but beta-amyloid accumulation is largely due to impaired clearance [32-40]. Mechanisms underlying deposition of beta-amyloid in vessel walls instead of parenchyma are unclear, however two competing hypotheses exist. The first hypothesis proposes vascular beta-amyloid arises locally from vascular smooth muscle cells [41, 42]. In contrast, the second hypothesis suggests beta-amyloid originates from neurons, and then accumulates in the vasculature [43, 44]. Preferential vascular beta-amyloid deposition is also associated with several features including specific mutations in the amyloid precursor protein (APP), beta-amyloid subtype, APOE allele status (*APOE*\* $\epsilon$ 2/\* $\epsilon$ 4), and presence of select co-deposited proteins [1, 45-48].

Several pathways are implicated in beta-amyloid clearance including phagocytosis, enzymatic degradation, perivascular drainage, and transport across the blood brain barrier (BBB) [49]. Studies have suggested between 40-60% of brain derived beta-amyloid may be cleared in the peripheral blood through the BBB, lymphatic vessels, and by cerebrospinal fluid absorption via arachnoid granules [50-52]. Although, the extent of involvement of each of these pathways in beta-amyloid clearance and their relation to the immune system is currently unclear [1]. Increasing understanding of peripheral clearance pathways and their interactions with brain resident beta-amyloid clearance strategies could offer significant clinical benefit in CAA populations, as therapeutics would not need to be permeable to the BBB. Further, strategies slowing or preventing beta-amyloid accumulation could prevent both ischemic and hemorrhagic brain injury, potentially slowing CAA-related cognitive decline.

### *1.2.2 Efflux receptors and immune cells*

Beta-amyloid is cleared from brain by several efflux receptors expressed on the BBB endothelium [53-55]. Apolipoprotein E4 binds beta-amyloid and mediates its clearance across the BBB via the VLDL pathway, while apolipoprotein E2 favors clearance of beta-amyloid through both LRP1 and VLDL receptors [54]. Other receptors involved in beta-amyloid efflux from brain include advanced glycation end product (RAGE), ATP binding cassette transporters (ABC transporters), organic anion transporting polypeptides (OATP), natriuretic peptide receptor C (Npr-C), low density lipoprotein receptor family (LDLD family – LRP1, LRP2), and insulin sensitive transporter [56].

Studies have suggested LRP1 may regulate recruitment of peripheral immune cells to sites of injury, contributing to monocyte differentiation and activation, and regulation of inflammation [57-60]. LRP1 is also implicated as an efflux receptor of beta-amyloid present on the BBB. As such, it is possible endothelial LRP1 on the BBB may interact with blood derived immune cells contributing to immune activation or altered beta-amyloid clearance in CAA. LRP1 is also expressed on monocytes and macrophages, suggesting beta-amyloid may bind immune cells directly via LRP1 [61-63]. LRP1 expressed by peripheral leukocytes and BBB endothelium may compete for beta-amyloid binding, perhaps altering clearance of beta-amyloid into blood. Future investigation of potential immune cell interactions with beta-amyloid efflux receptors expressed on the BBB is warranted, as these interactions could be targeted to promote beta-amyloid clearance in CAA. Evidence also suggests depletion of LRP1 in monocytes promotes NF- $\kappa$ B activation and pro-inflammatory signaling [60]. This may point towards a protective effect of LRP1 mediated interactions by immune cells in CAA, as LRP1 activity may assist with dampening inflammation, perhaps attenuating vascular damage in the brain.

Additionally, LRP1 expression is also reduced with age in AD, supporting a link between age related changes to beta-amyloid clearance in CAA [53, 64-66]. Thus, LRP1 has several links to immune cells in CAA including beta amyloid clearance, cerebrovascular damage, and inflammation that warrant evaluation to understand and potentially treat CAA.

### *1.2.3 Perivascular clearance of beta-amyloid*

Dysregulated perivascular clearance of beta-amyloid from the interstitial fluid (ISF) is also believed to play a role in CAA pathogenesis, supported by isotope labelling of beta-amyloid and PET imaging studies [1, 34, 35, 49, 67, 68]. Vascular damage and impaired vasoactivity in CAA likely contribute to reduced perivascular clearance of beta-amyloid [1, 69, 70]. Although the mechanisms of perivascular clearance are not well understood, glymphatic clearance along the venules and clearance by the intramural peri-arterial drainage pathways along basement membranes are thought to be involved [36-40, 71-73]. However, contributions of the glymphatic system remain contentious. To further understand perivascular clearance mechanisms, the development of non-invasive methods to better measure and visualize ISF clearance are required [1, 67, 74]. As isotope labelling of beta-amyloid and PET imaging are currently limited by off target binding and uptake of tracers by the brain [1, 67, 74]. If these limitations were addressed, potential treatments for improving clearance of beta-amyloid from the perivascular spaces and ISF could be developed.

### *1.2.4 Clearance of beta-amyloid in the peripheral blood*

Deposition of beta-amyloid in the cerebral vessels is integral to CAA pathology, however clearance of beta-amyloid by peripheral mechanisms is unclear. Recent evidence suggests beta-amyloid may be cleared from brain, to blood for final clearance by the kidney [32]. Indeed beta-amyloid was present in the blood and urine of patients with AD, with beta-amyloid levels being

higher in the blood of the renal artery compared to the renal vein in both humans and mice. Unilateral nephrectomy also increased brain beta-amyloid load, worsened AD pathology, neuroinflammation, and promoted cognitive deficits in APP/PS1 mice. In addition, an increase in beta-amyloid clearance in the blood has been associated with reduced beta-amyloid in the brain, again suggesting brain derived beta-amyloid may be cleared in the periphery [52, 75]. Further support of peripheral beta-amyloid clearance was demonstrated by long term furosemide treatment reducing levels of beta-amyloid in the brain and blood, while also improving AD pathologies, and cognitive deficits in APP/PS1 mice [32]. Neprilysin (NEP) a beta-amyloid degrading enzyme is highly expressed in the kidney [32]. This points towards a pathway where beta-amyloid can be degraded or eliminated by the kidney. Investigation of peripheral clearance mechanisms involving beta-amyloid in CAA are of value, as such methods could be exploited to enhance activity of a potential brain-blood-kidney clearance axis. Future investigation is required to validate such clearance pathways and evaluate the end location of brain derived beta-amyloid in the context of CAA.

Clearance of beta-amyloid in the periphery has also been linked to the complement system [76]. Complement receptor type 1 (CR1) is expressed on erythrocytes, monocytes, neutrophils and B-cells which regulates complement activation and endocytosis by phagocytic cells [77]. Genome wide association studies have associated a CR1 single nucleotide polymorphism (SNP) with CAA, including risk of ICH, and cerebrovascular beta-amyloid accumulation [20]. Beta-amyloid can be transported by CR1 on blood cells including erythrocytes by binding C3b, to be eliminated in the liver or kidney [56, 76]. However, in both patients with AD or mild cognitive impairment (MCI) lower levels of C3-opsonized beta-amyloid bound erythrocytes were observed compared to control participants [76]. Further, the



CR1 SNP associated with CAA is located on non-coding regions containing additional C3b binding sites [78-80]. Thus, a disruption of CR1-C3b binding may impair peripheral beta-amyloid removal in CAA, contributing to cerebral vascular accumulation of beta-amyloid. Investigation of potential beta-amyloid clearance through CR1-C3b interactions on peripheral leukocytes are of interest in future studies, as peripheral leukocytes could be targeted therapeutically in CAA.

Exploration into the potential for peripheral immune cell activity in systemic beta-amyloid clearance is of value, as leukocytes may be involved in clearing systemic beta-amyloid through interaction with the complement system, by direct uptake and phagocytosis, or by shuttling to end organs such as the kidneys for removal [32, 33, 49]. Potential systemic treatments promoting beta-amyloid clearance are of clinical interest, as issues of treatments needing to cross the BBB and potential adverse effects could be avoided in CAA treatment [81, 82].

### **1.3 Neutrophils and BBB disruption in Cerebral Amyloid Angiopathy**

#### *1.3.1 Introduction to neutrophils*

Neutrophils are phagocytic cells of the innate immune system, which mediate destruction of invading pathogens, cytokine production, and the recruitment of immune cells to sites of inflammation [30, 83, 84]. Damage to host tissues can result from neutrophil activity [85-91]. Neutrophils also promote tissue repair through involvement in vascular remodelling pathways, exhibiting a contrasting protective role in vascular maintenance [92-94].

### *1.3.2 Neutrophil infiltration into brain*

Neutrophil adhesion to cerebral endothelium can contribute to vascular injury, enhance production of metalloproteinases (MMPs), and reactive oxygen species (ROS) [95-99]. In human and mouse, beta-amyloid can enhance neutrophil adhesion to vascular endothelium and increase production of ROS [100]. Integrins are adhesion molecules involved in neutrophil adhesion and migration across the BBB. In a transgenic mouse model, beta-amyloid activated LFA-1 integrin, promoting neutrophil adhesion and infiltration across the BBB prior to the onset of cognitive decline [100]. Inhibiting LFA-1 reduced neutrophil adhesion resulting in slowed AD progression, with improvements in memory and a decrease in AD neuropathology. These findings suggest neutrophil infiltration into brain may contribute to development and progression of AD. Investigation of changes in adhesion molecule expression in patients at risk of CAA development, and in relation to CAA progression will be of interest to determine the role of neutrophils in CAA and cognitive decline.

Neutrophils from the peripheral blood may infiltrate into the brain and interact with vascular beta-amyloid in CAA. This is supported by 2-photon microscopy studies in AD mouse models which demonstrated neutrophil infiltration across the BBB, and migration to vessel associated beta-amyloid deposits [100, 101]. In transgenic AD mice neutrophils were found to co-localize with beta-amyloid, produce neutrophil extracellular traps (NETs) and IL-17 in regions of beta-amyloid accumulation [100]. NETs are extracellular web like structures which can trap pathogens and debris. NET release was also demonstrated in the cortical vessels and parenchyma of patients with AD, further supporting potential neutrophil involvement in CAA [102]. IL-17 is a pro-inflammatory cytokine released by CD4<sup>+</sup> T-cells (Th17) [103-106]. Th17 cells are a recently discovered lineage of CD4<sup>+</sup> helper T-cell and their biological roles are

largely elusive. Evidence suggests Th17 mediated IL-17 release promotes recruitment and activation of both monocytes and neutrophils, regulating tissue inflammation. Th17 cells also express toll like receptor (TLR) 1 and TLR2, pattern recognition receptors expressed by other peripheral leukocytes which have been demonstrated to be stimulated by beta-amyloid [107, 108]. As such, beta-amyloid may contribute to direct stimulation of Th17 cells leading to neutrophil recruitment in CAA. Further investigation is required to evaluate such an interaction. Th17-neutrophil interactions provide a potential link between innate and adaptive arms of the immune system in CAA pathogenesis. This is of interest, as novel mechanisms underlying beta-amyloid and Th17 signaling could possibly be targeted in future treatments of CAA.

### *1.3.3 Tissue repair by neutrophils*

Neutrophils have roles in removal of cellular debris following recruitment to sites of inflammation or injury [92, 109, 110]. Neutrophils have been shown to promote revascularization and angiogenesis through the release of metalloproteinases that activate vascular endothelial growth factor [92, 93]. Such processes could assist with repairing damaged cerebral vessels in CAA, through recruitment and activation of cells that promote repair [92]. Following repair processes, neutrophils are either cleared by macrophages or re-enter the blood, migrating to the bone marrow to die by apoptosis [111]. The exit or clearance of neutrophils from brain is supported by evidence indicating neutrophils release micro-vesicles containing molecules that attenuate further neutrophil recruitment and enhance shifting to anti-inflammatory macrophage phenotypes [94]. Neutrophils also express chemokine receptor 5 (CCR5) which acts as a cytokine scavenger, reducing levels of pro-inflammatory cytokines and thus inflammation [94, 112, 113]. This suggests exploration of a potentially protective role of neutrophils in CAA is warranted, as neutrophils may contribute to tissue repair, and then return to the peripheral blood.

Return of neutrophils to the blood following tissue repair processes in CAA would reduce risk of neutrophil promoted inflammation locally in the brain in CAA [114]. The potential shuttling of neutrophils in and out of the brain is important, as promotion of tissue repair processes by neutrophils could be targeted to reduce vascular damage or dampen inflammation characteristic of CAA.

## **1.4 Monocytes in Cerebral Amyloid Angiopathy**

### *1.4.1 Monocyte origins and function*

Monocytes are innate immune cells that arise from myeloid progenitor cells of the bone marrow and have roles in phagocytosis of debris, endothelial regulation, and inflammation [115-118]. Historically peripheral blood monocytes were thought to be the primary source of tissue macrophages [116]. However, recent studies suggest tissue resistant macrophages develop during embryogenesis arising from yolk sac precursors, then fetal liver monocytes, where they migrate to various tissues and maintain populations via self-renewal [116, 119, 120]. This has promoted a renewed curiosity of the roles of bone marrow derived peripheral blood monocytes and their roles in healthy and disease states [116, 121]. In CAA, beta-amyloid in the vascular wall may promote recruitment of peripheral blood monocytes into brain. This is supported by in vitro studies demonstrating beta-amyloid induced monocyte adhesion and infiltration across endothelium [122, 123]. Further, monocyte entry into brain was evidenced by live 2-photon microscopy indicating monocytes migrated towards beta-amyloid in the cerebral vessels and subsequently return to the blood in APP/PS1 AD mice [124]. This study also indicated depletion of monocytes increased beta-amyloid burden, suggesting a potential role of peripheral monocytes infiltrating brain and clearing amyloid burden locally.

#### *1.4.2 Monocytes and beta-amyloid in peripheral blood*

Evidence suggests beta-amyloid can be transported from brain into the peripheral blood, increasing clearance of beta-amyloid in the brain [32, 52, 125-128]. While no studies have explored peripheral blood monocyte activity specific to CAA, this is of interest as peripheral monocytes have been associated with beta-amyloid clearance in AD [108, 124]. Phagocytosis assays support the ability of blood monocytes to uptake beta-amyloid, as beta-amyloid uptake in assays was negatively associated with blood levels of beta-amyloid [108]. This supports potential for peripheral blood monocytes to uptake and clear beta-amyloid from the blood in CAA. Monocytes isolated from peripheral blood of AD patients exposed to beta-amyloid also demonstrated reduced phagocytosis, abnormal cytokine release, and increased apoptosis [127]. This suggests monocyte function may become impaired in settings of potentially chronic stimulation by beta-amyloid. Compensatory dampened peripheral blood monocytic response or dysregulated phagocytosis could be present in CAA, perhaps due to chronic stimulation with beta-amyloid. Exploration of peripheral monocyte activity in CAA is of importance as potential therapeutic agents could target monocyte activation and beta-amyloid uptake in blood.

#### *1.4.3 Receptor mediated endocytosis in monocytes*

Evidence suggests toll like receptors (TLRs) promote receptor mediated endocytosis in monocytes through mechanisms enhancing phagocytosis [108, 129]. Uptake of beta-amyloid was also indicated to proceed through TLR2 in peripheral blood monocytes in AD, supporting potential involvement of TLR signaling in CAA [108, 130, 131]. This supports a potential interaction between beta-amyloid and TLR in CAA, which may promote phagocytosis. Indeed, receptor mediated endocytosis of beta-amyloid was observed to increase early endosome formation and combination with lysosomes during beta-amyloid breakdown by proteases [108].

Lysosomal proteases implicated in beta-amyloid degradation include cathepsin D and cathepsin S, which were not found to be differentially expressed in peripheral monocytes of patients with AD. However, TLR2 expression was decreased in AD compared to controls. These results suggest monocyte dysfunction in AD may be linked to beta-amyloid-TLR alterations rather than enzymatic degradation issues in monocytes [108, 132]. In CAA, it is possible that beta-amyloid interacts with peripheral monocytes through TLR signaling perhaps leading to amyloid uptake and breakdown. Future investigation of pathways implicated in monocyte activation and endocytosis is of interest, as dysregulated monocyte activity may be involved in CAA specific beta-amyloid clearance from peripheral blood.

## **1.5 Perivascular macrophages**

### *1.5.1 Origin of perivascular macrophages*

Perivascular macrophages (PVMs) are brain resident immune cells distinguished by their localization to the perivascular spaces, expression of scavenger receptors, and phagocytic capacities [133]. PVMs are a type of border associated macrophage (BAM) [134]. BAMs include cells present in the perivascular spaces, choroid plexus, and meninges. Historically BAMs such as PVMs, meningeal macrophages (MGMs), and choroid plexus macrophages (CPMs) were thought to arise from peripheral monocytes after birth and then be replaced by bone marrow derived cells [135-141]. However, a recent study using parabiosis and fate mapping demonstrated stable BAM populations including PVMs instead likely originate from hematopoietic precursors during embryonic development [142].

### *1.5.2 Functional roles of perivascular macrophages*

In healthy states, PVMs are thought to maintain BBB integrity, act as phagocytes and antigen presenting cells, in addition to contributing to lymphatic clearance [133, 134]. However, under pathological conditions the role of PVMs remain unclear. Evidence suggests PVMs may facilitate cross talk between cerebral endothelial cells and peripheral immune cells to mediate immune activation [143]. BAM depletion decreased neutrophil infiltration, BBB disruption and reduced neurological deficits in rat stroke models supporting BAM activity in BBB maintenance [134]. Depletion of PVM in mouse stroke models led to granulocyte recruitment through increased expression of vascular endothelial growth factor (VEGF), which promoted BBB disruption and immune infiltration following stroke [134]. In conclusion, PVMs appear to play a role in BBB maintenance and potential peripheral immune cell infiltration.

PVMs may also enhance vascular damage by promoting oxidative stress within cerebral vessels [138, 144]. PVMs have been implicated in various neurological diseases including stroke, CAA, AD, multiple sclerosis, meningitis, and encephalitis [133, 134, 145-152]. PVM involvement in altering vascular health is supported by evidence demonstrating angiotensin II mediated activation of angiotensin II type 1 receptors in PVM led to increased production of ROS via the NOX2 superoxide producing enzyme [138, 153, 154]. These findings support a potential association between PVMs promoting oxidative stress and vascular damage, which may reduce neurovascular health when hypertension is present [138]. Given the known contribution of hypertension as a leading risk factor in vascular cognitive impairment and ICH, further investigation of the association between PVM and vascular oxidative stress is of interest [155]. In CAA PVMs might be implicated in promoting cognitive impairments through ROS production and NOX2 signaling, but further study is needed to explore this relationship and

potential associations with hypertension management. This is of clinical value, as vascular damage in CAA may increase risk of ICH or cognitive decline associated with CAA.

### *1.5.3 Perivascular macrophages and beta-amyloid*

PVMs have a proposed role in beta-amyloid clearance [146, 147, 156]. The investigation of PVM in CAA began with phagocytosis uptake assays where intracerebroventricular (ICV) injection of fluorescently labelled dextran tracers were observed to be taken up by PVMs [157-161]. This was indicated by the presence of fluorescently labelled phagosomes within PVMs, supporting phagocytic capabilities of PVMs [157-161]. In CAA mouse models (TgCRND8 mice), clodronate (CLO) mediated depletion of PVMs led to increased deposition of beta-amyloid within cerebral vessels while parenchymal beta-amyloid remained unchanged [162]. In another study using TgCRND8 mice, increased vascular beta-amyloid was found to be associated with PVM depletion while PVM stimulation with chitin attenuated CAA severity and beta-amyloid load [147]. CLO is toxic to PVM upon phagocytosis and was suggested to deplete PVMs by ICV injection of CLO-containing liposomes [146-149]. Importantly, CLO injection does not affect peripheral mononuclear cells or microglia cells [141]. Studies have illustrated PVMs express scavenger receptor class B (SR-B1), which is a high-density lipoprotein receptor that binds beta-amyloid [163-165]. SR-B1 expressing PVMs in J20 transgenic CAA mouse models were found to interact with beta-amyloid deposits in meningeal and cortical blood vessels, with J20 SR-B1<sup>+/-</sup> mice demonstrating increased vascular beta-amyloid deposits [148, 166].

Based on findings from PVM depletion studies and SR-B1 deficient CAA mouse models, there is evidence of a PVM or BAM in beta-amyloid clearance from the brain. However, these studies were limited by the inability to differentiate PVMs from MGMs which are often found in



overlapping locations [133, 167]. Additionally, markers specific and sensitive in PVM identification are essential before PVM involvement in CAA could be distinguished from other BAM involvement [133, 167]. Single cell RNA sequencing studies have attempted to differentiate various BAMs including PVMs and MGMs based on unique markers but have thus far been unsuccessful [168, 169]. Further investigation of unique BAM markers is of clinical interest, as they could help identify brain resident cell involvement specific to CAA. This could provide insight into future targeted strategies for clearing beta-amyloid locally within the brain.

## **1.6 CAA related inflammation**

### *1.6.1 An Introduction to CAA related inflammation and abeta related angiitis*

CAA related inflammation (CAA-ri) is a rare, potentially autoimmune related manifestation of CAA characterized by an inflammatory response to vascular beta-amyloid often presenting with subacute neurological symptoms [170, 171]. CAA-ri is thought to be a milder form of Abeta-related angiitis (ABRA) with features of perivascular inflammation, while ABRA is a type of vasculitis with transmural inflammation [172-174]. Although both CAA-ri and ABRA have similar clinical presentations and imaging findings, ABRA requires more aggressive immunosuppression treatment. Clinical presentation of these two syndromes includes acute or subacute cognitive decline, personality changes, new or persistent headache, seizure, memory impairment, confusion, progressive neurological signs, or altered level of consciousness. MRI often shows potentially reversible patchy or confluent white matter hyperintensities in the subcortical regions, and multiple microinfarcts are often seen [175]. Cerebrospinal fluid analysis may demonstrate pleocytosis with a lymphocytic predominance, mildly elevated protein, and the presence of anti-amyloid antibodies during the acute phase of inflammation. The presence of

antibodies is not detected during remission phases of CAA-ri, suggesting differences in immune system responses throughout CAA progression. In symptomatic patients, a diagnosis of probable CAA-ri is made in those 40 years or older, with the presence of one at least one of the following including headache, a decrease in consciousness, behavioural change, focal neurological signs, or seizures unrelated to acute ICH [176]. MRI must also demonstrate unifocal or multifocal WMH lesions, and the presence of either corticosubcortical hemorrhagic lesions, cerebral macrobleeds, or cSS in the absence of neoplasms, infection, or other causes of the lesions. Management of CAA-ri and ABRA include a course of high dose glucocorticoids, and immunosuppressive treatment [177-179].

#### *1.6.2 Immune system involvement in CAA-ri*

CAA-ri and ABRA have been suggested to be promoted by a potential autoimmune response against vascular beta-amyloid, which may contribute to beta-amyloid clearance or increased vasculitis [172, 180]. Intramural and perivascular infiltrates from patients with CAA-ri consist of CD68+ macrophages, multinucleated giant cells, and CD3+ T lymphocytes with both macrophages and giant cells containing intracellular beta-amyloid deposits [170, 172, 180, 181]. These findings suggest potential involvement of immune cells in beta-amyloid uptake during the acute phase response of CAA-ri. Flow cytometry of peripheral blood and CSF demonstrate lymphocytic pleocytosis during CAA-ri, indicating T cell responses may be upregulated as a response to brain vascular amyloid [181]. CD4+ T cells were the dominant subtype within perivascular infiltrates residing near MHC class II expressing microglia, macrophages, and multinucleated giant cells. This evidence suggests antigen presenting cells including macrophages and microglia could contribute to T cell activation in CAA-ri due to beta-amyloid presentation to T cells. Enhanced T cell responses could promote B cell activation and

production of anti beta-amyloid antibodies, potentially promoting immune activation and vascular inflammation during CAA-ri or ABRA. Antigen presenting cells may also respond to vascular beta-amyloid by increasing vessel inflammation and potentially worsening BBB integrity.

During the acute or subacute phase of CAA-ri an inflammatory and immune mediated response to cerebrovascular beta-amyloid deposits appears to occur. This transient production of anti-beta amyloid antibodies in the CSF could suggest the immune system may respond differently in CAA-ri as compared to states of remission, and sporadic or familial CAA where CSF appears normal. Comparison of immune system responses and peripheral leukocyte activation in CAA-ri and sporadic or familial forms of CAA is of interest as this could shed insight into distinct immune related mechanisms involving different CAA syndromes. The immune system may respond differently in patients presenting with CAA-ri, potentially suggesting immune response that could be targeted therapeutically in this specific subset of CAA patients. This is supported as glucocorticoids and immunosuppressants are clinically useful treatments for sporadic or familial CAA but are effective treatments for CAA-ri and ABRA [177-179]. Patients presenting with CAA-ri or ABRA may have altered immune system responsiveness, perhaps contributing to an elevated risk of CAA-ri type presentations as compared to other CAA related syndromes. Such changes could be explored to potentially reveal novel biomarkers or potential therapeutic targets associated with risk of CAA-ri, ABRA, or amyloid related imaging abnormalities an iatrogenic form of CAA-ri linked to trialed beta-amyloid specific therapies. Future investigation of peripheral leukocyte responses in during CAA-ri is of clinical interest, as such alterations in blood cell immune function could be modulated therapeutically and thus warrants future investigation.

## **1.7 Summary of immune system in CAA**

Further studies of the immune system specific to CAA are of interest to better understand the complexities underlying beta-amyloid clearance and CAA progression. With a globally aging population, strategies to slow progression of CAA and reduce cognitive decline are of great importance. Evaluation of immune contributions to various aspects of CAA in relation to severity are of interest as distinct alterations in immune system may be involved. As such, peripheral blood leukocyte changes could offer insight into new strategies for detecting diagnostic blood biomarkers in CAA. Early detection of CAA prior to manifestation of late-stage neuroimaging findings could be of clinical significance in detecting patients at risk of CAA progression, cognitive decline, and severe outcomes including ICH. Future evaluation of peripheral leukocyte involvement in CAA pathogenesis is of interest as a potential therapeutic target, as modulation of immune cell activation in the periphery could offer novel therapies to be trialed in CAA, CAA-ri or ABRA.

## *Chapter 2: Cerebral amyloid angiopathy blood gene expression profiling*

### **2.1 Abstract**

**Background:** Cerebral amyloid angiopathy (CAA) is a cerebral small vessel disease featuring beta-amyloid deposits within the cerebral vasculature. It is a major cause of cognitive decline and intracerebral hemorrhage in the elderly. This study evaluated whether gene expression profiles in peripheral blood can differentiate patients with CAA from vascular risk factor and healthy controls.

**Methods:** In 27 patients with CAA blood cell gene expression was compared to 55 controls. Total RNA was isolated from PAXgene tubes and measured by RNA sequencing. Differentially expressed genes between CAA and controls were identified by ANOVA adjusting for age and sex. Functional pathway analysis identified pathways associated with CAA. A prediction model to distinguish CAA from controls was developed using linear discriminant analysis with feature selection by forward selection. Model performance was evaluated by 10-fold leave-one-out cross validation.

**Results:** 686 differentially expressed genes were identified ( $p < 0.05$ , fold change  $> |1.2|$ ), of interest *ADAM15*, *CAMK1D*, *CAP1* and *TGFBI*. Canonical pathway analysis identified cell movement of phagocytes, activation of phagocytes, CREB, degranulation of leukocytes, immune response of cells, inflammatory response, and IL-23 signaling. A 24 gene panel differentiated patients with CAA from controls with  $>95\%$  sensitivity and specificity. The identified genes reveal differences in immune system regulation in patients with CAA compared to vascular risk

factor and healthy control patients. Differences identified include a potential shift in beta-amyloid uptake by phagocytes (*TGFB1*, *CREB*, *CAMK1D*), an increase in vascular extracellular matrix disruption (*ADAM15*, *CAP1*), and a possible alteration in amyloid precursor processing (*BRI3BP*, *SORCS3*).

**Conclusions:** Differences in blood gene expression are present in patients with CAA compared to control patients. These relate to differences in immune activation and signaling associated with CAA. The differences in blood cell gene expression shows promise to distinguish CAA from controls, though further evaluation in larger cohorts is required.

## **2.2 Introduction**

Cerebral amyloid angiopathy (CAA) is common amongst the elderly and is an important cause of spontaneous intracerebral hemorrhage (ICH), dementia and cognitive decline [2, 182-184]. Currently, no blood based diagnostic biomarkers for CAA exist. Improved understanding of the biological mechanisms in CAA pathogenesis is essential for the development of biomarkers. With an aging population, strategies to slow the progression of CAA are of increasing importance. A gap exists regarding the understanding of how the immune system response may contribute to CAA. In this study, we evaluated differences in blood cell gene expression signatures in patients with CAA to develop a gene panel that can predict patients with CAA from control patients.

A blood biomarker panel could be used as a tool for identifying patients with CAA. This is of clinical value as probable diagnosis of CAA relies on imaging findings associated with often late-stage, severe CAA manifestations [2]. Additionally, current blood and cerebrospinal fluid biomarkers of CAA lack adequate sensitivity and specificity to offer clinical utility [185]. Further, current proposed biomarkers require further replication and validation in larger cohorts [186, 187]. Early diagnosis of CAA is of importance, as strategies could be used to reduce risk of cognitive decline or future bleeding events and thus slow progression of CAA. Additionally, early detection of CAA could influence clinical management and prevention of ICH by avoiding use of anticoagulants, antiplatelets, and thrombolytics [188-193]. A biomarker panel could offer benefit in identifying CAA as these patients may present with different clinical features including transient focal neurological episodes, intracerebral hemorrhage, or cognitive decline [1, 194]. As such, development of diagnostic tools for identification of patients with CAA is of interest.

In this preliminary discovery-based study our aim was to evaluate if changes in peripheral blood gene expression profiles can distinguish patients with CAA from controls, and whether such changes can predict patients as having CAA. Our data suggests differentiation of patients with CAA compared to controls, and prediction of patients with CAA is achievable, however further investigation of this gene expression panel is required. Currently, the role of the immune system in CAA pathophysiology is not well understood. However, changes in peripheral leukocyte gene expression have been linked to various clinical features of CAA including ischemic stroke, hemorrhagic stroke, and white matter disease [30, 96, 98, 195-203]. Thus, investigation of changes in peripheral leukocyte gene expression in patients with CAA is of interest. Using RNA sequencing and prediction modelling a 24 gene profile that distinguished patients with CAA from control patients was developed. These genes were implicated in alterations in immune cell regulation and beta-amyloid clearance presenting potential for use as a tool in identifying patients with CAA.

## **2.3 Methods**

### Patients

Patients were recruited as part of the Functional Assessment of Vascular Reactivity (FAVR) study approved by the University of Alberta Health Research Ethics Board and University of Calgary Conjoint Health Research Ethics Board with each subject providing informed written consent. There were 27 patients with CAA and 55 controls recruited from the University of Alberta and the University of Calgary between 2016 and 2020. Probable CAA diagnosis was made by consensus of two board-certified neurologists using the Modified Boston Criteria on brain MRI [23]. Patients with lymphoma, leukemia, active infection, treatment with



immunomodulating therapy were not included. Control subjects had vascular risk factors but had no evidence of cognitive decline, no history of stroke, and did not have CAA.

### Sample Processing

Peripheral blood was collected by venipuncture into PAXgene tubes and stored at room temperature for 2 hours prior to being frozen at  $-80^{\circ}$  until RNA extraction. All samples were processed for RNA extraction in the same laboratory. RNA was isolated from PAXgene tubes using PAXgene Blood RNA kit (PreAnalytiX, Switzerland). RNA integrity and concentration was analyzed using the Agilent 2100 Bioanalyzer (Agilent, Santa Clara USA) and Nanodrop (Thermo Fisher Scientific, USA). Samples had an RNA integrity number (RIN)  $\geq 7.5$  and an  $A_{260}/A_{280}$  absorbance ratio of  $\geq 1.8$ .

### cDNA Library Preparation

RNA samples were processed using QuantSeq 3' mRNA-Seq Library Prep Kit FWD with Unique Dual Indices for cDNA library generation (Lexogen, Austria). Globin Block (RS-Globin Block) was used to prevent the generation of library fragments from globin mRNAs. cDNA library generation was initiated with 113ng RNA undergoing oligodT priming during strand synthesis and subsequent magnetic bead purification. PCR cycle optimization was performed by qPCR assay, and Lexogen UDI 12nt Unique Dual Indices were incorporated during amplification.

### RNA Sequencing Differential Expression and Pathway Analysis

Samples were sequenced by Illumina NovaSeq6000 sequencing. RNA sequencing (RNAseq) analysis was performed using the QuantSeq 3'mRNA-Seq pipeline in Partek Flow Bioinformatics software (Partek, Saint Louis, MO). Raw reads were trimmed for quality (Phred score >37), and adapters and unique dual indexing sequences were removed. Sequences were aligned to the human genome (hg38) using the STAR2.5.3a aligner. Reads were normalized using transcripts per kilobase million. ANOVA was used to generate a list of differentially expressed genes adjusted for age and sex. Genes were considered differentially expressed based on a  $p < 0.05$  and fold change  $> |1.2|$ . Ingenuity Pathway Analysis was used to identify enriched functional pathways from the identified gene list (IPA, Ingenuity Systems, QIAgen). Pathways were determined to be enriched using Fisher's exact test  $p < 0.05$  and a Benjamini-Hochberg false discovery rate (FDR  $< 0.05$ ) multiple comparisons correction.

### Gene Expression Analysis

Gene expression analysis, principal component analysis, hierarchical clustering analysis, and prediction modelling was performed using Partek Genomics Suite 6.06 (Partek Inc., St. Louis, MO). A prediction model was created using linear discriminant analysis with feature selection by forward selection. Model performance was tested by 10-fold leave-one-out cross validation.

## **2.4 Results**

### *Patient demographics*

Demographic and clinical features of patients with CAA (n=27) and control patients (n=55) are displayed in Table 1. The mean age of patients with CAA was 74.9 years, with 14

(51.8%) being female, 17 (63.0%) having hypertension, and 3 (11.1%) having diabetes. The mean age of control patients was 72.6, with 31 (56.4%) being female, 27 (49.0%) having hypertension, and 7 (11.1%) having diabetes. In patients with CAA the average white matter hyperintensity volume corrected for intracranial volume was 29.9 ( $\pm 23.6$ ) cm<sup>3</sup>, and the average cerebral microbleed count was 34.4 ( $\pm 85.6$ ). In control patients the average white matter hyperintensity volume corrected for intracranial volume was 4.75 ( $\pm 4.71$ ) cm<sup>3</sup>, and the average cerebral microbleed count was 0.11 ( $\pm 0.32$ ). Of the patients with CAA, the average perivascular space score (Wardlaw scale) in the basal ganglia at baseline was 1.90 ( $\pm 0.83$ ) and the average perivascular space score (Wardlaw scale) in the centrum semiovale was 2.23 ( $\pm 1.0$ ). Of the control patients, the average perivascular space score (Wardlaw scale) in the basal ganglia at baseline was 1.57 ( $\pm 0.65$ ) and the average perivascular space score (Wardlaw scale) in the centrum semiovale was 1.31 ( $\pm 0.63$ ). In patients with CAA, 12 (57.1%) of the patients had cortical superficial siderosis (cSS), with 7 (33.3%) having disseminated cSS, and 5 (23.8%) having focal cSS. In control patients, no patients had either focal or disseminated cSS. A 2-tailed t test or  $\chi^2$  test was used where appropriate to analyze differences in demographic and clinical data between CAA and control groups. There were no significant differences in age, sex, vascular risk factors, or years of education between groups. There were differences in neuroimaging features.

### *RNA Sequencing Differential Expression*

There were 686 differentially expressed genes identified from peripheral blood ( $p < 0.05$ , fold change  $> |1.2|$ ) (Table S1.1). 547 genes were downregulated in CAA compared to controls, including ADAM metalloproteinase domain 15 (*ADAMI5*), Transforming growth factor-beta 1

(*TGFB1*), Calcium/calmodulin-dependent protein kinase ID (*CAMK1D*), and Cyclase associated actin cytoskeleton regulatory protein 1 (*CAP1*). 139 genes were upregulated in CAA compared to controls.

### *Prediction of Cerebral Amyloid Angiopathy*

There were 27 patients with CAA, and 55 control patients. Clinical and demographic characteristics of patients used for comparison of CAA and control patients are displayed in Table 1.1. There were no significant differences in age, sex, vascular risk factors, or years or education between groups. There were differences in neuroimaging features.

A 24 gene profile was generated using linear discriminant analysis (LDA) with forward selection. The ability of the LDA model was assessed using cross validation. This 24 gene profile was then used to predict CAA patients from controls. Of the 82 samples, 96% of the 27 CAA patients and 98% of the 55 control patients were correctly predicted by the model. The gene profile demonstrated a sensitivity and specificity of >95%. The positive predictive value of the model was 96% and the negative predictive value was 94%.

A hierarchical cluster plot of the 24 genes that were significantly different between CAA and controls is shown in Figure 1.1. Subjects are clustered into groups based on diagnosis. Hierarchical clustering demonstrates a group of genes that are upregulated in CAA, and another group that is downregulated in controls. Another group of genes is downregulated in CAA and upregulated in controls. The control group also appears to cluster into two subgroups. The 24 genes separated CAA patients from controls by approximately 2 standard deviations as demonstrated by principal component analysis (Figure 1.2). Although these results are

hypothesis generating and need further assessment in larger cohorts, these findings suggest that gene expression profiling in blood can differentiate CAA from control patients.

### *Functional Pathway Analysis*

There were 686 genes that were significantly different between CAA patients and controls ( $p < 0.05$ , fold change  $> |1.2|$ ) (Table S1.1). Of these genes, 547 were downregulated in CAA and 139 were upregulated compared to controls. Functional pathway analysis utilizing this gene list of differentially expressed genes identified pathways associated with CAA. Enriched signaling pathways associated with CAA ( $p < 0.05$ ) are shown in Table 1.3. These pathways included cell movement of phagocytes, activation of phagocytes, CREB, degranulation of leukocytes, degranulation of phagocytes, immune response of cells, inflammatory response, and IL-23 signaling. Genes of interest present in the 24 gene profile and enriched signaling pathways include *ADAMI5*, *CAMK1D*, *CAP1* and *TGFBI* (Table 1.2).

## **2.5 Discussion**

We evaluated gene expression differences in blood to identify patients with CAA compared to controls. The identified genes and associated pathways provide insight to the relationship of the peripheral immune system to CAA. Differences identified include a potential shift in beta-amyloid uptake by phagocytes (*TGFBI*, *CREB*, *CAMK1D*), an increase in vascular extracellular matrix disruption (*ADAMI5*, *CAP1*), and a possible alteration in amyloid precursor processing (*BRI3BP*, *SORCS3*). A panel of 24 genes differentially expression in CAA showed promise to distinguish patients with CAA from controls.

Development of tools that can aid diagnosis of CAA is of tremendous clinical value, as probable CAA diagnosis is currently based on imaging features often characteristic of late-stage disease manifestations [2]. Early diagnosis of CAA could offer clinical benefit in altering pathways contributing to disease progression, to promote healthy brain aging and reduce cognitive decline in patients with CAA. The modified Boston Criteria is the currently accepted tool for probable CAA diagnosis, however relying on probable diagnosis may also produce more false positives and negatives when identifying patients with CAA [23]. Definitive diagnosis of CAA relies on histopathology which is limited by both sample size and generalizability, as brain tissue from biopsy, autopsy or hematoma evacuation is often acquired from patients with severe or aberrant clinical courses [23]. Currently blood and cerebrospinal fluid (CSF) biomarkers with diagnostic applications in CAA are limited by sensitivity and specificity, with CSF collections being invasive and time intensive [204, 205]. As such, development of minimally invasive tools that could aid diagnosis of CAA are of value.

TGF- $\beta$ 1 expression was reduced in patients with CAA (Figure 1.3, Table 1.2). The role of TGF- $\beta$ 1 is supported in CAA, as TGF- $\beta$ 1 variants are associated with increased beta-amyloid vascular deposition [206]. TGF- $\beta$ 1 is a cytokine produced by monocytes and lymphocytes, with roles in recruitment of peripheral leukocytes [207-211]. Signaling pathways including inflammatory response, immune response of cells, cell movement of phagocytes, and activation of phagocytes were also linked to TGF- $\beta$ 1 expression, further supporting involvement of TGF- $\beta$ 1 and immune regulation (Table 1.3). Targeting TGF- $\beta$ 1 has also been postulated to provide benefit in neurodegenerative or neuroinflammatory diseases including vascular dementia, Alzheimer's disease (AD), and stroke [208, 212, 213]. Indeed, TGF- $\beta$ 1 has been suggested to promote brain health following stroke [214-216]. TGF- $\beta$ 1 also promotes beta-amyloid uptake

and phagocytosis by polymorphonuclear leukocytes in AD [208, 217-219]. Thus, a decrease in TGF- $\beta$ 1 in CAA patients may impair beta-amyloid uptake by polymorphonuclear leukocytes, leading to increased amyloid burden in CAA. Immune cell interactions with chronic beta-amyloid stimulation involving TGF- $\beta$ 1 in CAA may contribute to altered immune responses and dysregulated beta-amyloid clearance. Impaired TGF- $\beta$  has been linked to activation of polymorphonuclear leukocytes, beta-amyloid accumulation, and the progression of neurodegeneration in AD, thus supporting potentially altered immune responses in CAA [220, 221]. Further investigation of immune system changes involving TGF- $\beta$ 1 and polymorphonuclear leukocytes is of interest, as this may provide a potential therapeutic target for the promotion of immune responses that promote brain health and beta-amyloid clearance.

In patients with CAA, CAMK1D expression was reduced, and signaling involving both CREB and immune response of cells were associated with CAA (Figure 1.3, Table 1.3). Signaling pathways including inflammatory response, immune response of cells, cell movement of phagocytes, and phagocytosis of cells were also linked to CAMK1D expression, supporting involvement of CAMK1D in immune cell responses (Table 1.3). CAMK1D is a protein kinase that regulates neutrophils through activation of the transcription factor CREB [222-224]. CREB has been associated with CAMK1D and is required for neutrophil proliferation and functioning [225]. Further, CREB has been linked to cognitive impairment in AD, memory, and synaptic plasticity [226-230]. This suggests neutrophil responses may be altered in CAA and contribute to cognitive decline. GWAS studies have identified CAMK1D single nucleotide polymorphisms to be associated with AD, and CAMK1D has also been linked to late onset AD [231, 232]. Protein level studies in AD patients have also indicated CAMK1D is differentially cleaved [233]. Further evaluation of neutrophils in CAA will be of interest to ascertain whether CAMK1D and CREB

signaling could be promoting beneficial immune system adaptations perhaps due to chronic beta-amyloid presence, or if CAMK1D-neutrophil interactions may be driving pathogenic immune responses in CAA linked to cognitive changes.

ADAM15 expression was reduced in patients with CAA (Figure 1.3, Table 1.2). ADAM15 is a metalloproteinase with roles in extracellular matrix (ECM) and tight junction (TJ) remodelling [234-240]. ADAM15 has also previously been found to affect endothelial permeability, by modulating blood brain barrier function and monocyte migration [240]. Thus, it may have effects on the ECM and immune cell interaction with cerebral endothelium in CAA. ADAM15 also negatively regulates toll-like receptor signalling, which dampens activation of the innate immune system and contributes to anti-inflammatory effects [241]. As such, ADAM15 expression may alter TLR signalling in CAA (Table 3). Peripheral monocytes can take up beta-amyloid [108]. However, uptake of beta-amyloid by peripheral monocytes was reduced in patients with AD alongside decreased TLR2 expression [108]. This suggests TLRs may be involved in beta-amyloid uptake in leukocytes, and ADAM15 may interact with these processes. Support of altered monocyte uptake of beta-amyloid related to ADAM15 is indicated by enriched cell movement of phagocytes signaling associated with CAA involving ADAM15 expression (Table 1.3). Further investigation of ADAM15 and TLR signalling in CAA is warranted, as elucidation of beta-amyloid interactions with TLR may provide insight to novel alterations in immune system responses present in CAA. Such responses could be of interest as potential therapeutic targets in CAA, as structural changes in the ECM and changes in immune system response may contribute to progression of CAA.

CAP1 expression was decreased in CAA. CAP1 was also involved in signaling pathways associated with CAA including degranulation of leukocytes and phagocytes (Figure 1.3, Table



1.3) CAP1 is an actin binding protein expressed by peripheral blood monocytes [242, 243]. Binding of CAP1 to actin is proposed to induce vascular inflammation by regulating adhesion and migration of monocytes [244, 245]. Vascular changes associated with CAP1 include endothelial cell contraction and blood brain barrier disruption. CAP1 also functions as a receptor for cytokines and upon activation promotes recruitment of immune cells [244, 246]. Activation of CAP1 is associated with chronic inflammatory conditions including atherosclerosis, obesity, diabetes, Huntington's disease and cardiometabolic diseases [243, 247-250]. As such, CAP1 may have a role in regulation of immune response in CAA related to cerebral vascular health. Further exploration of the association between CAP1 and altered immune response is important, as CAP1 may contribute to vascular inflammation and immune dysregulation in CAA.

Genes implicated in amyloid precursor processing were also identified in the prediction model, including *BRI3BP* and *SORCS3* (Table 1.2). *BRI3BP* expression was reduced in CAA. *BRI3BP* (Bri3 binding protein) binds *BRI3* which has been demonstrated to inhibit beta-amyloid production, through binding APP [251]. This suggests that *BRI3BP* may be a marker of enhanced APP processing in CAA. *SORCS3* expression was increased in CAA. *SORCS3* has also been associated with risk of AD, altered APP processing, and cognitive decline [252]. This evidence supports potential for *SORCS3* involvement in dysregulated beta-amyloid production in CAA, which may be contributing to worsening cognitive function. Thus, alterations in APP processing cascades present in CAA may be associated with cognition and thus could be of interest as potential therapeutic targets in slowing progression of CAA.

This study has several limitations including small sample size, thus further study in larger cohorts is required. Patients were matched for vascular risk factor controls, age, sex, and years of education, however other factors such as the heterogeneity of CAA could not be entirely

accounted for. Further investigation of gene expression signatures at various timepoints throughout CAA progression are of interest, as expression may differ based on disease progression and associated cognitive changes.

In conclusion, we provide preliminary evidence of gene expression differences in blood cells of patients with CAA. Genes assembled into a prediction panel were able to distinguish CAA from control patients. Genes of interest present in the prediction model suggest that immune system responses may adapt or be dysregulated in CAA potentially due to impairments in beta-amyloid clearance associated with peripheral immune cell alterations. These changes in immune responses demonstrated in CAA may alter brain health and potentially contribute to cognitive decline. With further evaluation in larger cohorts, gene expression profiles may offer diagnostic information in identifying CAA. Development of blood-based gene expression biomarkers are appealing as a tool in identifying CAA, as they are minimally invasive, and do not rely on access to magnetic resonance imaging.

## **2.6 Figures and Tables**

**Table 1.1:** Patient Demographics in patients with cerebral amyloid angiopathy compared to controls

	CAA n=27	Control n=55	P-value
Mean Age (years $\pm$ SD)	74.9 ( $\pm$ 7.34)	72.6 ( $\pm$ 11.6)	$1.64 \times 10^{-1}$
Sex Female, n (%)	14 (51.8)	31 (56.4)	$7.03 \times 10^{-1}$
Hypertension, n (%)	17 (63.0)	27 (49.0)	$2.41 \times 10^{-1}$
Diabetes, n (%)	3 (11.1)	7 (11.1)	$8.38 \times 10^{-1}$
Average CAA-SVD Score 0-4*	3.65 ( $\pm$ 1.20)	0.37 ( $\pm$ 0.67)	$3.38 \times 10^{-11}$
Years of Education ( $\pm$ SD)	14.5 ( $\pm$ 3.67)	16.1 ( $\pm$ 3.37)	$6.90 \times 10^{-2}$
Average White Matter Hyperintensity Volume corrected for	29.9 ( $\pm$ 23.6)	4.75 ( $\pm$ 4.71)	$4.28 \times 10^{-5}$

Intracranial Volume (cm <sup>3</sup> ±SD)			
Average Perivascular Space Score (Wardlaw scale) in Basal Ganglia at Baseline (0-4)**	1.90 (±0.83)	1.57 (±0.65) s	1.30x10 <sup>-2</sup>
Average Perivascular Space score (Wardlaw scale) in Centrum Semiovale (0-4)**	2.23 (±1.0)	1.31 (±0.63)	8.78x10 <sup>-5</sup>
Average Cerebral Microbleed Count	34.4 (±85.6)	0.11 (±0.32)	5.70x10 <sup>-2</sup>
cSS present, n (%)	12 (57.1%)	0 (0%)	1.42x10 <sup>-8</sup>
cSS focal, n (%)	5 (23.8%)	0 (0%)	3.00x10 <sup>-2</sup>
cSS disseminated, n (%)	7 (33.3%)	0 (0%)	8.29x10 <sup>-5</sup>

Values are mean ± standard deviation. \*Cerebral amyloid angiopathy small vessel disease score (CAA-SVD Score) as in Charidimou et al [253]. \*\*Enlarged perivascular spaces (EPVS) were scored using the Wardlaw score [254] on T2-weighted MRI were separated based on levels (0-4); level 0 being absent, level 1 (1-10 EPVS), level 2 (11-20 EPVS), level 3 (21-40 EPVS), and level 4 (>40 EPVS).

**Table 1.2:** Differentially expressed gene list comparing patients with cerebral amyloid angiopathy (CAA) and controls (CTL)

Gene Name	Fold Change Directionality	Fold Change (CAA vs CTL)	P-value
<i>ADAM15</i>	CAA down vs CTL	-1.28	3.72x10 <sup>-3</sup>
<i>TGFBI</i>	CAA down vs CTL	-1.29	4.02x10 <sup>-3</sup>
<i>CAP1</i>	CAA down vs CTL	-1.30	2.52x10 <sup>-4</sup>
<i>BRI3BP</i>	CAA down vs CTL	-1.35	4.56x10 <sup>-4</sup>
<i>POR</i>	CAA down vs CTL	-1.35	2.15x10 <sup>-4</sup>
<i>IL1B</i>	CAA down vs CTL	-1.33	6.45x10 <sup>-3</sup>
<i>CAMK1D</i>	CAA down vs CTL	-1.32	1.10x10 <sup>-3</sup>
<i>SORCS3</i>	CAA up vs CTL	2.30	1.00x10 <sup>-3</sup>
<i>PSMD2</i>	CAA down vs CTL	-1.27	1.71x10 <sup>-3</sup>

**Table 1.3:** Canonical pathways determined from differentially expressed genes in patients with cerebral amyloid angiopathy compared to controls

Canonical Pathway	Associated Genes	-log (p-value)
Activation of phagocytes	<i>ABHD12, ARG1, CD274, CD93, CERK, CSF1R, CST3, CXCL5, HMOX1, IDO1, IL1B, LGALS3BP, LGALS9B, MAP2K2, MT-CO1, MT-CYB, MT-ND2, MT-ND4, MT-ND5, MT-ND6,</i>	3.06

	<i>S100A12, S100A8, SPHK1, STAT3, TGFB1, TIMD4, TNFAIP8L2, TRAF3IP2</i>	
Cell movement of phagocytes	<i>ACKR2, ADAM15, ARG1, CAMK1D, CCR3, CD274, CLEC11A, CMKLR1, CSF1R, CST3, CTSZ, CXCL5, DIAPH1, FLNA, GDF15, GPSM1, GSK3B, GSN, HMOX1, IL15RA, IL1B, ILK, JAK1, MARCO, MMP8, PLGRKT, PTGDS, RIN3, S100A12, S100A8, SGK1, SPHK1, STAB1, STAT3, TERC, TGFB1, TNC, TNFAIP8L2, TNFRSF21, TPSAB1/TPSB2, TRAF3IP2, TRIO</i>	3.15
CREB Signaling	<i>ACKR4, ADCY6, ADGRE1, ADGRE3, CCR3, CMKLR1, FGFR2, GNB1L, GPR137, GRB2, GRID1, GRIK1, GRIN2B, MAP2K2, P2RY2, PIK3R6, PRKACA, PTGIR, SSTR2, TGFB1</i>	0.767
Degranulation of leukocytes	<i>ADGRE3, AGPAT2, ARG1, CAPI, CAPN1, CCR3, CD274, CD93, CST3, CTSH, CTSZ, CYB5R3, DIAPH1, FABP5, GSN, GSTP1, HLA-C, HMOX1, IL1B, INPP5B, MLEC, MMP8, ORAI2, P2RX4, PGAM1, PI4K2A, PRAM1, PSMD2, PSMD7, PTGDS, RHOF, S100A12, S100A8, SNAP29, SPHK1, STK10, TGFB1, TNFAIP6, UBR4, VCL</i>	5.70
Degranulation of phagocytes	<i>ADGRE3, AGPAT2, ARG1, CAPI, CAPN1, CCR3, CD93, CST3, CTSH, CTSZ, CYB5R3, DIAPH1, FABP5, GSN, GSTP1, HLA-C, HMOX1, IL1B, INPP5B, MLEC, MMP8, ORAI2, P2RX4, PGAM1, PRAM1, PSMD2, PSMD7, PTGDS, RHOF, S100A12, S100A8, SNAP29, SPHK1, STK10, TNFAIP6, UBR4, VCL</i>	5.72
Immune response of cells	<i>ABCF1, ARG1, BAK1, BAX, CAMK1D, CD274, CD93, CERK, CERS2, CSF1R, CST3, EIF4EBP1, ELF3, ELMO1, ELOVL1, FLNA, FSTL1, GP1BA, GRB2, GSN, HMOX1, IL15RA, IL1B, JAK1, LILRB1, MARCO, MYO1G, PRKAA2, PRKX, RELB, S100A12, S100A8, SGK1, SIGLEC1, SPHK1, STAT3, TGFB1, TIMD4, TLE3, TRAF3IP2, TRIM24, TRIM65, XRCC1</i>	3.45
Inflammatory response	<i>ABCF1, ABHD12, ACER3, ACKR2, ALDH2, ARG1, BAP1, BRD4, CAMK1D, CCR3, CD274, CMKLR1, CR2, CSF1R, CST3, CXCL5, DIAPH1, ELMO1, F12, FEM1A, GGT1, GPS2, GPSM1, GSK3B, GSN, HMOX1, IDO1, IL17RC, IL1B, LGALS3BP, LGALS9B, MAP2K2, MARCO, MMP8, MT-CO1, MT-CYB, MT-ND2, MT-ND4, MT-ND5, MT-ND6, NFKB2, NKIRAS2, PLGRKT, PRDX5, RIN3, S100A12, S100A8, SASH3, SPHK1, STAT3, TGFB1, TIMD4, TNC, TNFAIP6, TNFAIP8L2, TPSAB1/TPSB2, TPST1, TRAF3IP2</i>	4.23
IL-23 Signaling	<i>IL1B, NFKB2, PIK3R6, RELB, STAT3</i>	2.17

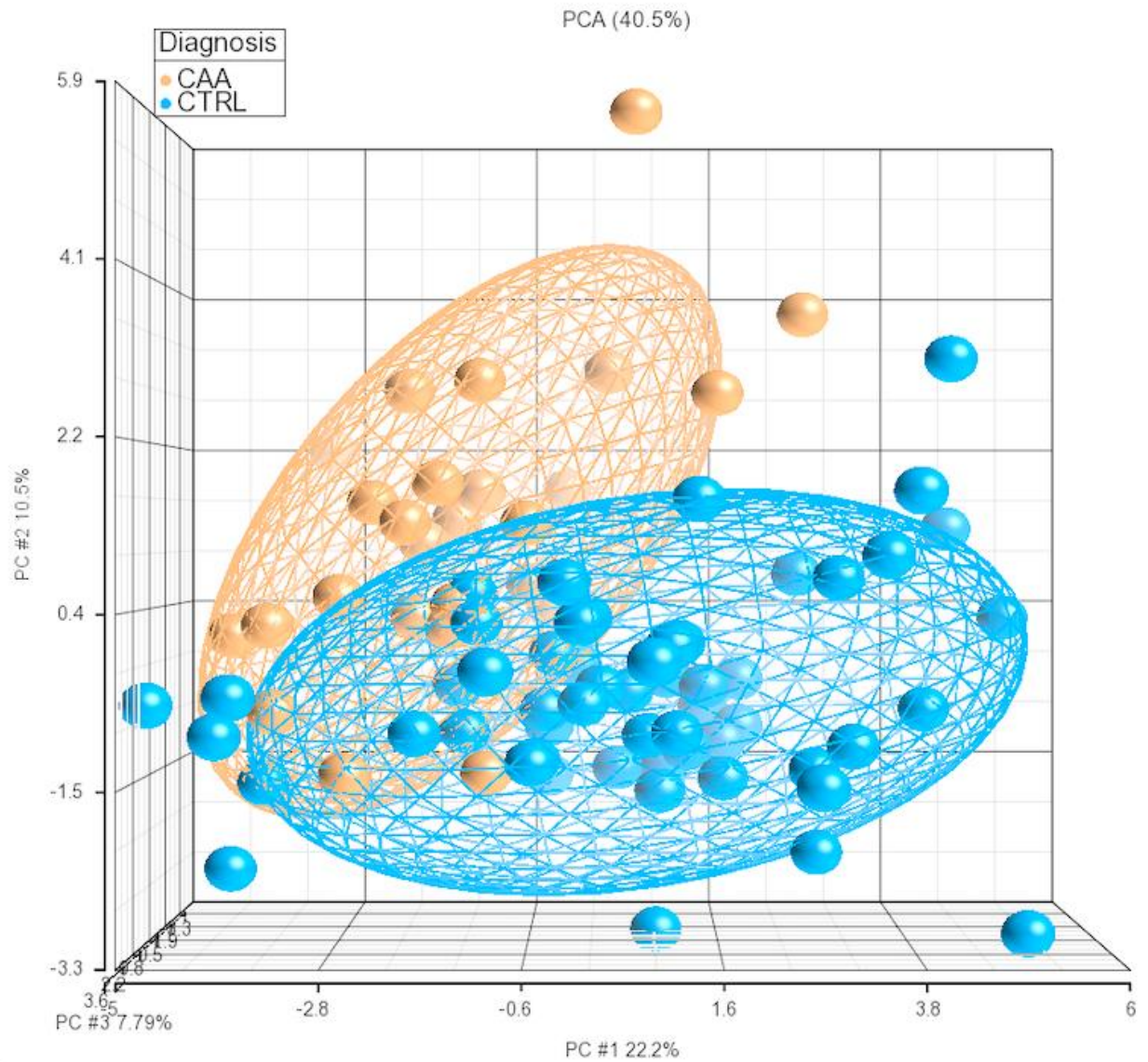


**Figure 1.1:** Principal components analysis of the 24 genes found to differentiate patients with cerebral amyloid angiopathy from control patients. Each sphere represents a single patient. CAA patients are shown in orange and control patients in blue. The ellipsoid represents 2 standard deviations from the group mean.

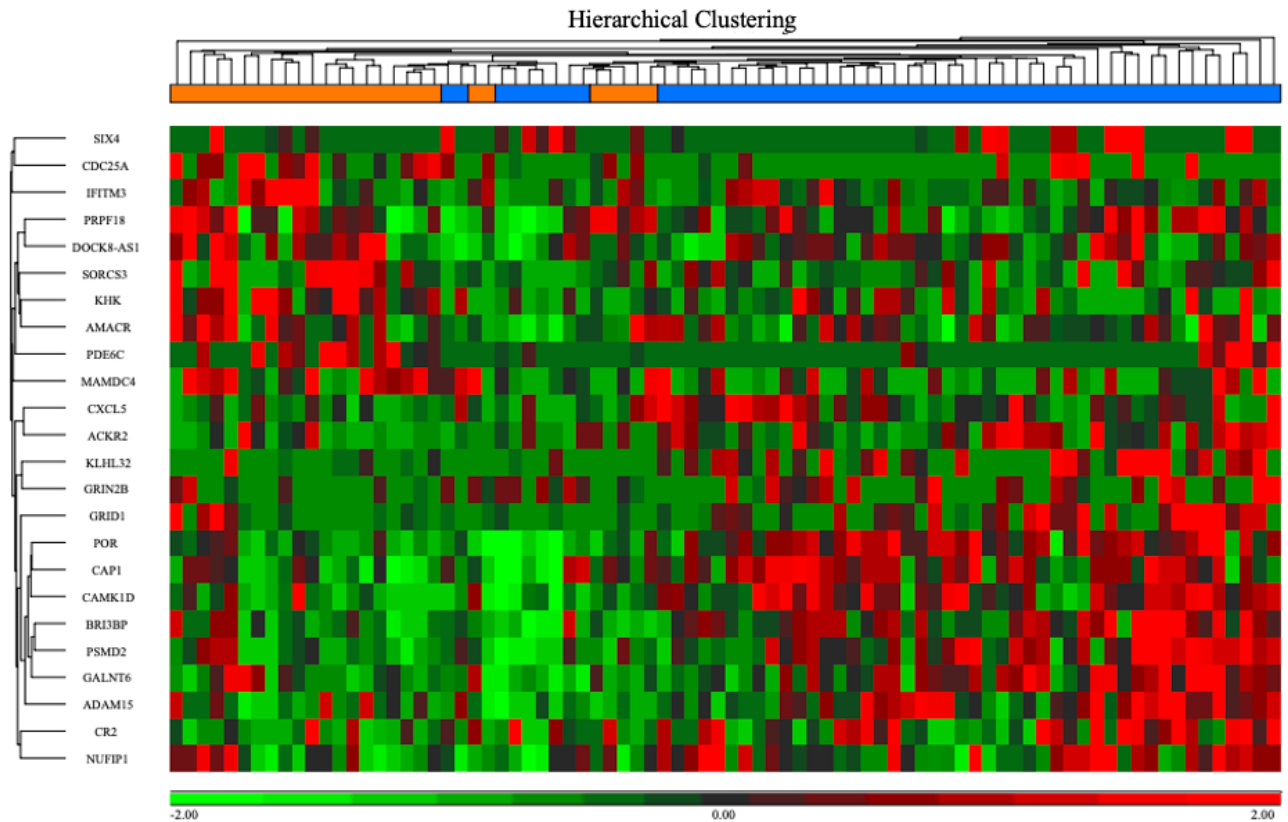


**Figure 1.2:** Hierarchical cluster plot of the 24 genes differentially expressed in patients with cerebral amyloid angiopathy compared to control patients. Genes are displayed on the y-axis and subjects are shown on the x-axis with CAA patients in orange and control patients in blue. Subjects are clustered by diagnosis. Upregulated genes are indicated in red, and downregulated genes are indicated in green. One group of genes has low expression in CAA and high expression in controls. Another group of genes has high expression in CAA and low expression in controls. The control group may cluster into two subgroups. Genes listed on the left from top to bottom are *SIX4*, *CDC25A*, *IFITM3*, *PRPF18*, *DOCK8-AS1*, *SORCS3*, *KHK*, *AMACR*, *PDE6C*, *MAMDC4*, *CXCL5*, *ACKR2*, *KLHL32*, *GRIN2B*, *GRID1*, *POR*, *CAPI*, *CAMK1D*, *BRI3BP*, *PSMD2*, *GALANT6*, *ADAM15*, *CR2*, *NUFIP1*.

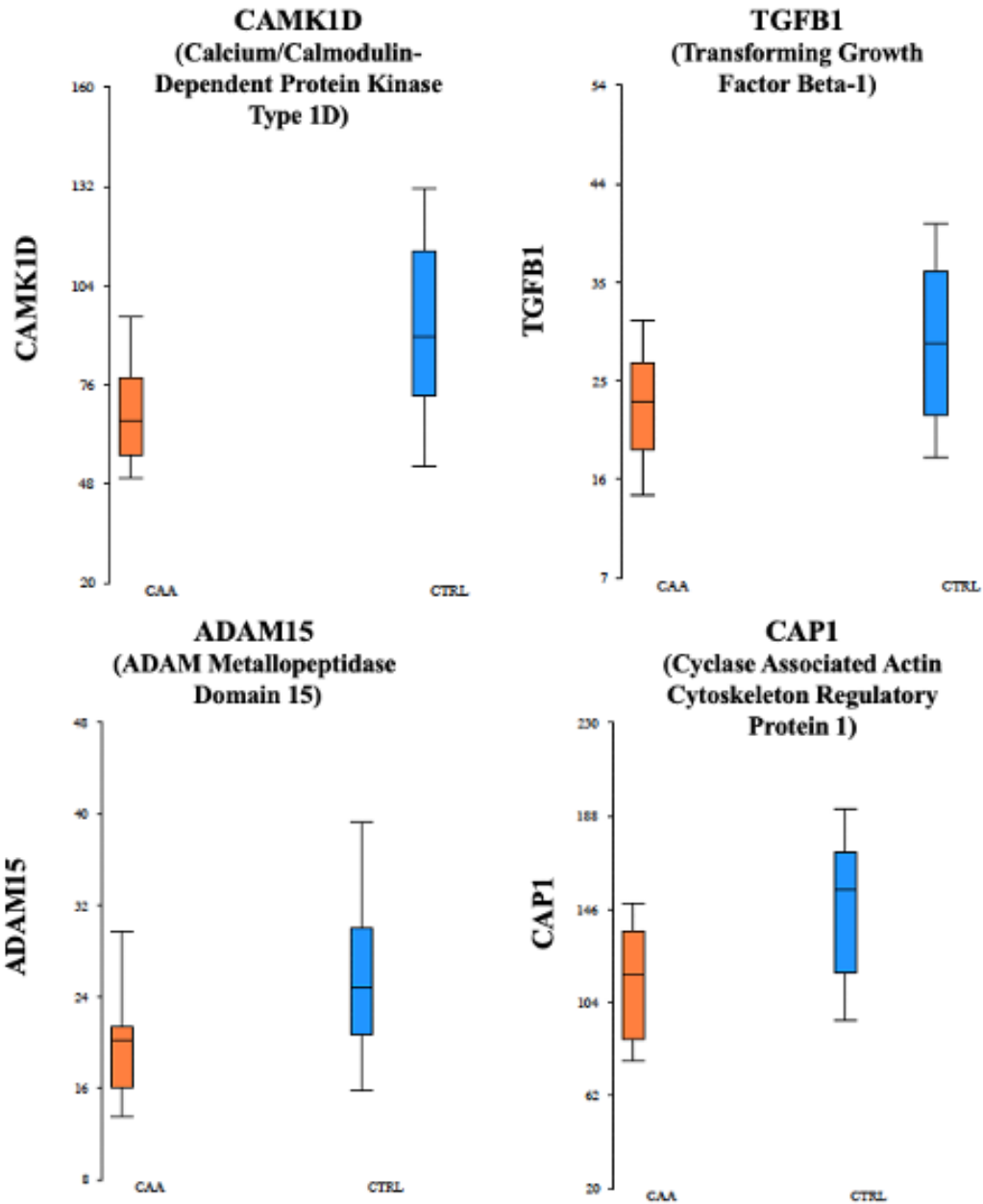


**Figure 1.3:** Box Plots of select differentially expressed genes comparing patients with cerebral amyloid angiopathy in orange and controls in blue ( $p < 0.05$ , fold change  $> |1.2|$ ).

### ***Chapter 3: Transcriptomic changes in peripheral blood leukocytes associated with cerebral amyloid angiopathy severity***

#### **3.1 Abstract**

**Background:** Cerebral amyloid angiopathy (CAA) is a cerebrovascular disease characterized by beta-amyloid deposition within cerebral vessels. Clinical markers of CAA severity include recurrent ICH, cognitive decline, and imaging features of CAA including microhemorrhage, dilated perivascular spaces, cortical superficial siderosis, and white matter hyperintensities. CAA is an important cause of cognitive decline and intracerebral hemorrhage in the elderly, leading to the need for CAA treatments. The contribution of the immune system to CAA severity is not well understood. This study sought to evaluate changes in peripheral leukocyte gene expression associated with CAA severity.

**Methods:** In 22 patients with CAA peripheral blood was collected into PAXgene tubes. RNA was isolated, and sequencing performed. Differentially expressed genes based on CAA small vessel disease (CAA-SVD) score as a marker of CAA severity were identified using ANOVA and functional pathway analysis. Memory, executive function, and processing speed were expressed as z-scores in relation to norms provided by test manuals. The relationship between gene expression, cognitive scores and CAA severity were assessed.

**Results:** Analysis of variance (ANOVA) was used to identify genes that were associated with CAA-SVD score ( $p \leq 0.05$ , partial correlation coefficient  $\geq |0.5|$ ). *HDAC11*, *IL23A*, *TRAIL*, *TRAILR1*, *TRAILR2*, and *ICAM-1* were associated with CAA severity (CAA-SVD score). Canonical pathway analysis identified included induction of T lymphocytes, binding of antigen



presentation cells, IL-12 signaling in macrophages/monocytes, activation of phagocytes, tight junction signaling, and activation of antigen presenting cells to be associated with CAA severity ( $p \leq 0.05$ ). Several genes associated with CAA severity were also associated with cognitive decline including a decrease in memory and executive functioning.

**Conclusions:** An association between the peripheral immune system and CAA severity was identified. Changes in neutrophil, monocyte, and Th17 cell gene expression in peripheral blood was associated with CAA severity. Further evaluation of immune system changes associated with CAA severity is needed to understand contribution to cerebral small vessel disease, cognitive decline, and potential roles as treatment targets or risk stratification markers in CAA.

### **3.2 Introduction**

CAA is an important cause of intracerebral hemorrhage (ICH), cognitive decline, and mortality [255-259]. The severity of CAA can be assessed using imaging features associated with CAA. These have been summarized into the CAA small vessel disease (CAA-SVD) score which is comprised of lobar cerebral microbleeds, cortical superficial siderosis, centrum semiovale perivascular spaces, and white matter hyperintensities [256]. The CAA-SVD score is associated with severity of vascular pathology [258]. Evidence demonstrates an association between the CAA-SVD score and cognitive function [260]. Patients with CAA also had lower scores in memory, executive function, and processing speed compared to norms [261]. In CAA patients with lobar ICH, higher CAA-SVD scores predicted recurrent ICH [258]. As such, patients with increased CAA severity have greater cognitive impairment and are at increased risk of ICH [258, 262, 263]. In this study we evaluated the relationship of blood cell gene expression to CAA severity to ascertain whether features of the immune system may relate to severity of CAA and cognitive parameters.

The relationship between CAA and the immune system is not well understood. Changes in peripheral leukocyte gene expression have been indicated in ischemic and hemorrhagic stroke, and white matter disease which are clinical features of CAA [30, 96, 98, 195-203]. Few studies have examined peripheral leukocytes in relation to CAA. In Alzheimer's disease (AD) peripheral monocytes have a proposed role in the clearance of beta-amyloid [108, 124]. Beta-amyloid from the brain may be taken up by circulating leukocytes and cleared in the kidney or liver [32, 52, 56, 57, 75, 76, 125-127, 129]. Indeed, a decrease in leukocyte phagocytosis of beta-amyloid increases vascular beta-amyloid in AD [108, 122-124]. In CAA leukocytes may have a similar contribution that may relate to severity of CAA.

In this study we examined differences in peripheral leukocyte gene expression associated with CAA severity. Involving induction of T lymphocytes, binding of antigen presentation cells, IL-12 signaling in macrophages, activation of phagocytes, tight junction signaling, and activation of antigen presenting cells pathways. Specific genes of interest implicated in peripheral leukocyte activation include *HDAC11*, *IL23A*, *TRAIL*, *TRAILR1*, *TRAILR2* and *ICAM-1*. This supports immune system involvement specific to CAA pathogenesis. Such differences could elucidate novel biomarkers associated with CAA. Further, novel biomarkers specific to CAA may also be potential therapeutic targets for slowing CAA progression and reduction of bleeding events. Early detection of biomarkers associated with severity could be targeted to therapeutically slow progression, reduce risk of ICH, cognitive decline, and CAA related mortality. This could provide value, in offering potential novel therapeutic targets in CAA.

### **3.3 Methods**

#### **Patients**

The study protocol was approved by the University of Alberta Health Research Ethics Board and University of Calgary Conjoint Health Research Ethics Board with each subject providing informed written consent. There were 22 patients with CAA recruited from the University of Alberta and the University of Calgary between 2016 and 2020. Participants were recruited from cognitive clinic or stroke prevention clinic. Probable CAA diagnosis was made by consensus of two board-certified neurologists using the Modified Boston Criteria on brain MRI [23]. CAA-SVD scores were determined by a board-certified neurologist and were utilized as a marker of CAA-severity scored from 0 to 6 [256]. Patients with lymphoma, leukemia, active infection, treatment with immunomodulating therapy were not included in the study.

### Sample Processing and RNA Isolation

Peripheral blood was collected by venipuncture into PAXgene tubes and stored at room temperature for 2 hours prior to being frozen at  $-80^{\circ}$  until RNA extraction. All samples were processed for RNA extraction in the same laboratory. Total RNA was isolated from PAXgene tubes using PAXgene Blood RNA kit (PreAnalytiX, Switzerland). RNA integrity and concentration was analyzed using the Agilent 2100 Bioanalyzer (Agilent, Santa Clara USA) and Nanodrop (Thermo Fisher Scientific, USA). Samples had an RNA integrity number (RIN)  $\geq 7.5$  and an  $A_{260}/A_{280}$  absorbance ratio of  $\geq 1.8$ .

### cDNA Library Preparation

RNA samples were processed using QuantSeq 3' mRNA-Seq Library Prep Kit FWD with Unique Dual Indices for cDNA library generation (Lexogen, Austria). Globin Block (RS-Globin Block) was used to prevent the generation of library fragments from globin mRNAs. cDNA library generation was initiated with 113ng RNA undergoing oligodT priming during strand synthesis and subsequent magnetic bead purification. PCR cycle optimization was performed by qPCR assay, and Lexogen 12nt Unique Dual Indices were incorporated during amplification.

### RNA Sequencing and Analysis

Samples were sequenced by Illumina NovaSeq6000 sequencing. RNA sequencing (RNAseq) analysis was performed using the QuantSeq 3' mRNA-Seq pipeline in Partek Flow Bioinformatics software (Partek Inc., St. Louis, MO). Raw reads were trimmed for quality (Phred score  $>37$ ), and adapters and unique dual indexing sequences were removed. Sequences

were aligned to the human genome (hg38) using the STAR2.5.3a aligner. Reads were normalized using transcripts per kilobase million.

### Cognitive Assessments

The National Institute for Neurological Diseases and Stroke-Canadian Stroke Network test battery was used for neuropsychological assessment as previously described by Case et al [261, 264]. The test battery included Trail Making A (TMT-A) and B (TMT-B), Controlled Oral Word Association Test-FAS (COWAT-FAS), Digit Symbol Coding (DSC) subtest of the WAIS-IV, Rey-Osterrieth Complex Figure Test (ROCFT), and verbal learning and memory (California Verbal Learning Test – CVLT-II) [265-269]. Neuropsychological tests were assessed based on three domains including episodic memory (average of the delayed recall portions of the CBLT-II and ROCFT), executive function (average of the TMT-B and COWAT-FAS), perceptual and processing speed (average of the DSC and TMT-A) [261].

### Statistical Analysis

Partek Genomics Suite was used for statistical analysis. Differential gene expression based on CAA severity (CAA-SVD score) was assessed using ANOVA. Genes considered to be associated with CAA severity had a  $p\text{-value} \leq 0.05$  and partial correlation coefficient  $r \geq |0.5|$ . Genes significantly associated with CAA severity were evaluated using Ingenuity Pathway Analysis to identify enriched functional pathways from our gene list (IPA, Ingenuity Systems, QIAGEN). Pathways were determined to be enriched using Fisher's exact test  $p \leq 0.05$  and a Benjamini-Hochberg false discovery rate (FDR  $< 0.05$ ) multiple comparisons correction. Genes of interest were not found to be independently associated with age, sex, or other vascular risk

factors. Neuropsychological test scores were converted to z-scores after adjusting for age, sex, and years of education based on normative data in the test manuals as previously described by Case et al [261]. A 1-sample *t*-test was used to identify differences from published norms. Cognitive tests were grouped into 3 domains including episodic memory (average of the delayed recall portions of the CVLT-II and ROCFT), executive function (average of the TMT-B and COWAT-FAS), and perceptual processing speed (average of the DSC and TMT-A). A mean z-score of  $\leq 1$  was considered to indicate cognitive impairment.

### **3.4 Results**

#### *Patient demographics*

Characteristics of patients with CAA are displayed in Table 2.1. The mean age of patients with CAA was 74.0 ( $\pm 6.14$ ) years, with 11 (50%) being female, 14 (64%) having hypertension, 2 (9%) having diabetes. The average CAA-SVD score being 3.5 ( $\pm 1.30$ ), the average white matter hyperintensity volume corrected for intracranial volume being 28.8 cm<sup>3</sup> ( $\pm 23.8$ ), and the average cerebral microbleed count being 33.0 ( $\pm 83.8$ ). The average perivascular space score (Wardlaw scale) in the basal ganglia at baseline was 1.91 ( $\pm 0.82$ ) and the average perivascular space score (Wardlaw scale) in the centrum semiovale was 2.23 ( $\pm 0.97$ ). Of the 22 CAA patients, 12 (55%) of the patients had cortical superficial siderosis (cSS), with 7 (32%) having disseminated cSS, and 5 (23%) having focal cSS.

#### *Differential RNA Expression associated with CAA Severity*

There were 414 genes associated with CAA-SVD score identified from peripheral blood ( $p \leq 0.05$ ,  $r \geq |0.5|$ ) (Table S2.1). 284 genes were positively associated with CAA severity,

including *IL23A* ( $p=0.003$ ,  $r=0.61$ ), *TRAILR1* ( $p=0.004$ ,  $r=0.59$ ), *TRAILR2* ( $p=0.02$ ,  $r=0.51$ ) (Table 2.2). 130 genes were negatively associated with CAA severity, including *HDAC11* ( $p=0.006$ ,  $r=-0.56$ ), *TRAIL* ( $p=0.02$ ,  $r=-0.50$ ) and *ICAM-1* ( $p=0.004$ ,  $r=-0.61$ ) (Table 2.2). These genes of interest demonstrate differences in leukocyte gene expression associated with CAA-SVD score.

### *Functional Pathway Analysis*

There were 414 genes that were associated with CAA severity ( $p \leq 0.05$ ,  $r \geq |0.5|$ ) (Table S2.1). Of these genes, 284 were positively associated with CAA severity and 130 were negatively associated with CAA severity. Functional pathway analysis utilizing this gene list of differentially expressed genes identified pathways associated with severe CAA. Enriched signaling pathways associated with CAA severity ( $p < 0.05$ ) are shown in Table 2.3. Genes of interest were indicated to be involved in these enriched signaling pathways. Functional pathways found to be enriched based on associations with CAA severity (CAA-SVD score) included induction of T lymphocytes (*IL23*), binding of antigen presentation cells (*ICAM1*), IL-12 signaling in macrophages (*IL23*), activation of phagocytes (*C5*, *ICAM1*, *IL23*, *TRAIL2R*), and activation of antigen presenting cells (*ICAM1*, *IL23*, *TRAIL2R*) (Table 2.3).

### *Cognitive Assessments*

Several of the genes of interest were associated with a decrease in cognitive performance compared to norms ( $z\text{-score} \leq 1.0$ ) including ICAM-1, TRAIL, and TRAIL2. Low ICAM-1 expression was associated with CAA severity (Figure 2.2). CAA patients expressing low ICAM-1 also demonstrated poorer executive functioning on cognitive assessments compared to norms

(z-score -1.73). CAA patients expressing low TRAIL, had decreased memory (z-score -1.71) and executive functioning (z-score -1.47). In patients with moderate to severe CAA (CAA-SVD score >3) and increased TRAIL2R expression, memory (z-score -2.28), executive function (z-score -1.82) and processing speed scores (z-score -1.14) were all decreased compared to norms.

### **3.5 Discussion**

Differences in blood cell gene expression by CAA severity were identified. Genes associated with CAA severity include *HDAC11*, *IL23A*, *TRAIL*, *TRAILR1*, *TRAILR2*, and *ICAM-1*. Pathway analysis revealed enrichment in signaling related to induction of T lymphocytes, binding and activation of antigen presentation cells, IL-12 signaling in monocytes/macrophages, and activation of phagocytes. The functional effects of these genes in CAA requires further study but highlight immune system differences in patients with CAA related to severity that may have potential to slow progression of CAA or stratify CAA severity.

CAA severity can be assessed by neuropathological evaluation or neuroimaging. Both have limitations. Neuropathology can only be performed post-mortem. Neuroimaging findings associated with CAA severity including white matter hyperintensities, enlarged perivascular spaces (PVS) on MRI, lobar lacunes, and cortical microinfarcts [270, 271]. The total CAA-SVD score is also associated with CAA related vasculopathic changes and severe CAA presentations including symptomatic ICH, supporting the use of the CAA-SVD score as a marker of CAA severity [253]. CAA severity represented by the (CAA-SVD) score is associated with both cognitive decline and recurrent ICH [258, 260, 262, 263]. Thus, risk stratification markers of CAA severity could provide utility in identifying patients at risk of severe CAA related outcomes and cognitive decline. However, there are presently no blood-based biomarkers associated with



CAA-severity. Investigation of potential peripheral immune system involvement related to CAA severity may provide insights into mechanisms underlying CAA progression and present novel risk stratification biomarkers. Changes in immune system responses may be contributing to cognitive decline and severe CAA presentations including ICH. Evaluation of immune cell interactions associated with CAA severity could reveal novel targets for future therapies aimed at slowing CAA progression. This study sought to evaluate changes in peripheral leukocyte gene expression associated with CAA severity based on the CAA-SVD score.

A reduction in *HDAC11* expression was associated with increasing CAA severity (Table 2.2). HDAC11 is a histone deacetylase that regulates gene expression at an epigenetic level [272, 273]. Modulation of HDAC11 has been suggested as a therapeutic strategy for diseases involving autoimmunity, neurodegeneration, and chronic inflammation [272, 274, 275]. HDAC11 regulates neutrophil differentiation, and HDAC11 deficient neutrophils demonstrate a pro-inflammatory phenotype with enhanced migration and phagocytosis abilities [273]. Neutrophils with an inflammatory and phagocytic phenotype in CAA are supported by CAA severity being associated with pathways of phagocyte activation, and activation of antigen presenting cells (Table 2.3). These signaling pathways include genes related to neutrophil recruitment and activity associated with CAA severity including *ICAM-1*, *MYD88*, *TRAILR2*, *IL27*, and *C5* (Table 2.3). Potential for neutrophil phagocytosis of beta-amyloid in the peripheral blood is further supported by evidence demonstrating neutrophils co-localize with beta-amyloid in AD mice, beta-amyloid clearance was increased upon targeting increased C5 signaling in neutrophils, and C5a receptor agonists in AD mice increased phagocytosis of beta-amyloid by neutrophils [101, 276, 277]. A decrease in ICAM-1 was also associated with CAA severity (Figure 2.2). CAA patients expressing low ICAM-1 also demonstrated poorer executive

functioning on cognitive assessments compared to norms (z-score -1.73). ICAM-1 is an adhesion molecule required for neutrophil infiltration across the blood brain barrier into brain [30, 278, 279]. A reduction in ICAM-1 associated with CAA severity may have a role in impaired clearance of beta-amyloid due to altered neutrophil responses which may be linked to changes in cognitive functioning. Further investigation of HDAC11 in inflammatory neutrophils in relation to CAA severity is warranted to ascertain whether targeting of neutrophil phenotypes and phagocytic activity may have potential as a therapeutic strategy for CAA.

TRAIL was decreased in patients with more severe CAA (Table 2.2). TRAIL is expressed by monocytes, neutrophils, natural killer cells and natural killer T-cells [280-283]. TRAIL binds TRAILR1 and TRAILR2, both of which were associated with CAA severity [282, 284] (Table 2.2). While the role of TRAIL-TRAIL receptor interactions in CAA remains unclear, they are associated with inflammation, neurodegeneration and iNOS signaling [285]. iNOS signaling was also demonstrated to be associated with CAA severity (Table 2.2). Evidence suggests monocytes deficient in TRAIL demonstrated impaired functioning and a pro-inflammatory phenotype [286]. Additionally, TRAIL infusion in an AD mouse model resulted in reduced beta-amyloid deposition, improved cognition and reduced brain inflammation [287]. We also found CAA patients expressing low TRAIL, had decreased memory (z-score -1.71) and executive functioning (z-score -1.47). This further supports a link between TRAIL signalling in monocytes and CAA progression. In severe CAA, monocyte functioning may become dysregulated, potentially contributing to CAA pathogenesis and cognitive decline. While further studies are needed, blood monocytes with reduced TRAIL signaling may contribute to inflammation and cognitive decline in CAA. Future investigation of the interaction between

beta-amyloid and TRAIL signaling in blood leukocytes is of interest as this may provide a novel target for reducing inflammation and cognitive decline in CAA.

Increased expression of TRAILR2 (the TRAIL receptor) was also associated with CAA severity (Figure 2.2). TRAILR2 is highly expressed on monocyte cell surfaces and has opposing roles in the cell cycle [288-290]. Other genes associated with monocyte activation in relationship to CAA severity were *TRIM71*, *IL23*, and enriched IL-12 signaling (Table 2.3, Figure 2.2). These further indicate monocyte activation is altered in patients with severe CAA. In patients with moderate to severe CAA (CAA-SVD score >3) and increased TRAIL2R expression, memory (z-score -2.28), executive function (z-score -1.82) and processing speed scores (z-score -1.14) were all decreased compared to norms. This again suggests TRAIL signaling in monocytes may be implicated in cognitive decline associated with CAA severity. Monocytes may uptake beta-amyloid and contribute to its clearance from the blood in CAA, as has been described in AD [108, 130, 131]. Alternately, evidence suggests beta-amyloid may bind monocyte receptors and be shuttled to end organs such as the liver or kidneys for clearance from the blood [56, 76]. While clearance of beta-amyloid in CAA requires further study, investigation of monocyte activity and their role in beta amyloid clearance will be of interest as a potential strategy to treat CAA.

*IL23A* expression was increased in patients with more severe CAA (Figure 2.2). IL-23 is a pro-inflammatory cytokine produced by activated monocytes, macrophages, and dendritic cells [291-295]. IL-23 promotes differentiation of Th17 cells, a T cell subset implicated in chronic inflammation and peripheral leukocyte recruitment [294, 296-298]. Several pathways involving *IL23A* expression were associated with CAA severity, including induction of T lymphocytes, activation of phagocytes, and activation of antigen presenting cells (Table 2.3). *PGLYRP2* was

also associated with CAA severity, which limits overactivation of Th17 signaling, further supporting potential Th17 involvement in CAA [299]. In CAA the increase in IL-23 signaling may promote a shift towards Th17 cells in the peripheral blood, which may contribute to brain injury. Beta-amyloid can also stimulate Th17 cells through TLR1 and TLR2, further supporting potential for Th17 activity in CAA [107, 108]. As such, evaluation of IL-23 signaling and Th17 cells in CAA will be of interest as novel targets for CAA treatments may be identified.

Limitations of our discovery-based study include small cohort sizes, therefore future investigation and validation in larger cohorts is required. Although there were no statistically significant differences in age, sex, or vascular risk factors by severity of CAA, it remains possible that other factors could be involved. Due to the heterogenous nature of CAA, further evaluation of associations between peripheral leukocyte gene expression and individual imaging markers comprising the CAA-SVD score will be of interest. This could provide information about mechanisms contributing to each of these imaging findings. The role of peripheral leukocytes provides a novel contribution to CAA pathogenesis and thus justifies future investigation.

This study provides preliminary evidence that differences in peripheral leukocyte gene expression are associated with CAA severity. While further evaluation is needed, the peripheral immune system including neutrophils and monocytes may contribute to clearance of beta-amyloid, leading to decreased amyloid burden in the brain [32, 52, 56, 57, 75, 76, 125-127, 129]. Th17 cells may also contribute to inflammation and altered peripheral leukocytes responses in CAA. Alterations in immune cell gene expression were also related to changes in cognitive parameters, supporting a relationship of peripheral immune system to severity of CAA. Future investigation of peripheral leukocyte involvement in CAA is of value, as immune cell

interactions could be targeted to potentially enhance beta amyloid clearance, reduce inflammation and cognitive decline in patients with CAA.

### **3.6 Figures and Tables**

**Table 2.1:** Patient demographics in patients with cerebral amyloid angiopathy (n=22)

Mean Age (years $\pm$ SD)	74 ( $\pm$ 6.14)
Sex Female, n (%)	11 (50%)
Hypertension, n (%)	14 (64%)
Diabetes, n (%)	2 (9%)
Average Boston Criteria Score (0-6)	2 (0)
Average CAA-SVD Score (0-4)*	3.5 ( $\pm$ 1.30)
cSS present, n (%)	12 (55%)
cSS focal, n (%)	5 (23%)
cSS disseminated, n (%)	7 (32%)
Average White Matter Hyperintensity Volume corrected for Intracranial Volume ( $\text{cm}^3 \pm$ SD)	28.8 ( $\pm$ 23.8)
Average Perivascular Space Score (Wardlaw scale) in Basal Ganglia at Baseline (0-4)**	1.91 ( $\pm$ 0.82)
Average Perivascular Space score (Wardlaw scale) in Centrum Semiovale (0-4)**	2.23 ( $\pm$ 0.97)
Average Cerebral Microbleed Count ( $\pm$ SD)	33.0 ( $\pm$ 83.8)

Values are mean  $\pm$  the standard deviation. \* Cerebral amyloid angiopathy small vessel disease score (CAA-SVD Score) as in Charidimou et al [253]. \*\*Enlarged perivascular spaces (EPVS) were scored using the Wardlaw score [254] on T2-weighted MRI were separated based on levels (0-4); level 0 being absent, level 1 (1-10 EPVS), level 2 (11-20 EPVS), level 3 (21-40 EPVS), and level 4 (>40 EPVS).

**Table 2.2** Biologically significant genes associated with CAA-severity (CAA-SVD score)

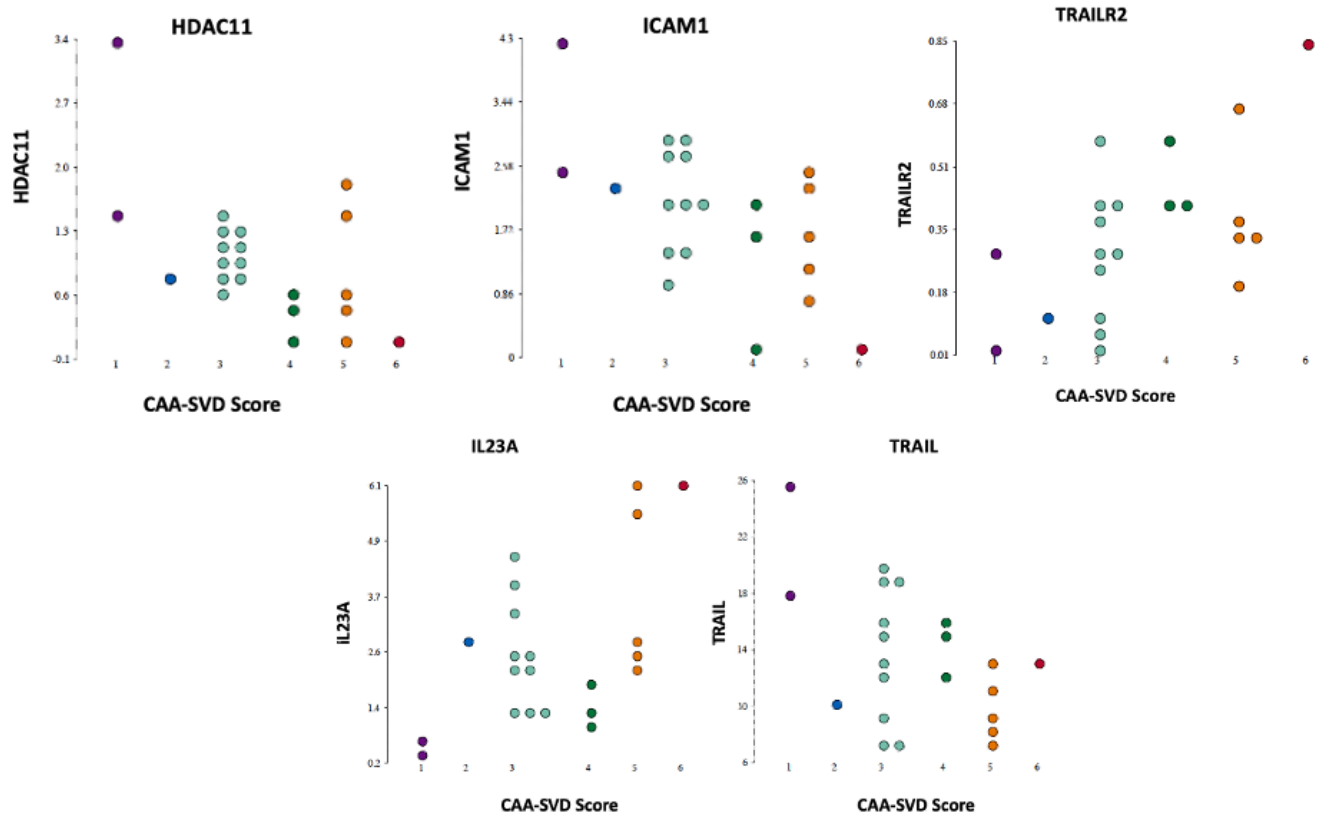
Gene Name	Partial Correlation Coefficient (r)	P-value
<i>IL23A</i>	0.61	0.00279
<i>HDAC11</i>	-0.56	0.00644
<i>TRAILR2</i>	0.51	0.01520
<i>TRAILR1</i>	0.59	0.00356
<i>ICAM1</i>	-0.61	0.00241
<i>TRAIL</i>	-0.50	0.01730
<i>PGLYRP2</i>	0.52	0.01220
<i>C5</i>	0.53	0.01050

**Table 2.3:** Biological pathways determined by ingenuity pathway analysis associated with CAA severity (CAA-SVD Score)

Functional Pathway	Associated Genes	-log(p-value)	Number of Associated Genes
Induction of T lymphocytes	<i>CD4, IL23A, IL27, MYD88, RELB</i>	2.65	5
Binding of Antigen Presentation Cells	<i>ALOX15, CD4, FCGR1A, ICAM1, PLAUI, RELB</i>	2.26	6
Tight junction Signaling	<i>BET1L, CLDN10, CLDN16, NECTIN2, RELB, STX1A</i>	1.33	6
IL-12 Signaling and Production in Macrophages	<i>ALOX15, IL23A, MAP2K1, MYD88, RELB</i>	1.31	5
Activation of Antigen Presenting Cells	<i>CD4, CRT3, FCGR1A, GDNF, ICAM1, IL23A, MAP2K1, MFN2, MYD88, PSMB8, RELB, SCN9A, SERPIN1, TNFRSF10B, TSHR, TSPAN32</i>	2.70	16
Activation of Phagocytes	<i>C5, CASR, CD4, CRT3, GDNF, ICAM1, IL23A, IL27, MAP2K1, MFN2, MYD88, NECTIN2, SCN9A, SERPIN1, TNFRSF10B, TSPAN32</i>	2.05	16

A Benjamini-Hochberg corrected  $p$ -value  $< 0.05$  corresponds to  $-\log_{10}$  (Benjamini-Hochberg corrected  $p$ -value)  $> 1.3$ .

**Figure 2.1:** Dot plots of select differentially expressed genes based on CAA-severity (CAA-SVD Score)



## ***Chapter 4: Conclusions and Future Directions***

### **4.1 Summary of Findings**

This study investigates changes in peripheral leukocyte gene expression that distinguishes CAA from control patients and is associated with CAA severity. Differences in gene expression delineating CAA from control patients included potential changes in beta-amyloid uptake by phagocytes (*TGFB1*, *CAMK1D*), extracellular matrix remodelling (*ADAM15*, *CAP1*), and potential alterations in amyloid precursor processing (*BRI3BP*, *SORCS3*). A panel of 24 genes differentially expressed in CAA demonstrate promise for distinguishing patients with CAA from controls. Differences in blood cell gene expression associated with CAA severity were identified. CAA severity associated genes included *HDAC11*, *IL23A*, *TRAIL*, *TRAILR1*, *TRAILR2*, and *ICAM-1*. Pathway analysis revealed enrichment in signaling related to induction of T lymphocytes, binding and activation of antigen presentation cells, IL-12 signaling in monocytes/macrophages, and activation of phagocytes. The functional effects of these genes require further evaluation but demonstrate differences in immune system responses in patients with CAA compared to controls and in relation to CAA severity.

### **4.2 Limitations**

Limitations of these discovery-based studies include small cohort sizes, thus future investigation and validation in larger cohorts is required. Although there were no significant differences in age, sex, or vascular risk factors between patients with CAA and controls or by CAA severity, it remains possible that other factors could be involved. Due to the heterogenous nature of CAA, further evaluation of gene expression changes associated with the CAA-SVD score and individual imaging markers will be of interest. Additionally, it is possible that



differences in mechanisms contributing to ischemic and hemorrhagic brain injury pathways may be associated with different immune responses [300]. Further study in larger cohorts is required, as there were limited patients on either end of the CAA-SVD score severity spectrum. In summary, the role of peripheral leukocytes provides a novel contribution to CAA pathogenesis and thus justifies future investigation in larger cohorts.

### **4.3 Future Directions**

Future investigation of peripheral gene expression changes in CAA is of clinical interest, as it could provide diagnostic or risk stratification information. Validation studies in larger cohorts assessing the utility of the 24 gene prediction model in identifying patients with CAA is warranted. Evaluation and validation of peripheral gene expression changes associated with CAA severity is justified, as this may provide insight into novel risk stratification markers of CAA. Further exploration of peripheral gene expression targets identified may shed insight into mechanisms of CAA progression which could be evaluated for potential as therapeutic targets for slowing CAA progression and cognitive decline. Protein level studies and investigation of the proposed gene targets of interest may also be of interest to explore their functional effects in CAA pathogenesis. Gene expression and protein level changes could also be evaluated in relation to cognitive changes over time in CAA populations, potentially broadening our understanding of pathways implicated in CAA related cognitive decline and progression. Investigation of gene expression changes associated with individual markers of CAA-severity could also provide information regarding the contribution of various features of the CAA-SVD score to CAA. Lastly, exploration of expression level changes over time associated with ischemic (microinfarcts, ischemic stroke, WMH progression) and hemorrhagic lesion burden

(ICH, CMBs, cSS) may be of clinical value in determining differences in immune contribution to brain injury present in CAA.

#### **4.4 Conclusions**

Immune system activation in cerebral amyloid angiopathy was explored through evaluation of changes in peripheral leukocyte gene expression. A gene expression profile was used to distinguish patients with CAA from control patients with a sensitivity and specificity >95%. Differences identified by the gene expression profile included changes in beta-amyloid uptake by phagocytes, structural changes to the extracellular matrix, and potentially altered amyloid precursor protein processing. Overall, this suggests altered peripheral immune cell responses may be contributing to CAA pathogenesis. With further investigation in larger cohorts, this gene expression profile could potentially provide useful diagnostic information in CAA. Alterations in leukocyte gene expression associated with CAA severity using the CAA-SVD score were also presented. These changes in immune cell gene expression could be beneficial in CAA risk stratification or identification of novel therapeutic targets. Alterations in peripheral blood T cell, monocyte, and neutrophil responses were associated with CAA severity supporting the contribution of altered blood immune cell activity in CAA. While this data was discovery based and requires validation, the alterations in immune responses identified could be further investigated for potential application in CAA diagnosis and risk stratification. Gene targets identified to be differentially expressed in CAA and associated with CAA severity offer insight into pathways contributing to CAA progression. These genes of interest and related signaling pathways could be further explored for potential therapeutic targets in future CAA treatments. Targeting of immune cell responses could provide clinical benefit in slowing CAA progression and cognitive decline.

## References

1. Greenberg, S.M., et al., *Cerebral amyloid angiopathy and Alzheimer disease - one peptide, two pathways*. Nature reviews. Neurology, 2020. **16**(1): p. 30-42.
2. Charidimou, A., et al., *Emerging concepts in sporadic cerebral amyloid angiopathy*. Brain : a journal of neurology, 2017. **140**(7): p. 1829-1850.
3. Esiri, M., et al., *Pathological correlates of late-onset dementia in a multicentre, community-based population in England and Wales*. Lancet, 2001.
4. Thal, D.R., et al., *Cerebral amyloid angiopathy and its relationship to Alzheimer's disease*. Acta neuropathologica, 2008. **115**(6): p. 599-609.
5. Auriel, E. and S.M. Greenberg, *The pathophysiology and clinical presentation of cerebral amyloid angiopathy*. Current atherosclerosis reports, 2012. **14**(4): p. 343-350.
6. Smith, E.E., et al., *Cerebral Amyloid Angiopathy–Related Transient Focal Neurologic Episodes*. Neurology, 2021. **97**(5): p. 231-238.
7. Greenberg, S.M. and J.-P.G. Vonsattel, *Diagnosis of cerebral amyloid angiopathy: sensitivity and specificity of cortical biopsy*. Stroke, 1997. **28**(7): p. 1418-1422.
8. Boyle, P.A., et al., *Person-specific contribution of neuropathologies to cognitive loss in old age*. Annals of neurology, 2018. **83**(1): p. 74-83.
9. Keage, H.A., et al., *Population studies of sporadic cerebral amyloid angiopathy and dementia: a systematic review*. BMC neurology, 2009. **9**(1): p. 1-8.
10. Jäkel, L., et al., *Prevalence of cerebral amyloid angiopathy: A systematic review and meta-analysis*. Alzheimer's & Dementia, 2022. **18**(1): p. 10-28.
11. van Etten, E.S., et al., *Recurrent hemorrhage risk and mortality in hereditary and sporadic cerebral amyloid angiopathy*. Neurology, 2016. **87**(14): p. 1482-1487.
12. Attems, J., et al., *Review: Sporadic cerebral amyloid angiopathy*. Neuropathology and Applied Neurobiology, 2011. **37**(1): p. 75-93.
13. Revesz, T., et al., *Sporadic and familial cerebral amyloid angiopathies*. Brain pathology, 2002. **12**(3): p. 343-357.
14. Nicoll, J.A., et al., *High frequency of apolipoprotein E  $\epsilon$ 2 allele in hemorrhage due to cerebral amyloid angiopathy*. Annals of neurology, 1997. **41**(6): p. 716-721.
15. Greenberg, S., et al., *Association of apolipoprotein E  $\epsilon$ 2 and vasculopathy in cerebral amyloid angiopathy*. Neurology, 1998. **50**(4): p. 961-965.
16. Greenberg, S.M., et al., *Apolipoprotein E  $\epsilon$ 4 and cerebral hemorrhage associated with amyloid angiopathy*. Annals of neurology, 1995. **38**(2): p. 254-259.
17. Greenberg, S.M. and J. Rosand, *Genetic associations with brain microbleeds: Systematic review and meta-analyses*. 2021.
18. O'Donnell, H.C., et al., *Apolipoprotein E genotype and the risk of recurrent lobar intracerebral hemorrhage*. New England Journal of Medicine, 2000. **342**(4): p. 240-245.
19. Rannikmäe, K., et al., *Genetics of cerebral amyloid angiopathy: systematic review and meta-analysis*. Journal of Neurology, Neurosurgery & Psychiatry, 2013. **84**(8): p. 901-908.
20. Biffi, A., et al., *Genetic variation at CR1 increases risk of cerebral amyloid angiopathy*. Neurology, 2012. **78**(5): p. 334-341.
21. Knudsen, K.A., et al., *Clinical diagnosis of cerebral amyloid angiopathy: Validation of the Boston Criteria*. Neurology, 2001. **56**(4): p. 537-539.

22. Linn, J., et al., *Prevalence of superficial siderosis in patients with cerebral amyloid angiopathy*. *Neurology*, 2010. **74**(17): p. 1346-1350.
23. Greenberg, S.M. and A. Charidimou, *Diagnosis of cerebral amyloid angiopathy: evolution of the Boston criteria*. *Stroke*, 2018. **49**(2): p. 491-497.
24. Bettcher, B.M., et al., *Peripheral and central immune system crosstalk in Alzheimer disease—a research prospectus*. *Nature Reviews Neurology*, 2021. **17**(11): p. 689-701.
25. Heppner, F.L., R.M. Ransohoff, and B. Becher, *Immune attack: the role of inflammation in Alzheimer disease*. *Nature Reviews Neuroscience*, 2015. **16**(6): p. 358-372.
26. Fu, Y., et al., *Immune interventions in stroke*. *Nature Reviews Neurology*, 2015. **11**(9): p. 524-535.
27. Sykes, G.P., et al., *Aging Immune System in Acute Ischemic Stroke: A Transcriptomic Analysis*. *Stroke*, 2021. **52**(4): p. 1355-1361.
28. Montaner, J., et al., *Multilevel omics for the discovery of biomarkers and therapeutic targets for stroke*. *Nature Reviews Neurology*, 2020. **16**(5): p. 247-264.
29. Jickling, G.C. and F.R. Sharp, *Improving the translation of animal ischemic stroke studies to humans*. *Metabolic brain disease*, 2015. **30**(2): p. 461-467.
30. Jickling, G.C., et al., *Targeting neutrophils in ischemic stroke: translational insights from experimental studies*. *Journal of Cerebral Blood Flow & Metabolism*, 2015. **35**(6): p. 888-901.
31. Revesz, T., et al., *Genetics and molecular pathogenesis of sporadic and hereditary cerebral amyloid angiopathies*. *Acta neuropathologica*, 2009. **118**(1): p. 115-130.
32. Tian, D.-Y., et al., *Physiological clearance of amyloid-beta by the kidney and its therapeutic potential for Alzheimer's disease*. *Molecular Psychiatry*, 2021. **26**(10): p. 6074-6082.
33. Sun, B.-l., et al., *Critical thinking on amyloid-beta-targeted therapy: challenges and perspectives*. *Science China Life Sciences*, 2021. **64**(6): p. 926-937.
34. Weller, R.O., et al., *Perivascular drainage of amyloid-beta peptides from the brain and its failure in cerebral amyloid angiopathy and Alzheimer's disease*. *Brain pathology (Zurich, Switzerland)*, 2008. **18**(2): p. 253-266.
35. Carare, R., et al., *cerebral amyloid angiopathy, prion angiopathy, CADASIL and the spectrum of protein elimination failure angiopathies (PEFA) in neurodegenerative disease with a focus on therapy*. *Neuropathology and applied neurobiology*, 2013. **39**(6): p. 593-611.
36. Carare, R.O., et al., *Solutes, but not cells, drain from the brain parenchyma along basement membranes of capillaries and arteries: significance for cerebral amyloid angiopathy and neuroimmunology*. *Neuropathology and Applied Neurobiology*, 2008. **34**(2): p. 131-144.
37. Albargothy, N.J., et al., *Convective influx/glymphatic system: tracers injected into the CSF enter and leave the brain along separate periarterial basement membrane pathways*. *Acta neuropathologica*, 2018. **136**(1): p. 139-152.
38. Keable, A., et al., *Deposition of amyloid  $\beta$  in the walls of human leptomeningeal arteries in relation to perivascular drainage pathways in cerebral amyloid angiopathy*. *Biochimica et biophysica acta*, 2016. **1862**(5): p. 1037-1046.
39. Iliff, J.J., et al., *A paravascular pathway facilitates CSF flow through the brain parenchyma and the clearance of interstitial solutes, including amyloid  $\beta$* . *Science translational medicine*, 2012. **4**(147): p. 147ra111-147ra111.

40. Benveniste, H., et al., *The glymphatic system and waste clearance with brain aging: a review*. Gerontology, 2019. **65**(2): p. 106-119.
41. Wisniewski, H. and J. Wegiel,  *$\beta$ -amyloid formation by myocytes of leptomeningeal vessels*. Acta neuropathologica, 1994. **87**(3): p. 233-241.
42. Frackowiak, J., et al., *Secretion and accumulation of  $A\beta$  by brain vascular smooth muscle cells from  $A\beta$ PP-Swedish transgenic mice*. Journal of Neuropathology & Experimental Neurology, 2003. **62**(6): p. 685-696.
43. Calhoun, M.E., et al., *Neuronal overexpression of mutant amyloid precursor protein results in prominent deposition of cerebrovascular amyloid*. Proceedings of the National Academy of Sciences, 1999. **96**(24): p. 14088-14093.
44. Herzig, M.C., et al.,  *$A\beta$  is targeted to the vasculature in a mouse model of hereditary cerebral hemorrhage with amyloidosis*. Nature neuroscience, 2004. **7**(9): p. 954-960.
45. Kakuda, N., et al., *Distinct deposition of amyloid- $\beta$  species in brains with Alzheimer's disease pathology visualized with MALDI imaging mass spectrometry*. Acta neuropathologica communications, 2017. **5**(1): p. 1-8.
46. Harigaya, Y., et al., *Amyloid  $\beta$  protein starting pyroglutamate at position 3 is a major component of the amyloid deposits in the Alzheimer's disease brain*. Biochemical and biophysical research communications, 2000. **276**(2): p. 422-427.
47. Revesz, T., et al., *Cerebral amyloid angiopathies: a pathologic, biochemical, and genetic view*. Journal of Neuropathology & Experimental Neurology, 2003. **62**(9): p. 885-898.
48. Wattendorff, A., et al., *Hereditary cerebral haemorrhage with amyloidosis, Dutch type (HCHWA-D): clinicopathological studies*. Journal of Neurology, Neurosurgery & Psychiatry, 1995. **58**(6): p. 699-705.
49. Tarasoff-Conway, J.M., et al., *Clearance systems in the brain—implications for Alzheimer disease*. Nature reviews neurology, 2015. **11**(8): p. 457-470.
50. Qosa, H., et al., *Differences in amyloid- $\beta$  clearance across mouse and human blood–brain barrier models: kinetic analysis and mechanistic modeling*. Neuropharmacology, 2014. **79**: p. 668-678.
51. Yuede, C.M., et al., *Rapid in vivo measurement of  $\beta$ -amyloid reveals biphasic clearance kinetics in an Alzheimer's mouse model*. Journal of Experimental Medicine, 2016. **213**(5): p. 677-685.
52. Xiang, Y., et al., *Physiological amyloid-beta clearance in the periphery and its therapeutic potential for Alzheimer's disease*. Acta neuropathologica, 2015. **130**(4): p. 487-499.
53. Silverberg, G.D., et al., *Amyloid efflux transporter expression at the blood-brain barrier declines in normal aging*. Journal of Neuropathology & Experimental Neurology, 2010. **69**(10): p. 1034-1043.
54. Deane, R., et al., *apoE isoform–specific disruption of amyloid  $\beta$  peptide clearance from mouse brain*. The Journal of clinical investigation, 2008. **118**(12): p. 4002-4013.
55. Deane, R., Z. Wu, and B.V. Zlokovic, *RAGE (yin) versus LRP (yang) balance regulates Alzheimer amyloid  $\beta$ -peptide clearance through transport across the blood–brain barrier*. Stroke, 2004. **35**(11\_suppl\_1): p. 2628-2631.
56. Qi, X.-m. and J.-f. Ma, *The role of amyloid beta clearance in cerebral amyloid angiopathy: more potential therapeutic targets*. Translational neurodegeneration, 2017. **6**(1): p. 1-12.

57. Wujak, L., et al., *LRP1: a chameleon receptor of lung inflammation and repair*. Matrix Biology, 2018. **68**: p. 366-381.
58. Steinmüller, M., et al., *Endotoxin induced peritonitis elicits monocyte immigration into the lung: implications on alveolar space inflammatory responsiveness*. Respiratory research, 2006. **7**(1): p. 1-8.
59. May, P., H.H. Bock, and J.-R. Nofer, *Low density receptor-related protein 1 (LRP1) promotes anti-inflammatory phenotype in murine macrophages*. Cell and tissue research, 2013. **354**(3): p. 887-889.
60. Potere, N., et al., *Low density lipoprotein receptor-related protein-1 in cardiac inflammation and infarct healing*. Frontiers in cardiovascular medicine, 2019. **6**: p. 51.
61. Ranganathan, S., et al., *Molecular basis for the interaction of low density lipoprotein receptor-related protein 1 (LRP1) with integrin  $\alpha$ M $\beta$ 2: identification of binding sites within  $\alpha$ M $\beta$ 2 for LRP1*. Journal of Biological Chemistry, 2011. **286**(35): p. 30535-30541.
62. Staudt, N.D., et al., *Myeloid cell receptor LRP1/CD91 regulates monocyte recruitment and angiogenesis in tumors*. Cancer research, 2013. **73**(13): p. 3902-3912.
63. Ferrer, D.G., et al., *Standardized flow cytometry assay for identification of human monocytic heterogeneity and LRP1 expression in monocyte subpopulations: decreased expression of this receptor in nonclassical monocytes*. Cytometry Part A, 2014. **85**(7): p. 601-610.
64. Sagare, A.P., R. Deane, and B.V. Zlokovic, *Low-density lipoprotein receptor-related protein 1: a physiological  $A\beta$  homeostatic mechanism with multiple therapeutic opportunities*. Pharmacology & therapeutics, 2012. **136**(1): p. 94-105.
65. Kanekiyo, T. and G. Bu, *The low-density lipoprotein receptor-related protein 1 and amyloid- $\beta$  clearance in Alzheimer's disease*. Frontiers in aging neuroscience, 2014. **6**: p. 93.
66. Osgood, D., et al., *Aging alters mRNA expression of amyloid transporter genes at the blood-brain barrier*. Neurobiology of aging, 2017. **57**: p. 178-185.
67. De Leon, M.J., et al., *Cerebrospinal fluid clearance in Alzheimer disease measured with dynamic PET*. Journal of Nuclear Medicine, 2017. **58**(9): p. 1471-1476.
68. Weller, R.O., et al., *Cerebral amyloid angiopathy: amyloid  $\beta$  accumulates in putative interstitial fluid drainage pathways in Alzheimer's disease*. The American journal of pathology, 1998. **153**(3): p. 725-733.
69. Beaudin, A.E., et al., *Cerebrovascular Reactivity Across the Entire Brain in Cerebral Amyloid Angiopathy*. Neurology, 2022. **98**(17): p. e1716-e1728.
70. Fierstra, J., et al., *Measuring cerebrovascular reactivity: what stimulus to use?* The Journal of physiology, 2013. **591**(23): p. 5809-5821.
71. Plog, B.A. and M. Nedergaard, *The glymphatic system in central nervous system health and disease: past, present, and future*. Annual Review of Pathology: Mechanisms of Disease, 2018. **13**: p. 379-394.
72. Smith, A.J., et al., *Test of the 'glymphatic' hypothesis demonstrates diffusive and aquaporin-4-independent solute transport in rodent brain parenchyma*. elife, 2017. **6**: p. e27679.
73. Carare, R.O., et al., *Clearance of interstitial fluid (ISF) and CSF (CLIC) group—part of Vascular Professional Interest Area (PIA) Cerebrovascular disease and the failure of elimination of Amyloid- $\beta$  from the brain and retina with age and Alzheimer's disease-*

- Opportunities for Therapy*. Alzheimer's & Dementia: Diagnosis, Assessment & Disease Monitoring, 2020. **12**(1): p. e12053.
74. Mawuenyega, K.G., et al., *Decreased clearance of CNS  $\beta$ -amyloid in Alzheimer's disease*. Science, 2010. **330**(6012): p. 1774-1774.
  75. Jin, W.-S., et al., *Peritoneal dialysis reduces amyloid-beta plasma levels in humans and attenuates Alzheimer-associated phenotypes in an APP/PS1 mouse model*. Acta neuropathologica, 2017. **134**(2): p. 207-220.
  76. Rogers, J., et al., *Peripheral clearance of amyloid  $\beta$  peptide by complement C3-dependent adherence to erythrocytes*. Neurobiology of aging, 2006. **27**(12): p. 1733-1739.
  77. Funkhouser, T. and D. Vik, *Complement receptor type 1 gene regulation: retinoic acid and cytosine arabinoside increase CR1 expression*. Scandinavian journal of immunology, 1999. **49**(1): p. 21-28.
  78. Brouwers, N., et al., *Alzheimer risk associated with a copy number variation in the complement receptor 1 increasing C3b/C4b binding sites*. Molecular psychiatry, 2012. **17**(2): p. 223-233.
  79. Jacquet, M., et al., *Deciphering complement receptor type 1 interactions with recognition proteins of the lectin complement pathway*. The Journal of Immunology, 2013. **190**(7): p. 3721-3731.
  80. Larvie, M., et al., *Mannose-binding lectin binds to amyloid  $\beta$  protein and modulates inflammation*. Journal of Biomedicine and Biotechnology, 2012. **2012**.
  81. Liu, Y.-H., et al., *Immunotherapy for Alzheimer disease—the challenge of adverse effects*. Nature Reviews Neurology, 2012. **8**(8): p. 465-469.
  82. Iijima-Ando, K., et al., *Overexpression of neprilysin reduces alzheimer amyloid- $\beta$ 42 (A $\beta$ 42)-induced neuron loss and intraneuronal A $\beta$ 42 deposits but causes a reduction in cAMP-responsive element-binding protein-mediated transcription, age-dependent axon pathology, and premature death in Drosophila*. Journal of Biological Chemistry, 2008. **283**(27): p. 19066-19076.
  83. Pham, C.T., *Neutrophil serine proteases: specific regulators of inflammation*. Nature Reviews Immunology, 2006. **6**(7): p. 541-550.
  84. Meyer-Hoffert, U. and O. Wiedow, *Neutrophil serine proteases: mediators of innate immune responses*. Current opinion in hematology, 2011. **18**(1): p. 19-24.
  85. Brinkmann, V., et al., *Neutrophil extracellular traps kill bacteria*. science, 2004. **303**(5663): p. 1532-1535.
  86. Lood, C., et al., *Neutrophil extracellular traps enriched in oxidized mitochondrial DNA are interferogenic and contribute to lupus-like disease*. Nature medicine, 2016. **22**(2): p. 146-153.
  87. Urban, C.F., et al., *Neutrophil extracellular traps capture and kill Candida albicans yeast and hyphal forms*. Cellular microbiology, 2006. **8**(4): p. 668-676.
  88. Saitoh, T., et al., *Neutrophil extracellular traps mediate a host defense response to human immunodeficiency virus-1*. Cell host & microbe, 2012. **12**(1): p. 109-116.
  89. Abi Abdallah, D.S., et al., *Toxoplasma gondii triggers release of human and mouse neutrophil extracellular traps*. Infection and immunity, 2012. **80**(2): p. 768-777.
  90. Walker, M.J., et al., *DNase Sda1 provides selection pressure for a switch to invasive group A streptococcal infection*. Nature medicine, 2007. **13**(8): p. 981-985.

91. Branzk, N., et al., *Neutrophils sense microbe size and selectively release neutrophil extracellular traps in response to large pathogens*. *Nature immunology*, 2014. **15**(11): p. 1017-1025.
92. Castanheira, F.V. and P. Kubes, *Neutrophils and NETs in modulating acute and chronic inflammation*. *Blood, The Journal of the American Society of Hematology*, 2019. **133**(20): p. 2178-2185.
93. Christoffersson, G., et al., *VEGF-A recruits a proangiogenic MMP-9-delivering neutrophil subset that induces angiogenesis in transplanted hypoxic tissue*. *Blood, The Journal of the American Society of Hematology*, 2012. **120**(23): p. 4653-4662.
94. Peiseler, M. and P. Kubes, *More friend than foe: the emerging role of neutrophils in tissue repair*. *The Journal of clinical investigation*, 2019. **129**(7): p. 2629-2639.
95. Jayaraj, R.L., et al., *Neuroinflammation: friend and foe for ischemic stroke*. *Journal of neuroinflammation*, 2019. **16**(1): p. 1-24.
96. Jickling, G.C., et al., *Hemorrhagic transformation after ischemic stroke in animals and humans*. *Journal of Cerebral Blood Flow & Metabolism*, 2014. **34**(2): p. 185-199.
97. Shichita, T., M. Ito, and A. Yoshimura, *Post-ischemic inflammation regulates neural damage and protection*. *Frontiers in cellular neuroscience*, 2014. **8**: p. 319.
98. Jickling, G.C., et al., *RNA in blood is altered prior to hemorrhagic transformation in ischemic stroke*. *Annals of neurology*, 2013. **74**(2): p. 232-240.
99. Kim, J.Y., et al., *Inflammation after ischemic stroke: the role of leukocytes and glial cells*. *Experimental neurobiology*, 2016. **25**(5): p. 241.
100. Zenaro, E., et al., *Neutrophils promote Alzheimer's disease-like pathology and cognitive decline via LFA-1 integrin*. *Nature medicine*, 2015. **21**(8): p. 880-886.
101. Baik, S.H., et al., *Migration of neutrophils targeting amyloid plaques in Alzheimer's disease mouse model*. *Neurobiology of aging*, 2014. **35**(6): p. 1286-1292.
102. Pietronigro, E.C., et al., *NETosis in Alzheimer's disease*. *Frontiers in Immunology*, 2017. **8**: p. 211.
103. Gelderblom, M., et al., *Neutralization of the IL-17 axis diminishes neutrophil invasion and protects from ischemic stroke*. *Blood, The Journal of the American Society of Hematology*, 2012. **120**(18): p. 3793-3802.
104. Harrington, L.E., et al., *Interleukin 17-producing CD4<sup>+</sup> effector T cells develop via a lineage distinct from the T helper type 1 and 2 lineages*. *Nature immunology*, 2005. **6**(11): p. 1123-1132.
105. Park, H., et al., *A distinct lineage of CD4 T cells regulates tissue inflammation by producing interleukin 17*. *Nature immunology*, 2005. **6**(11): p. 1133-1141.
106. Dong, C., *Diversification of T-helper-cell lineages: finding the family root of IL-17-producing cells*. *Nature Reviews Immunology*, 2006. **6**(4): p. 329-334.
107. Martin, B., et al., *Interleukin-17-producing  $\gamma\delta$  T cells selectively expand in response to pathogen products and environmental signals*. *Immunity*, 2009. **31**(2): p. 321-330.
108. Chen, S.-H., et al., *Amyloid-beta uptake by blood monocytes is reduced with ageing and Alzheimer's disease*. *Translational psychiatry*, 2020. **10**(1): p. 1-11.
109. Slaba, I., et al., *Imaging the dynamic platelet-neutrophil response in sterile liver injury and repair in mice*. *Hepatology*, 2015. **62**(5): p. 1593-1605.
110. Wang, J., *Neutrophils in tissue injury and repair*. *Cell and tissue research*, 2018. **371**(3): p. 531-539.



111. Wang, J., et al., *Visualizing the function and fate of neutrophils in sterile injury and repair*. Science, 2017. **358**(6359): p. 111-116.
112. Dobaczewski, M., et al., *CCR5 signaling suppresses inflammation and reduces adverse remodeling of the infarcted heart, mediating recruitment of regulatory T cells*. The American journal of pathology, 2010. **176**(5): p. 2177-2187.
113. Jones, H.R., et al. *The role of neutrophils in inflammation resolution*. in *Seminars in immunology*. 2016. Elsevier.
114. Kim, Y.R., et al., *Neutrophils Return to Bloodstream Through the Brain Blood Vessel After Crosstalk With Microglia During LPS-Induced Neuroinflammation*. Frontiers in Cell and Developmental Biology, 2020. **8**.
115. Passaro, A.P., et al., *Immune Response in Neurological Pathology: Emerging Role of Central and Peripheral Immune Crosstalk*. Frontiers in Immunology, 2021: p. 2085.
116. Jakubzick, C.V., G.J. Randolph, and P.M. Henson, *Monocyte differentiation and antigen-presenting functions*. Nature Reviews Immunology, 2017. **17**(6): p. 349-362.
117. Auffray, C., et al., *Monitoring of blood vessels and tissues by a population of monocytes with patrolling behavior*. Science, 2007. **317**(5838): p. 666-670.
118. Shalhoub, J., et al., *Innate immunity and monocyte-macrophage activation in atherosclerosis*. Journal of inflammation, 2011. **8**(1): p. 1-17.
119. Ginhoux, F. and S. Jung, *Monocytes and macrophages: developmental pathways and tissue homeostasis*. Nature Reviews Immunology, 2014. **14**(6): p. 392-404.
120. Hopkinson-Woolley, J., et al., *Macrophage recruitment during limb development and wound healing in the embryonic and foetal mouse*. Journal of cell science, 1994. **107**(5): p. 1159-1167.
121. Hettinger, J., et al., *Origin of monocytes and macrophages in a committed progenitor*. Nature immunology, 2013. **14**(8): p. 821-830.
122. Giri, R., et al.,  *$\beta$ -Amyloid-induced migration of monocytes across human brain endothelial cells involves RAGE and PECAM-1*. American Journal of Physiology-Cell Physiology, 2000. **279**(6): p. C1772-C1781.
123. Zhang, K., et al., *CXCL1 contributes to  $\beta$ -amyloid-induced transendothelial migration of monocytes in Alzheimer's disease*. PloS one, 2013. **8**(8): p. e72744.
124. Michaud, J.-P., et al., *Real-time in vivo imaging reveals the ability of monocytes to clear vascular amyloid beta*. Cell reports, 2013. **5**(3): p. 646-653.
125. Maness, L.M., et al., *Passage of human amyloid  $\beta$ -protein 1–40 across the murine blood-brain barrier*. Life sciences, 1994. **55**(21): p. 1643-1650.
126. Roberts, K.F., et al., *Amyloid- $\beta$  efflux from the central nervous system into the plasma*. Annals of neurology, 2014. **76**(6): p. 837-844.
127. Deane, R., et al., *Clearance of amyloid- $\beta$  peptide across the blood-brain barrier: implication for therapies in Alzheimer's disease*. CNS & Neurological Disorders-Drug Targets (Formerly Current Drug Targets-CNS & Neurological Disorders), 2009. **8**(1): p. 16-30.
128. Wang, J., et al., *A systemic view of Alzheimer disease—insights from amyloid- $\beta$  metabolism beyond the brain*. Nature reviews neurology, 2017. **13**(10): p. 612-623.
129. Brandt, K.J., et al., *TLR2 ligands induce NF- $\kappa$ B activation from endosomal compartments of human monocytes*. PloS one, 2013. **8**(12): p. e80743.

130. Richard, K.L., et al., *Toll-like receptor 2 acts as a natural innate immune receptor to clear amyloid  $\beta$ 1–42 and delay the cognitive decline in a mouse model of Alzheimer's disease*. Journal of Neuroscience, 2008. **28**(22): p. 5784-5793.
131. Udan, M.L., et al., *Toll-like receptors 2 and 4 mediate  $A\beta$  (1–42) activation of the innate immune response in a human monocytic cell line*. Journal of neurochemistry, 2008. **104**(2): p. 524-533.
132. Koronyo-Hamaoui, M., et al., *Peripherally derived angiotensin converting enzyme-enhanced macrophages alleviate Alzheimer-related disease*. Brain, 2020. **143**(1): p. 336-358.
133. Yang, T., R. Guo, and F. Zhang, *Brain perivascular macrophages: Recent advances and implications in health and diseases*. CNS neuroscience & therapeutics, 2019. **25**(12): p. 1318-1328.
134. Pedragosa, J., et al., *CNS-border associated macrophages respond to acute ischemic stroke attracting granulocytes and promoting vascular leakage*. Acta neuropathologica communications, 2018. **6**(1): p. 1-19.
135. Prinz, M. and J. Priller, *Microglia and brain macrophages in the molecular age: from origin to neuropsychiatric disease*. Nature Reviews Neuroscience, 2014. **15**(5): p. 300-312.
136. Aguzzi, A., B.A. Barres, and M.L. Bennett, *Microglia: scapegoat, saboteur, or something else?* science, 2013. **339**(6116): p. 156-161.
137. Hickey, W.F., K. Vass, and H. Lassmann, *Bone marrow-derived elements in the central nervous system: an immunohistochemical and ultrastructural survey of rat chimeras*. Journal of neuropathology and experimental neurology, 1992. **51**(3): p. 246-256.
138. Faraco, G., et al., *Perivascular macrophages mediate the neurovascular and cognitive dysfunction associated with hypertension*. The Journal of clinical investigation, 2016. **126**(12): p. 4674-4689.
139. Hannocks, M.-J., et al., *Molecular characterization of perivascular drainage pathways in the murine brain*. Journal of Cerebral Blood Flow & Metabolism, 2018. **38**(4): p. 669-686.
140. Chinnery, H.R., M.J. Ruitenberg, and P.G. McMenamin, *Novel characterization of monocyte-derived cell populations in the meninges and choroid plexus and their rates of replenishment in bone marrow chimeric mice*. Journal of Neuropathology & Experimental Neurology, 2010. **69**(9): p. 896-909.
141. Polfliet, M.M., et al., *A method for the selective depletion of perivascular and meningeal macrophages in the central nervous system*. Journal of neuroimmunology, 2001. **116**(2): p. 188-195.
142. Goldmann, T., et al., *Origin, fate and dynamics of macrophages at central nervous system interfaces*. Nature immunology, 2016. **17**(7): p. 797-805.
143. Faraco, G., et al., *Brain perivascular macrophages: characterization and functional roles in health and disease*. Journal of molecular medicine (Berlin, Germany), 2017. **95**(11): p. 1143-1152.
144. Foulquier, S., *Brain perivascular macrophages: connecting inflammation to autonomic activity in hypertension*. Hypertension Research, 2020. **43**(2): p. 148-150.
145. Rajan, W.D., et al., *Defining molecular identity and fates of CNS-border associated macrophages after ischemic stroke in rodents and humans*. Neurobiology of disease, 2020. **137**: p. 104722.

146. Park, L., et al., *Brain perivascular macrophages initiate the neurovascular dysfunction of Alzheimer A $\beta$  peptides*. *Circulation research*, 2017. **121**(3): p. 258-269.
147. Hawkes, C.A. and J. McLaurin, *Selective targeting of perivascular macrophages for clearance of  $\beta$ -amyloid in cerebral amyloid angiopathy*. *Proceedings of the National Academy of Sciences*, 2009. **106**(4): p. 1261-1266.
148. Thanopoulou, K., et al., *Scavenger receptor class B type I (SR-BI) regulates perivascular macrophages and modifies amyloid pathology in an Alzheimer mouse model*. *Proceedings of the National Academy of Sciences*, 2010. **107**(48): p. 20816-20821.
149. Steel, C.D., et al., *Distinct macrophage subpopulations regulate viral encephalitis but not viral clearance in the CNS*. *Journal of neuroimmunology*, 2010. **226**(1-2): p. 81-92.
150. Kösel, S., et al., *Long-lasting perivascular accumulation of major histocompatibility complex class II-positive lipophages in the spinal cord of stroke patients: possible relevance for the immune privilege of the brain*. *Acta neuropathologica*, 1997. **94**(6): p. 532-538.
151. Polfliet, M.M., et al., *Meningeal and perivascular macrophages of the central nervous system play a protective role during bacterial meningitis*. *The Journal of Immunology*, 2001. **167**(8): p. 4644-4650.
152. Polfliet, M.M., et al., *The role of perivascular and meningeal macrophages in experimental allergic encephalomyelitis*. *Journal of neuroimmunology*, 2002. **122**(1-2): p. 1-8.
153. Pizzolla, A., et al., *Reactive oxygen species produced by the NADPH oxidase 2 complex in monocytes protect mice from bacterial infections*. *The Journal of Immunology*, 2012. **188**(10): p. 5003-5011.
154. Yanagitani, Y., et al., *Angiotensin II type 1 receptor-mediated peroxide production in human macrophages*. *Hypertension*, 1999. **33**(1): p. 335-339.
155. Gorelick, P.B., et al., *Vascular contributions to cognitive impairment and dementia: a statement for healthcare professionals from the American Heart Association/American Stroke Association*. *stroke*, 2011. **42**(9): p. 2672-2713.
156. Hawkes, C.A., et al., *Regional differences in the morphological and functional effects of aging on cerebral basement membranes and perivascular drainage of amyloid- $\beta$  from the mouse brain*. *Aging cell*, 2013. **12**(2): p. 224-236.
157. Bechmann, I., et al., *Immune surveillance of mouse brain perivascular spaces by blood-borne macrophages*. *European Journal of Neuroscience*, 2001. **14**(10): p. 1651-1658.
158. del Rey, A., et al., *A cytokine network involving brain-borne IL-1 $\beta$ , IL-1ra, IL-18, IL-6, and TNF $\alpha$  operates during long-term potentiation and learning*. *Brain, behavior, and immunity*, 2013. **33**: p. 15-23.
159. Bechmann, I., et al., *Turnover of rat brain perivascular cells*. *Experimental neurology*, 2001. **168**(2): p. 242-249.
160. Kim, W.-K., et al., *CD163 identifies perivascular macrophages in normal and viral encephalitic brains and potential precursors to perivascular macrophages in blood*. *The American journal of pathology*, 2006. **168**(3): p. 822-834.
161. Faraco, G., et al., *Perivascular macrophages mediate the neurovascular and cognitive dysfunction associated with hypertension*. *The Journal of clinical investigation*, 2016. **126**(12): p. 4674-4689.
162. De Strooper, B. and E. Karran, *The cellular phase of Alzheimer's disease*. *Cell*, 2016. **164**(4): p. 603-615.

163. Steinberg, D., *A docking receptor for HDL cholesterol esters*. Science, 1996. **271**(5248): p. 460-460.
164. Paresce, D.M., R.N. Ghosh, and F.R. Maxfield, *Microglial cells internalize aggregates of the Alzheimer's disease amyloid  $\beta$ -protein via a scavenger receptor*. Neuron, 1996. **17**(3): p. 553-565.
165. Husemann, J., et al., *Scavenger receptor class B type I (SR-BI) mediates adhesion of neonatal murine microglia to fibrillar  $\beta$ -amyloid*. Journal of neuroimmunology, 2001. **114**(1-2): p. 142-150.
166. Mucke, L., et al., *High-level neuronal expression of  $A\beta$ 1-42 in wild-type human amyloid protein precursor transgenic mice: synaptotoxicity without plaque formation*. Journal of Neuroscience, 2000. **20**(11): p. 4050-4058.
167. Faraco, G., et al., *Brain perivascular macrophages: characterization and functional roles in health and disease*. Journal of Molecular Medicine, 2017. **95**(11): p. 1143-1152.
168. Zeisel, A., et al., *Cell types in the mouse cortex and hippocampus revealed by single-cell RNA-seq*. Science, 2015. **347**(6226): p. 1138-1142.
169. Van Hove, H., et al., *A single-cell atlas of mouse brain macrophages reveals unique transcriptional identities shaped by ontogeny and tissue environment*. Nature neuroscience, 2019. **22**(6): p. 1021-1035.
170. Eng, J.A., et al., *Clinical manifestations of cerebral amyloid angiopathy-related inflammation*. Annals of Neurology: Official Journal of the American Neurological Association and the Child Neurology Society, 2004. **55**(2): p. 250-256.
171. Kinnecom, C., et al., *Course of cerebral amyloid angiopathy-related inflammation*. Neurology, 2007. **68**(17): p. 1411-1416.
172. Fountain, N.B. and D.A. Eberhard, *Primary angiitis of the central nervous system associated with cerebral amyloid angiopathy: report of two cases and review of the literature*. Neurology, 1996. **46**(1): p. 190-197.
173. Scolding, N.J., et al.,  *$A\beta$ -related angiitis: primary angiitis of the central nervous system associated with cerebral amyloid angiopathy*. Brain, 2005. **128**(3): p. 500-515.
174. Schwab, P., et al., *Cerebral amyloid angiopathy associated with primary angiitis of the central nervous system: report of 2 cases and review of the literature*. Arthritis Care & Research, 2003. **49**(3): p. 421-427.
175. Wu, J.-J., M. Yao, and J. Ni, *Cerebral amyloid angiopathy-related inflammation: current status and future implications*. Chinese Medical Journal, 2021. **134**(06): p. 646-654.
176. Charidimou, A., et al., *Cortical superficial siderosis: detection and clinical significance in cerebral amyloid angiopathy and related conditions*. Brain, 2015. **138**(8): p. 2126-2139.
177. Kimura, A., et al., *Corticosteroid therapy in a patient with cerebral amyloid angiopathy-related inflammation*. Journal of Neuroinflammation, 2013. **10**(1): p. 1-9.
178. Antolini, L., et al., *Spontaneous ARIA-like events in cerebral amyloid angiopathy-related inflammation: a multicenter prospective longitudinal cohort study*. Neurology, 2021. **97**(18): p. e1809-e1822.
179. Kloppenborg, R.P., et al., *Steroid responsive encephalopathy in cerebral amyloid angiopathy: a case report and review of evidence for immunosuppressive treatment*. Journal of neuroinflammation, 2010. **7**(1): p. 1-6.

180. Salvarani, C., et al., *Primary central nervous system vasculitis: comparison of patients with and without cerebral amyloid angiopathy*. *Rheumatology*, 2008. **47**(11): p. 1671-1677.
181. Melzer, N., et al., *CD4+ T cells predominate in cerebrospinal fluid and leptomeningeal and parenchymal infiltrates in cerebral amyloid  $\beta$ -related angiitis*. *Archives of neurology*, 2012. **69**(6): p. 773-777.
182. Yamada, M., et al., *Cerebral amyloid angiopathy in the aged*. *Journal of neurology*, 1987. **234**(6): p. 371-376.
183. Masuda, J., et al., *Autopsy study of incidence and distribution of cerebral amyloid angiopathy in Hisayama, Japan*. *Stroke*, 1988. **19**(2): p. 205-210.
184. Hirohata, M., et al., *Clinical features of non-hypertensive lobar intracerebral hemorrhage related to cerebral amyloid angiopathy*. *European journal of neurology*, 2010. **17**(6): p. 823-829.
185. Margraf, N.G., et al., *Cerebrospinal Fluid Biomarkers in Cerebral Amyloid Angiopathy: New Data and Quantitative Meta-Analysis*. *Frontiers in Aging Neuroscience*, 2022. **14**.
186. Banerjee, G., et al., *Cerebrospinal fluid biomarkers in cerebral amyloid angiopathy*. *Journal of Alzheimer's disease*, 2020. **74**(4): p. 1189-1201.
187. Charidimou, A., et al., *Core cerebrospinal fluid biomarker profile in cerebral amyloid angiopathy: a meta-analysis*. *Neurology*, 2018. **90**(9): p. e754-e762.
188. Greenberg, S.M., et al., *2022 Guideline for the Management of Patients With Spontaneous Intracerebral Hemorrhage: A Guideline From the American Heart Association/American Stroke Association*. *Stroke*: p. 10.1161/STR.0000000000000407.
189. Rosand, J., et al., *Warfarin-associated hemorrhage and cerebral amyloid angiopathy: a genetic and pathologic study*. *Neurology*, 2000. **55**(7): p. 947-951.
190. Hart, R.G., B.S. Boop, and D.C. Anderson, *Oral anticoagulants and intracranial hemorrhage: facts and hypotheses*. *Stroke*, 1995. **26**(8): p. 1471-1477.
191. Ward, R., et al. *Utility of HAS-BLED and CHA2DS2-VASc scores among patients with atrial fibrillation and imaging evidence of cerebral amyloid angiopathy*. in *Mayo Clinic Proceedings*. 2020. Elsevier.
192. Sloan, M., et al., *Clinical features and pathogenesis of intracerebral hemorrhage after rt-PA and heparin therapy for acute myocardial infarction: the Thrombolysis in Myocardial Infarction (TIMI) II Pilot and Randomized Clinical Trial combined experience*. *Neurology*, 1995. **45**(4): p. 649-658.
193. Charidimou, A., et al., *Microbleeds, cerebral hemorrhage, and functional outcome after stroke thrombolysis: individual patient data meta-analysis*. *Stroke*, 2017. **48**(8): p. 2084-2090.
194. Smith, E.E., *Cerebral amyloid angiopathy as a cause of neurodegeneration*. *Journal of Neurochemistry*, 2017. **144**(5): p. 651-658.
195. Sharp, F.R., et al., *Molecular markers and mechanisms of stroke: RNA studies of blood in animals and humans*. *Journal of Cerebral Blood Flow & Metabolism*, 2011. **31**(7): p. 1513-1531.
196. Sharp, F.R. and G.C. Jickling, *Whole genome expression of cellular response to stroke*. *Stroke*, 2013. **44**(6\_suppl\_1): p. S23-S25.
197. Agnihotri, S., et al., *Peripheral leukocyte counts and outcomes after intracerebral hemorrhage*. *Journal of neuroinflammation*, 2011. **8**(1): p. 1-4.

198. Meller, R., et al., *Blood transcriptome changes after stroke in an African American population*. *Annals of clinical and translational neurology*, 2016. **3**(2): p. 70-81.
199. Jickling, G.C., et al., *microRNA expression in peripheral blood cells following acute ischemic stroke and their predicted gene targets*. *PloS one*, 2014. **9**(6): p. e99283.
200. Jickling, G.C., et al., *Progression of cerebral white matter hyperintensities is related to leukocyte gene expression*. *Brain*, 2022.
201. Jickling, G.C. and F.R. Sharp, *Blood biomarkers of ischemic stroke*. *Neurotherapeutics*, 2011. **8**(3): p. 349-360.
202. Jickling, G.C., et al., *Signatures of cardioembolic and large-vessel ischemic stroke*. *Annals of neurology*, 2010. **68**(5): p. 681-692.
203. Jickling, G.C., et al., *Ischemic transient neurological events identified by immune response to cerebral ischemia*. *Stroke*, 2012. **43**(4): p. 1006-1012.
204. Foidl, B.M., et al., *Platelet and plasma phosphatidylcholines as biomarkers to diagnose cerebral amyloid angiopathy*. *Frontiers in Neurology*, 2020. **11**: p. 359.
205. Humpel, C., *Identifying and validating biomarkers for Alzheimer's disease*. *Trends in biotechnology*, 2011. **29**(1): p. 26-32.
206. Wyss-Coray, T., et al., *TGF- $\beta$ 1 promotes microglial amyloid- $\beta$  clearance and reduces plaque burden in transgenic mice*. *Nature medicine*, 2001. **7**(5): p. 612-618.
207. Paglinawan, R., et al., *TGF $\beta$  directs gene expression of activated microglia to an anti-inflammatory phenotype strongly focusing on chemokine genes and cell migratory genes*. *Glia*, 2003. **44**(3): p. 219-231.
208. Rustenhoven, J., et al., *TGF-beta1 regulates human brain pericyte inflammatory processes involved in neurovasculature function*. *Journal of neuroinflammation*, 2016. **13**(1): p. 1-15.
209. Smith, A.M., et al., *Adult human glia, pericytes and meningeal fibroblasts respond similarly to IFN $\gamma$  but not to TGF $\beta$ 1 or M-CSF*. *PloS one*, 2013. **8**(12): p. e80463.
210. Brionne, T.C., et al., *Loss of TGF- $\beta$ 1 leads to increased neuronal cell death and microgliosis in mouse brain*. *Neuron*, 2003. **40**(6): p. 1133-1145.
211. Branton, M.H. and J.B. Kopp, *TGF- $\beta$  and fibrosis*. *Microbes and infection*, 1999. **1**(15): p. 1349-1365.
212. Von Bernhardi, R., et al., *Role of TGF $\beta$  signaling in the pathogenesis of Alzheimer's disease*. *Frontiers in cellular neuroscience*, 2015: p. 426.
213. Kandasamy, M., et al., *TGF- $\beta$  signaling: a therapeutic target to reinstate regenerative plasticity in vascular dementia?* *Aging and disease*, 2020. **11**(4): p. 828.
214. Buisson, A., et al., *Transforming growth factor- $\beta$  and ischemic brain injury*. *Cellular and molecular neurobiology*, 2003. **23**(4): p. 539-550.
215. Wang, X., et al., *Transforming growth factor- $\beta$ 1 exhibits delayed gene expression following focal cerebral ischemia*. *Brain research bulletin*, 1995. **36**(6): p. 607-609.
216. Ma, M., et al., *Intranasal delivery of transforming growth factor-beta1 in mice after stroke reduces infarct volume and increases neurogenesis in the subventricular zone*. *BMC neuroscience*, 2008. **9**(1): p. 1-10.
217. Donninelli, G., et al., *Interleukin-9 regulates macrophage activation in the progressive multiple sclerosis brain*. *Journal of Neuroinflammation*, 2020. **17**(1): p. 1-14.
218. Hampton, M.B., A.J. Kettle, and C.C. Winterbourn, *Inside the neutrophil phagosome: oxidants, myeloperoxidase, and bacterial killing*. *Blood, The Journal of the American Society of Hematology*, 1998. **92**(9): p. 3007-3017.

219. Rosales, C. and E. Uribe-Querol, *Phagocytosis: a fundamental process in immunity*. BioMed research international, 2017. **2017**.
220. Caraci, F., et al., *Neurobiological links between depression and AD: the role of TGF- $\beta$ 1 signaling as a new pharmacological target*. Pharmacological research, 2018. **130**: p. 374-384.
221. Tesseur, I., et al., *Deficiency in neuronal TGF- $\beta$  signaling promotes neurodegeneration and Alzheimer's pathology*. The Journal of clinical investigation, 2006. **116**(11): p. 3060-3069.
222. Gaines, P., et al., *A cascade of Ca<sup>2+</sup>/calmodulin-dependent protein kinases regulates the differentiation and functional activation of murine neutrophils*. Experimental hematology, 2008. **36**(7): p. 832-844.
223. Verploegen, S., et al., *Identification and characterization of CKLiK, a novel granulocyte Ca<sup>++</sup>/calmodulin-dependent kinase*. Blood, The Journal of the American Society of Hematology, 2000. **96**(9): p. 3215-3223.
224. Verploegen, S., et al., *Characterization of the role of CaMKI-like kinase (CKLiK) in human granulocyte function*. Blood, 2005. **106**(3): p. 1076-1083.
225. Chen, Y. and W.G. Junger, *Measurement of oxidative burst in neutrophils, in Leucocytes*. 2012, Springer. p. 115-124.
226. Barco, A., C. Pittenger, and E.R. Kandel, *CREB, memory enhancement and the treatment of memory disorders: promises, pitfalls and prospects*. Expert opinion on therapeutic targets, 2003. **7**(1): p. 101-114.
227. Bourtchuladze, R., et al., *Deficient long-term memory in mice with a targeted mutation of the cAMP-responsive element-binding protein*. Cell, 1994. **79**(1): p. 59-68.
228. Won, J. and A.J. Silva, *Molecular and cellular mechanisms of memory allocation in neuronetworks*. Neurobiology of learning and memory, 2008. **89**(3): p. 285-292.
229. Ortega-Martínez, S., *A new perspective on the role of the CREB family of transcription factors in memory consolidation via adult hippocampal neurogenesis*. Frontiers in molecular neuroscience, 2015. **8**: p. 46.
230. Lee, Y.-S. and A.J. Silva, *The molecular and cellular biology of enhanced cognition*. Nature Reviews Neuroscience, 2009. **10**(2): p. 126-140.
231. Liang, X., et al., *Effect of heterogeneity on the chromosome 10 risk in late-onset Alzheimer disease*. Human mutation, 2007. **28**(11): p. 1065-1073.
232. Desikan, R.S., et al., *Polygenic overlap between C-reactive protein, plasma lipids, and Alzheimer disease*. Circulation, 2015. **131**(23): p. 2061-2069.
233. Müller, M., et al., *Constitutive cAMP response element binding protein (CREB) activation by Alzheimer's disease presenilin-driven inositol trisphosphate receptor (InsP3R) Ca<sup>2+</sup> signaling*. Proceedings of the National Academy of Sciences, 2011. **108**(32): p. 13293-13298.
234. Böhm, B.B., et al., *Homeostatic effects of the metalloproteinase disintegrin ADAM15 in degenerative cartilage remodeling*. Arthritis & Rheumatism, 2005. **52**(4): p. 1100-1109.
235. Charrier-Hisamuddin, L., C.L. Laboisie, and D. Merlin, *ADAM-15: a metalloprotease that mediates inflammation*. The FASEB Journal, 2008. **22**(3): p. 641-653.
236. Mattern, J., et al., *ADAM15 mediates upregulation of Claudin-1 expression in breast cancer cells*. Scientific reports, 2019. **9**(1): p. 1-14.

237. Charrier, L., et al., *ADAM-15 inhibits wound healing in human intestinal epithelial cell monolayers*. American Journal of Physiology-Gastrointestinal and Liver Physiology, 2005. **288**(2): p. G346-G353.
238. Herren, B., E.W. Raines, and R. Ross, *Expression of a disintegrin-like protein in cultured human vascular cells and in vivo*. The FASEB Journal, 1997. **11**(2): p. 173-180.
239. Ham, C., et al., *ADAM15 is an adherens junction molecule whose surface expression can be driven by VE-cadherin*. Experimental cell research, 2002. **279**(2): p. 239-247.
240. Sun, C., et al., *A disintegrin and metalloproteinase 15 contributes to atherosclerosis by mediating endothelial barrier dysfunction via Src family kinase activity*. Arteriosclerosis, thrombosis, and vascular biology, 2012. **32**(10): p. 2444-2451.
241. Ahmed, S., et al., *TRIF-mediated TLR3 and TLR4 signaling is negatively regulated by ADAM15*. The Journal of Immunology, 2013. **190**(5): p. 2217-2228.
242. Kakurina, G.V., et al., *Circulating Actin-Binding Proteins in Laryngeal Cancer: Its Relationship with Circulating Tumor Cells and Cells of the Immune System*. Acta Naturae, 2021. **13**(4): p. 64-68.
243. Chang, K.-H., et al., *Downregulation of genes involved in metabolism and oxidative stress in the peripheral leukocytes of Huntington's disease patients*. 2012.
244. Lee, S., et al., *Adenylyl cyclase-associated protein 1 is a receptor for human resistin and mediates inflammatory actions of human monocytes*. Cell metabolism, 2014. **19**(3): p. 484-497.
245. Cho, Y., et al., *Adipokine resistin is a key player to modulate monocytes, endothelial cells, and smooth muscle cells, leading to progression of atherosclerosis in rabbit carotid artery*. Journal of the American College of Cardiology, 2011. **57**(1): p. 99-109.
246. Zhang, H., et al., *Mammalian adenylyl cyclase-associated protein 1 (CAPI) regulates cofilin function, the actin cytoskeleton, and cell adhesion*. Journal of biological chemistry, 2013. **288**(29): p. 20966-20977.
247. Filková, M., et al., *The role of resistin as a regulator of inflammation: Implications for various human pathologies*. Clinical immunology, 2009. **133**(2): p. 157-170.
248. Reilly, M.P., et al., *Resistin is an inflammatory marker of atherosclerosis in humans*. Circulation, 2005. **111**(7): p. 932-939.
249. Zhang, Y., et al., *Association between serum resistin concentration and hypertension: A systematic review and meta-analysis*. Oncotarget, 2017. **8**(25): p. 41529.
250. Perovic, E., et al., *Diagnostic and prognostic role of resistin and copeptin in acute ischemic stroke*. Topics in stroke rehabilitation, 2017. **24**(8): p. 614-618.
251. Matsuda, S., Y. Matsuda, and L. D'Adamio, *BRI3 inhibits amyloid precursor protein processing in a mechanistically distinct manner from its homologue dementia gene BRI2*. Journal of Biological Chemistry, 2009. **284**(23): p. 15815-15825.
252. Reitz, C., et al., *Independent and epistatic effects of variants in VPS10-d receptors on Alzheimer disease risk and processing of the amyloid precursor protein (APP)*. Translational psychiatry, 2013. **3**(5): p. e256-e256.
253. Charidimou, A., et al., *Total magnetic resonance imaging burden of small vessel disease in cerebral amyloid angiopathy: an imaging-pathologic study of concept validation*. JAMA neurology, 2016. **73**(8): p. 994-1001.
254. MacLulich, A., et al., *Enlarged perivascular spaces are associated with cognitive function in healthy elderly men*. Journal of Neurology, Neurosurgery & Psychiatry, 2004. **75**(11): p. 1519-1523.



255. Moulin, S., et al., *Dementia risk after spontaneous intracerebral haemorrhage: a prospective cohort study*. The Lancet Neurology, 2016. **15**(8): p. 820-829.
256. Charidimou, A., et al., *Total MRI small vessel disease burden in cerebral amyloid angiopathy: a concept validation imaging-pathological study*. JAMA neurology, 2016. **73**(8): p. 994.
257. Yilmaz, P., et al., *Application of an imaging-based sum score for cerebral amyloid angiopathy to the general population: risk of major neurological diseases and mortality*. Frontiers in neurology, 2019: p. 1276.
258. Boulouis, G., et al., *Hemorrhage recurrence risk factors in cerebral amyloid angiopathy: comparative analysis of the overall small vessel disease severity score versus individual neuroimaging markers*. Journal of the neurological sciences, 2017. **380**: p. 64-67.
259. Charidimou, A., et al., *Cortical superficial siderosis and intracerebral hemorrhage risk in cerebral amyloid angiopathy*. Neurology, 2013. **81**(19): p. 1666-1673.
260. Matsuda, K., et al., *Investigation of hypertensive arteriopathy-related and cerebral amyloid angiopathy-related small vessel disease scores in patients from a memory clinic: a prospective single-centre study*. BMJ open, 2021. **11**(4): p. e042550.
261. Case, N.F., et al., *Cerebral amyloid angiopathy is associated with executive dysfunction and mild cognitive impairment*. Stroke, 2016. **47**(8): p. 2010-2016.
262. Arvanitakis, Z., et al., *Cerebral amyloid angiopathy pathology and cognitive domains in older persons*. Annals of neurology, 2011. **69**(2): p. 320-327.
263. Xiong, L., et al., *Dementia incidence and predictors in cerebral amyloid angiopathy patients without intracerebral hemorrhage*. Journal of Cerebral Blood Flow & Metabolism, 2018. **38**(2): p. 241-249.
264. Hachinski, V., et al., *National Institute of Neurological Disorders and Stroke–Canadian stroke network vascular cognitive impairment harmonization standards*. Stroke, 2006. **37**(9): p. 2220-2241.
265. Reitan, R.M., *Validity of the Trail Making Test as an indicator of organic brain damage*. Perceptual and motor skills, 1958. **8**(3): p. 271-276.
266. Benton, A.L., K. deS, and A.B. Sivan, *Multilingual aphasia examination*. 1994: AJA associates.
267. Wechsler, D., *Wechsler adult intelligence scale*. Archives of Clinical Neuropsychology, 1955.
268. Osterrieth, P.A., *Le test de copie d'une figure complexe; contribution a l'etude de la perception et de la memoire*. Archives de psychologie, 1944.
269. Delis, D.C., et al., *California Verbal Learning Test*. Assessment, 1987.
270. Love, S., et al., *Development, appraisal, validation and implementation of a consensus protocol for the assessment of cerebral amyloid angiopathy in post-mortem brain tissue*. American journal of neurodegenerative disease, 2014. **3**(1): p. 19.
271. Reijmer, Y.D., S.J. Van Veluw, and S.M. Greenberg, *Ischemic brain injury in cerebral amyloid angiopathy*. Journal of Cerebral Blood Flow & Metabolism, 2016. **36**(1): p. 40-54.
272. Yanginlar, C. and C. Logie, *HDAC11 is a regulator of diverse immune functions*. Biochimica et Biophysica Acta (BBA)-Gene Regulatory Mechanisms, 2018. **1861**(1): p. 54-59.
273. Sahakian, E., et al., *Essential role for histone deacetylase 11 (HDAC11) in neutrophil biology*. Journal of leukocyte biology, 2017. **102**(2): p. 475-486.

274. Bondarev, A.D., et al., *Recent developments of HDAC inhibitors: Emerging indications and novel molecules*. British Journal of Clinical Pharmacology, 2021. **87**(12): p. 4577-4597.
275. Shukla, S. and B.L. Tekwani, *Histone deacetylases inhibitors in neurodegenerative diseases, neuroprotection and neuronal differentiation*. Frontiers in pharmacology, 2020. **11**: p. 537.
276. Fella, E., et al., *Pharmacological stimulation of phagocytosis enhances amyloid plaque clearance; evidence from a transgenic mouse model of ATTR neuropathy*. Frontiers in molecular neuroscience, 2017. **10**: p. 138.
277. Panayiotou, E., et al., *C5aR agonist enhances phagocytosis of fibrillar and non-fibrillar A $\beta$  amyloid and preserves memory in a mouse model of familial Alzheimer's disease*. PloS one, 2019. **14**(12): p. e0225417.
278. Gorina, R., et al.,  *$\beta$ 2 integrin-mediated crawling on endothelial ICAM-1 and ICAM-2 is a prerequisite for transcellular neutrophil diapedesis across the inflamed blood-brain barrier*. The Journal of Immunology, 2014. **192**(1): p. 324-337.
279. Spronk, E., et al., *Hemorrhagic transformation in ischemic stroke and the role of inflammation*. Frontiers in Neurology, 2021. **12**: p. 597.
280. Evstratova, Y.V., et al., *Monocyte-Macrophage Differentiation Suppresses the Expression of Proapoptotic Receptors to Apo2L/TRAIL and Increases Resistance to TRAIL-Induced Apoptosis*. Biophysics, 2019. **64**(5): p. 729-731.
281. Halaas, O., et al., *Lipopolysaccharide induces expression of APO2 ligand/TRAIL in human monocytes and macrophages*. Scandinavian journal of immunology, 2000. **51**(3): p. 244-250.
282. Almasan, A. and A. Ashkenazi, *Apo2L/TRAIL: apoptosis signaling, biology, and potential for cancer therapy*. Cytokine & growth factor reviews, 2003. **14**(3-4): p. 337-348.
283. Sayers, T.J. and W.J. Murphy, *Combining proteasome inhibition with TNF-related apoptosis-inducing ligand (Apo2L/TRAIL) for cancer therapy*. Cancer Immunology, Immunotherapy, 2006. **55**(1): p. 76-84.
284. Uberti, D., et al., *TRAIL is expressed in the brain cells of Alzheimer's disease patients*. Neuroreport, 2004. **15**(4): p. 579-581.
285. Cantarella, G., et al., *Neutralization of TRAIL death pathway protects human neuronal cell line from  $\beta$ -amyloid toxicity*. Cell Death & Differentiation, 2003. **10**(1): p. 134-141.
286. Cartland, S.P., et al., *TRAIL-expressing monocyte/macrophages are critical for reducing inflammation and atherosclerosis*. Iscience, 2019. **12**: p. 41-52.
287. Cantarella, G., et al., *Neutralization of TNFSF10 ameliorates functional outcome in a murine model of Alzheimer's disease*. Brain, 2015. **138**(1): p. 203-216.
288. Falschlehner, C., et al., *TRAIL signalling: decisions between life and death*. The international journal of biochemistry & cell biology, 2007. **39**(7-8): p. 1462-1475.
289. Liguori, M., et al., *Functional TRAIL receptors in monocytes and tumor-associated macrophages: a possible targeting pathway in the tumor microenvironment*. Oncotarget, 2016. **7**(27): p. 41662.
290. Secchiero, P., et al., *Tumor necrosis factor-related apoptosis-inducing ligand induces monocytic maturation of leukemic and normal myeloid precursors through a caspase-dependent pathway*. Blood, The Journal of the American Society of Hematology, 2002. **100**(7): p. 2421-2429.

291. Tang, C., et al., *Interleukin-23: as a drug target for autoimmune inflammatory diseases*. Immunology, 2012. **135**(2): p. 112-124.
292. Puccetti, P., M.L. Belladonna, and U. Grohmann, *Effects of IL-12 and IL-23 on antigen-presenting cells at the interface between innate and adaptive immunity*. Critical Reviews™ in Immunology, 2002. **22**(5-6).
293. Maloy, K. and M. Kullberg, *IL-23 and Th17 cytokines in intestinal homeostasis*. Mucosal immunology, 2008. **1**(5): p. 339-349.
294. McKenzie, B.S., R.A. Kastelein, and D.J. Cua, *Understanding the IL-23–IL-17 immune pathway*. Trends in immunology, 2006. **27**(1): p. 17-23.
295. Belladonna, M.L., et al., *IL-23 and IL-12 have overlapping, but distinct, effects on murine dendritic cells*. The Journal of Immunology, 2002. **168**(11): p. 5448-5454.
296. Langrish, C.L., et al., *IL-23 drives a pathogenic T cell population that induces autoimmune inflammation*. The Journal of experimental medicine, 2005. **201**(2): p. 233-240.
297. Dai, H., et al., *IL-23 limits the production of IL-2 and promotes autoimmunity in lupus*. The Journal of Immunology, 2017. **199**(3): p. 903-910.
298. Croxford, A.L., F. Mair, and B. Becher, *IL-23: one cytokine in control of autoimmunity*. European journal of immunology, 2012. **42**(9): p. 2263-2273.
299. Park, S.Y., et al., *Peptidoglycan recognition protein Pglyrp2 protects mice from psoriasis-like skin inflammation by promoting regulatory T cells and limiting Th17 responses*. The journal of immunology, 2011. **187**(11): p. 5813-5823.
300. van Veluw, S.J., et al., *Different microvascular alterations underlie microbleeds and microinfarcts*. Annals of neurology, 2019. **86**(2): p. 279-292.

## Appendices

**Table S1.1** Differentially expressed genes in patients with cerebral amyloid angiopathy compared to controls

Gene	<i>p</i>	Fold Change	Gene	<i>p</i>	Fold Change	Gene	<i>p</i>	Fold Change
<i>POR</i>	0.0002	-1.35	<i>CMIP</i>	0.0164	-1.24	<i>EPHA10</i>	0.0325	-2.25
<i>CAP1</i>	0.0003	-1.30	<i>HEATR5A</i>	0.0166	-1.24	<i>ZNF467</i>	0.0326	-1.25
<i>BRI3BP</i>	0.0004	-1.35	<i>SYCP2L</i>	0.0167	-3.47	<i>UBE2Q2P2</i>	0.0327	-1.73
<i>SCARNA7</i>	0.0007	2.61	<i>OR7E13P</i>	0.0167	-1.65	<i>UBXN10</i>	0.0327	2.90
<i>PNPLA6</i>	0.0007	-1.38	<i>RELB</i>	0.0167	-1.21	<i>OGFOD3</i>	0.0328	-1.25
<i>MT-TA</i>	0.0009	-1.71	<i>ZBED1</i>	0.0167	-1.21	<i>SASH3</i>	0.0328	-1.24
<i>SORCS3</i>	0.0010	2.30	<i>COQ8A</i>	0.0168	-1.28	<i>GOLGA8O</i>	0.0329	-1.37
<i>CAMK1D</i>	0.0011	-1.32	<i>RPS7P10</i>	0.0169	2.55	<i>EMSLR</i>	0.0329	-6.35
<i>MT-TS1</i>	0.0012	-1.48	<i>PIGZ</i>	0.0169	-2.23	<i>PCBP2P1</i>	0.0329	-2.21
<i>ZNF596</i>	0.0013	2.41	<i>DEPDC7</i>	0.0170	2.52	<i>CELF3</i>	0.0329	1.34
<i>SEPTIN7P6</i>	0.0014	-1.41	<i>GYPE</i>	0.0170	1.84	<i>PTGIR</i>	0.0330	-1.23
<i>BCAS1</i>	0.0015	-2.47	<i>RABAC1</i>	0.0171	-1.21	<i>PLGRKT</i>	0.0330	-1.48
<i>FAM107A</i>	0.0016	3.29	<i>CWF19L1</i>	0.0171	-1.27	<i>MT-TS2</i>	0.0331	-1.30
<i>KCNK6</i>	0.0016	-1.30	<i>SNX10</i>	0.0172	-1.21	<i>TBPL1</i>	0.0333	1.31
<i>PSMD2</i>	0.0017	-1.27	<i>TMPRSS5</i>	0.0173	2.67	<i>MT2P1</i>	0.0334	2.90
<i>VAC14</i>	0.0020	-1.55	<i>CTR9</i>	0.0173	-1.21	<i>AURKAP1</i>	0.0336	-1.32
<i>KLHL32</i>	0.0021	-5.51	<i>PRSS33</i>	0.0174	-1.69	<i>SEPTIN14P8</i>	0.0336	-3.35
<i>RPSAP36</i>	0.0023	-1.70	<i>PLEKHJ1</i>	0.0174	-1.25	<i>CCHCR1</i>	0.0336	-1.60
<i>CHAF1A</i>	0.0024	-1.37	<i>SNRPEP2</i>	0.0174	6.75	<i>MBD3</i>	0.0340	-1.25
<i>GGT1</i>	0.0025	-1.50	<i>MT-ATP6</i>	0.0175	-1.37	<i>EPHB3</i>	0.0340	-1.90
<i>SLCO1A2</i>	0.0025	3.15	<i>CAPN1</i>	0.0175	-1.23	<i>CNTNAP2</i>	0.0341	-1.98
<i>AGPAT2</i>	0.0025	-1.34	<i>MTARC2</i>	0.0175	3.59	<i>LILRB1</i>	0.0342	-1.23
<i>ATF5</i>	0.0026	-1.39	<i>SUGP1</i>	0.0176	-1.22	<i>TECTA</i>	0.0343	3.46
<i>RPL12P25</i>	0.0027	4.17	<i>MRPS7</i>	0.0176	-1.24	<i>FAM157C</i>	0.0343	-1.28
<i>ZNF574</i>	0.0028	-1.56	<i>TLE3</i>	0.0177	-1.23	<i>ACKR2</i>	0.0343	-1.85
<i>CMKLR1</i>	0.0028	-1.42	<i>BMS1P1</i>	0.0177	-1.41	<i>FGFR2</i>	0.0344	-2.54
<i>ADGRE1</i>	0.0029	-1.47	<i>MARCO</i>	0.0178	-1.49	<i>RPL4P5</i>	0.0344	-1.47
<i>LBX2</i>	0.0029	-3.77	<i>EVA1B</i>	0.0180	-1.43	<i>MAP4K3</i>	0.0344	1.37
<i>CLEC11A</i>	0.0029	-2.06	<i>TLL4</i>	0.0180	-1.32	<i>RBFOX3</i>	0.0344	-2.05
<i>MT-CO3</i>	0.0032	-1.33	<i>ILK</i>	0.0181	-1.27	<i>COLCA1</i>	0.0345	-2.46
<i>SH3BGRL3</i>	0.0032	-1.26	<i>SUSD4</i>	0.0181	-1.96	<i>C1DP5</i>	0.0346	-2.37
<i>TBL1X</i>	0.0033	-1.27	<i>POLG</i>	0.0183	-1.22	<i>TNFAIP8L2</i>	0.0346	-1.30
<i>PLEKHB2</i>	0.0034	-1.21	<i>WNT5B</i>	0.0184	-3.14	<i>GRIK1</i>	0.0347	-2.42
<i>GRB2</i>	0.0034	-1.24	<i>ZNF524</i>	0.0184	-1.25	<i>RCAN1</i>	0.0349	-1.24
<i>SNX17</i>	0.0034	-1.23	<i>AP3D1</i>	0.0186	-1.22	<i>LOXL1</i>	0.0349	1.53
<i>LFNG</i>	0.0036	-1.28	<i>CAPN15</i>	0.0186	-1.22	<i>PTPA</i>	0.0350	-1.25
<i>HMOX1</i>	0.0036	-1.35	<i>GPS2</i>	0.0187	-1.21	<i>CCS</i>	0.0351	-1.25
<i>VCL</i>	0.0036	-1.28	<i>TMEM160</i>	0.0187	-1.35	<i>RASA4B</i>	0.0351	-1.78
<i>RRP1</i>	0.0037	-1.49	<i>CCDC144A</i>	0.0188	-2.07	<i>NIPAL1</i>	0.0351	-1.92
<i>EVI2A</i>	0.0037	1.58	<i>ALDH2</i>	0.0188	-1.24	<i>GUCA1B</i>	0.0354	-1.59
<i>TLCD5</i>	0.0037	3.47	<i>ATG4B</i>	0.0189	-1.21	<i>ORAI2</i>	0.0354	-1.20
<i>ADAM15</i>	0.0037	-1.28	<i>ARMC9</i>	0.0189	-2.20	<i>PAQR7</i>	0.0354	-1.42
<i>NHP2</i>	0.0037	-1.33	<i>VPS37C</i>	0.0190	-1.24	<i>OR8H1</i>	0.0355	2.75
<i>RPL39P3</i>	0.0038	6.70	<i>CHD4</i>	0.0190	-1.22	<i>CALD1</i>	0.0355	-1.51
<i>GSTP1</i>	0.0038	-1.21	<i>ZNF138</i>	0.0192	1.60	<i>IMPA2</i>	0.0357	-1.23
<i>IFITM3</i>	0.0038	1.80	<i>ZNF440</i>	0.0192	-1.31	<i>HNRNPKP2</i>	0.0359	-1.49
<i>TPST1</i>	0.0038	1.67	<i>MT-TF</i>	0.0192	-1.40	<i>NAGPA</i>	0.0359	-1.29
<i>GET3</i>	0.0039	-1.29	<i>NBPF10</i>	0.0193	-1.29	<i>SAC3D1</i>	0.0359	-1.30

<i>MT-ND6</i>	0.0039	-1.37	<i>PACSI</i>	0.0193	-1.21	<i>RHOBTB3</i>	0.0361	-1.26
<i>TGFB1</i>	0.0040	-1.29	<i>RPL23AP46</i>	0.0194	-2.22	<i>NOC2LP1</i>	0.0362	2.58
<i>PRICKLE1</i>	0.0041	-1.67	<i>GPATCH3</i>	0.0195	-1.26	<i>LIN37</i>	0.0363	-1.35
<i>C5orf17</i>	0.0041	3.49	<i>SOX4</i>	0.0195	-1.21	<i>FSTL1</i>	0.0363	-1.65
<i>IPO13</i>	0.0042	-1.47	<i>PI4KAP1</i>	0.0196	-1.64	<i>FAM43A</i>	0.0363	-1.21
<i>ST20</i>	0.0044	1.35	<i>NFIC</i>	0.0196	-1.26	<i>LY6E</i>	0.0363	1.71
<i>SUPT16HP1</i>	0.0046	-1.32	<i>DDX31</i>	0.0196	-1.42	<i>AKAP3</i>	0.0363	1.89
<i>MCM5</i>	0.0047	-1.31	<i>SLC66A2</i>	0.0197	-1.26	<i>PITPNM1</i>	0.0363	-1.33
<i>SETD1A</i>	0.0049	-1.44	<i>ATG101</i>	0.0197	-1.27	<i>PRPH2</i>	0.0364	-1.39
<i>RIN3</i>	0.0050	-1.26	<i>POLD2</i>	0.0197	-1.35	<i>SNHG8</i>	0.0365	1.60
<i>CIC</i>	0.0051	-1.37	<i>GSK3A</i>	0.0198	-1.26	<i>RBM7</i>	0.0366	-1.22
<i>MT-ND2</i>	0.0052	-1.31	<i>MYO1G</i>	0.0198	-1.24	<i>CDIP1</i>	0.0367	-1.21
<i>GSN</i>	0.0055	-1.27	<i>UBE2M</i>	0.0198	-1.27	<i>NAP1L4P1</i>	0.0367	-1.26
<i>C8G</i>	0.0056	3.36	<i>CERK</i>	0.0200	-1.26	<i>HNRNPA1P76</i>	0.0367	2.24
<i>LRRFIP1P1</i>	0.0056	-1.44	<i>WDHD1</i>	0.0201	-1.60	<i>RCAN2</i>	0.0367	2.70
<i>NOTCH2NLA</i>	0.0056	-1.28	<i>HMMR</i>	0.0203	-1.92	<i>CCDC71</i>	0.0367	-1.30
<i>R3HCC1</i>	0.0056	-1.47	<i>TCF7L2</i>	0.0204	-1.25	<i>ZNF555</i>	0.0367	-1.32
<i>MKNK2</i>	0.0057	-1.24	<i>GNB1L</i>	0.0207	-1.46	<i>RN7SKP16</i>	0.0369	2.01
<i>ACTB</i>	0.0057	-1.25	<i>RSU1</i>	0.0208	-1.23	<i>GRID1</i>	0.0372	-2.26
<i>FLII</i>	0.0058	-1.25	<i>CLEC16A</i>	0.0208	-1.30	<i>SSTR2</i>	0.0374	-2.08
<i>NKIRAS2</i>	0.0059	-1.25	<i>GALNT6</i>	0.0208	-1.29	<i>DCAF6</i>	0.0375	-1.23
<i>AKAP17A</i>	0.0060	-1.28	<i>FHL3</i>	0.0208	-1.37	<i>MTRNR2L3</i>	0.0376	-1.61
<i>SCML2</i>	0.0060	2.96	<i>WDR25</i>	0.0209	-1.40	<i>NUDT1</i>	0.0379	-1.30
<i>PRIM1</i>	0.0060	1.58	<i>RN7SKP30</i>	0.0211	-1.31	<i>SLC48A1</i>	0.0379	-1.41
<i>MIIP</i>	0.0060	-1.33	<i>JADE3</i>	0.0211	2.00	<i>HILPDA</i>	0.0381	-1.44
<i>CARHSP1</i>	0.0061	-1.28	<i>CENPN</i>	0.0212	2.18	<i>LGALS9B</i>	0.0381	-2.19
<i>ABHD2</i>	0.0062	-1.28	<i>ACSM3</i>	0.0212	-1.39	<i>ZNF213</i>	0.0383	-1.37
<i>ANKMY1</i>	0.0062	-1.38	<i>DPP9</i>	0.0214	-1.23	<i>WDR90</i>	0.0383	-1.34
<i>COPA</i>	0.0063	-1.21	<i>ZNF749</i>	0.0215	-1.73	<i>CLPTM1</i>	0.0384	-1.24
<i>PAPLN</i>	0.0063	-1.46	<i>CTSH</i>	0.0219	-1.22	<i>S100Z</i>	0.0384	-1.30
<i>BAP1</i>	0.0064	-1.24	<i>CLTB</i>	0.0219	-1.24	<i>GRIN2B</i>	0.0385	-2.70
<i>IL1B</i>	0.0065	-1.33	<i>ARFGAP2</i>	0.0219	-1.23	<i>RN7SL47P</i>	0.0386	3.08
<i>MSNPI</i>	0.0065	-1.35	<i>TRIM65</i>	0.0219	-1.30	<i>AP5S1</i>	0.0387	-1.29
<i>MIR181A2HG</i>	0.0066	-1.95	<i>NFKB2</i>	0.0219	-1.23	<i>CFAP97D1</i>	0.0389	-1.96
<i>MT-CO1</i>	0.0066	-1.25	<i>HADHAP2</i>	0.0220	-1.28	<i>ABCF1</i>	0.0391	-1.23
<i>SIPA1</i>	0.0067	-1.25	<i>CYB5R3</i>	0.0221	-1.24	<i>ZNF613</i>	0.0391	1.40
<i>CCDC15</i>	0.0067	-1.40	<i>RNF165</i>	0.0221	-1.47	<i>PCA3</i>	0.0391	-3.70
<i>RPUSD1</i>	0.0067	-1.49	<i>MOXD1</i>	0.0223	2.21	<i>CFAP69</i>	0.0393	-3.71
<i>PNPLA1</i>	0.0067	1.86	<i>TIMM13</i>	0.0224	-1.23	<i>MSH6</i>	0.0394	-1.21
<i>MRPL28</i>	0.0067	-1.34	<i>LSM10</i>	0.0224	-1.23	<i>GUK1</i>	0.0395	-1.39
<i>TACSTD2</i>	0.0069	2.30	<i>THAP3</i>	0.0224	-1.40	<i>SIX4</i>	0.0395	-4.19
<i>RABL6</i>	0.0069	-1.27	<i>ALG14</i>	0.0224	-1.46	<i>ACKR4</i>	0.0396	1.90
<i>MGAT3</i>	0.0069	2.63	<i>GPSM1</i>	0.0224	2.38	<i>HMGB1P44</i>	0.0397	1.64
<i>KSR1</i>	0.0070	-1.34	<i>IMMP2L</i>	0.0225	1.50	<i>DPM2</i>	0.0399	-1.41
<i>C10orf105</i>	0.0070	1.51	<i>FSD1</i>	0.0226	-2.08	<i>NCLN</i>	0.0399	-1.21
<i>ZMIZ1</i>	0.0071	-1.27	<i>PRDX5</i>	0.0226	-1.35	<i>SESN2</i>	0.0400	-1.21
<i>ELOVL1</i>	0.0071	-1.30	<i>ADAP2</i>	0.0226	-1.28	<i>BATF2</i>	0.0402	1.62
<i>MT-TM</i>	0.0072	-1.39	<i>PRAM1</i>	0.0226	-1.21	<i>ATP13A1</i>	0.0403	-1.35
<i>INPP5B</i>	0.0073	-1.53	<i>CASP7</i>	0.0226	1.36	<i>FILIP1L</i>	0.0404	-1.51
<i>FAM126A</i>	0.0074	-1.29	<i>PPIL6</i>	0.0228	1.74	<i>FLNA</i>	0.0406	-1.20
<i>ACAP3</i>	0.0074	-1.48	<i>ADGRE3</i>	0.0229	-1.31	<i>TNFRSF21</i>	0.0406	1.64
<i>MT-TY</i>	0.0075	-1.52	<i>OPA3</i>	0.0229	-1.26	<i>KIAA1143P1</i>	0.0406	-1.64
<i>CCNT2</i>	0.0076	-1.27	<i>GSK3B</i>	0.0229	-1.22	<i>TERF1P3</i>	0.0407	2.28
<i>DUSP13</i>	0.0076	2.35	<i>GP1BA</i>	0.0230	-1.88	<i>WWC1</i>	0.0407	1.71
<i>HIP1</i>	0.0076	-1.44	<i>DIAPH1</i>	0.0230	-1.21	<i>PROX1</i>	0.0408	2.56
<i>SSC4D</i>	0.0077	4.02	<i>EFR3B</i>	0.0231	-1.77	<i>MT2A</i>	0.0409	1.31

ZSCAN5A	0.0078	-1.73	ABCF3	0.0231	-1.29	PCDHGB7	0.0410	1.91
C12orf43	0.0079	-1.31	PFKM	0.0231	-1.67	CEP112	0.0411	-1.84
ARID3A	0.0079	-1.26	COASY	0.0232	-1.23	XAF1	0.0412	1.44
MIGA2	0.0080	-1.31	DCAF7	0.0233	-1.21	XRCC1	0.0414	-1.26
IL17RC	0.0080	-1.82	MLF2	0.0233	-1.21	SOWAHD	0.0414	-1.26
KALRN	0.0080	-1.60	GATAD2A	0.0233	-1.21	GHRLOS	0.0415	-1.23
ARG1	0.0081	1.92	MRPS18A	0.0233	-1.38	TBC1D10A	0.0416	-1.30
NLN	0.0081	-1.38	SMG1P6	0.0235	1.75	SDAD1P1	0.0416	-1.29
MT-TE	0.0082	-1.41	AMACR	0.0235	1.33	ERF	0.0416	-1.20
GARNL3	0.0082	-2.10	H19	0.0236	1.89	TIMD4	0.0417	-3.54
IDO1	0.0083	-1.70	HSD17B12	0.0238	-1.21	MYOM3	0.0417	2.65
LDHAL6A	0.0084	-1.34	MINPP1	0.0240	1.39	GOT2	0.0417	-1.23
C14orf39	0.0086	-1.27	ELF3	0.0240	1.98	PDE8B	0.0420	-1.46
XPOT	0.0087	-1.39	RFLNB	0.0241	-1.21	CCR3	0.0420	-1.40
CSF1R	0.0088	-1.35	ARFIP2	0.0242	-1.47	HTD2	0.0422	-2.32
STYXL1	0.0088	-1.35	SIGLEC1	0.0242	2.25	ZRSR2P1	0.0422	-1.28
BORCS8	0.0091	-1.27	SPATS2L	0.0242	1.69	FASN	0.0422	-1.29
SF3B3	0.0091	-1.28	SH3GL1	0.0243	-1.21	EEF1B2P6	0.0423	1.59
ANKRD34B	0.0092	-1.73	SI00A12	0.0246	1.29	PAFAH2	0.0423	-1.21
FBXO8	0.0092	1.60	MLF1	0.0247	2.70	ATP6V1G2	0.0423	1.67
CDC25A	0.0092	2.78	XRCC3	0.0248	-1.48	ZNF883	0.0423	2.13
SHLD2P1	0.0092	-1.96	TRIM24	0.0248	-1.23	GRK6P1	0.0424	-1.72
RN7SL774P	0.0093	-38.80	COBL	0.0250	-3.94	MAMDC4	0.0425	1.66
SNX29P2	0.0093	-1.58	GATD1	0.0250	-1.27	LETM1P2	0.0426	-2.33
TGOLN2	0.0093	-1.22	TIGAR	0.0251	-1.28	FAM207A	0.0426	-1.29
SI00A8	0.0094	1.45	CD82	0.0252	-1.22	SYNM	0.0428	1.86
RAI2	0.0095	-3.23	CCDC157	0.0252	-1.71	PTGFRN	0.0428	1.79
CHST11	0.0096	-1.23	TNC	0.0253	2.13	STAT3	0.0429	-1.21
ABHD12	0.0096	-1.29	WRAP53	0.0253	-1.29	CDC27P1	0.0432	-1.37
STK10	0.0098	-1.22	RHOF	0.0254	-1.28	ARL6	0.0432	1.98
MAP3K3	0.0098	-1.22	SLC6A12	0.0255	-1.97	MYZAP	0.0435	-1.69
EBAG9	0.0100	-1.27	COG5	0.0256	-1.24	TMEM183B	0.0435	1.90
SORD2P	0.0100	-1.32	MRPL2	0.0257	-1.35	SULT1C4	0.0435	-3.86
DHPS	0.0100	-1.31	SIK3	0.0257	-1.23	TBC1D10B	0.0435	-1.21
SNAP29	0.0100	-1.23	DGKG	0.0257	-1.27	P2RX4	0.0435	-1.26
PCBP2	0.0100	-1.21	NR4A1AS	0.0257	2.28	DCAF15	0.0435	-1.30
CST3	0.0100	-1.22	MICALL2	0.0259	-1.96	COMMD6	0.0435	1.72
SCAF1	0.0101	-1.40	WBP11P1	0.0259	-1.51	PLEKHD1	0.0436	-1.56
FAAP100	0.0102	-1.36	ARF3	0.0260	-1.21	PNMA6F	0.0437	-4.22
FADS1	0.0102	-1.32	SGK1	0.0260	-1.28	FRRS1	0.0437	-1.52
YBX1P6	0.0102	-1.43	MMP8	0.0261	1.93	LRCH4	0.0437	-1.20
PRELID1	0.0103	-1.21	LRRC57	0.0262	-1.20	PDE6C	0.0438	2.64
DNASE2	0.0103	-1.21	TPK1	0.0265	-1.25	ITGA7	0.0439	1.65
SOX10	0.0103	3.04	XIST	0.0266	-1.53	RIPOR1	0.0439	-1.21
MED15	0.0103	-1.26	RBM42	0.0266	-1.21	DCHS1	0.0440	-1.90
MPST	0.0104	-1.29	CXCL5	0.0267	-1.46	HDAC11	0.0440	-1.40
MT-TN	0.0104	-1.76	BAK1	0.0267	-1.22	NT5DC3	0.0440	-1.42
SAMHD1	0.0104	-1.23	GDF15	0.0268	6.34	LGALS3BP	0.0441	1.41
MLEC	0.0105	-1.22	STAB1	0.0272	-1.46	PAOX	0.0442	-1.42
MRM3	0.0106	-1.45	CD274	0.0273	1.37	CAPN5	0.0442	-1.56
MT-TH	0.0106	-1.43	TPSB2	0.0273	-9.70	PYMI	0.0443	-1.27
ZBTB24	0.0106	-1.25	CR2	0.0274	-1.63	FAM110A	0.0444	-1.23
FBXO6	0.0107	-1.82	TBC1D17	0.0276	-1.25	BAX	0.0444	-1.23
TNFAIP6	0.0107	1.41	TOR2A	0.0276	-1.29	ZNF703	0.0446	-1.37
CTSZ	0.0108	-1.41	EVI5	0.0278	-1.21	COPRS	0.0447	-1.32
RPL7AP50	0.0109	2.42	INCENP	0.0278	-1.38	IFI44	0.0449	1.73

<i>SF3A2</i>	0.0109	-1.39	<i>PIK3R6</i>	0.0278	-1.45	<i>HOXA10</i>	0.0450	-1.42
<i>OASL</i>	0.0110	1.65	<i>MINDY4</i>	0.0280	2.70	<i>OAS3</i>	0.0450	1.73
<i>DYRK1B</i>	0.0111	-1.30	<i>SCRN3</i>	0.0280	1.30	<i>C8orf58</i>	0.0450	-1.32
<i>AKT1S1</i>	0.0111	-1.39	<i>MFAP1</i>	0.0281	-1.22	<i>LNX2</i>	0.0450	1.34
<i>CFAP74</i>	0.0112	-2.55	<i>PEA15</i>	0.0281	-1.22	<i>MARK4</i>	0.0450	-1.24
<i>SEC61A1</i>	0.0113	-1.31	<i>C10orf55</i>	0.0281	2.06	<i>PEMT</i>	0.0451	-1.30
<i>ADCY6</i>	0.0114	-4.71	<i>IFI44L</i>	0.0282	2.32	<i>RPS15AP38</i>	0.0451	1.79
<i>ELOB</i>	0.0115	-1.23	<i>MACROH2A2</i>	0.0282	1.67	<i>RHOQP3</i>	0.0452	-1.68
<i>CICP27</i>	0.0115	-1.33	<i>RNF207</i>	0.0282	-2.37	<i>VSTM1</i>	0.0452	-1.33
<i>MRPL23</i>	0.0116	-1.41	<i>RPAP1</i>	0.0284	-1.28	<i>TDRG1</i>	0.0452	-2.87
<i>MCRIP2</i>	0.0116	-1.57	<i>GRK3</i>	0.0284	-1.25	<i>ARHGAP35</i>	0.0452	-1.23
<i>KHK</i>	0.0118	1.84	<i>AACS</i>	0.0286	-1.30	<i>SND1</i>	0.0453	-1.21
<i>MT-CYB</i>	0.0120	-1.28	<i>ARMCX1</i>	0.0287	1.90	<i>LETMI</i>	0.0453	-1.24
<i>ZFP42</i>	0.0121	2.28	<i>RBM8B</i>	0.0287	-1.24	<i>SCIN</i>	0.0453	-2.46
<i>DIAPH3</i>	0.0121	-1.77	<i>BRD4</i>	0.0287	-1.21	<i>BLVRB</i>	0.0454	-1.39
<i>P2RY2</i>	0.0121	-1.90	<i>ZNF430</i>	0.0287	-1.23	<i>ZNF366</i>	0.0454	-1.39
<i>ZNF117</i>	0.0122	1.35	<i>C19orf44</i>	0.0287	-2.15	<i>WASH2P</i>	0.0457	-1.22
<i>SLC35D2</i>	0.0122	1.42	<i>H4C14</i>	0.0288	-1.55	<i>VWCE</i>	0.0457	-1.64
<i>PTMAP3</i>	0.0123	-2.56	<i>GPR137</i>	0.0289	-1.33	<i>BCL11A</i>	0.0459	-1.27
<i>PGAM1</i>	0.0125	-1.21	<i>TRIO</i>	0.0289	-1.32	<i>SRP68</i>	0.0460	-1.24
<i>SMARCD2</i>	0.0125	-1.21	<i>COPG1</i>	0.0289	-1.23	<i>PI4K2A</i>	0.0460	-1.22
<i>H2AJ</i>	0.0125	-1.29	<i>FAHD2CP</i>	0.0289	2.03	<i>SGF29</i>	0.0461	-1.25
<i>PHEX</i>	0.0127	1.65	<i>TMED8</i>	0.0291	-1.20	<i>RRAGB</i>	0.0462	-1.45
<i>CSNK1A1P1</i>	0.0127	-2.27	<i>SERP2</i>	0.0292	2.87	<i>C17orf99</i>	0.0462	-1.68
<i>SLC25A11</i>	0.0129	-1.23	<i>SPHK1</i>	0.0292	-1.61	<i>SLC37A2</i>	0.0462	-1.25
<i>VDAC1P1</i>	0.0129	-3.54	<i>C19orf73</i>	0.0292	2.02	<i>CLIC3</i>	0.0462	-1.30
<i>GSTM2</i>	0.0129	-2.05	<i>MAP2K2</i>	0.0294	-1.20	<i>STK32B</i>	0.0463	-2.28
<i>CCNYL5</i>	0.0130	-2.47	<i>MTND1P23</i>	0.0294	-1.38	<i>PRPF18</i>	0.0465	1.21
<i>ZNF653</i>	0.0131	-1.53	<i>MAST4</i>	0.0295	-1.29	<i>FGGY</i>	0.0465	-1.41
<i>JAK1</i>	0.0133	-1.21	<i>EIF4EBP1</i>	0.0295	-1.34	<i>MCM6</i>	0.0466	-1.30
<i>MT-ND4</i>	0.0134	-1.30	<i>MEF2C</i>	0.0295	-1.22	<i>NBAS</i>	0.0466	-1.21
<i>MT-TP</i>	0.0134	-1.41	<i>NUFIP1</i>	0.0296	-1.30	<i>ZMIZ2</i>	0.0466	-1.22
<i>PTGDS</i>	0.0134	-1.65	<i>RGS17P1</i>	0.0297	-1.33	<i>NAXE</i>	0.0467	-1.22
<i>NUDT7</i>	0.0138	1.70	<i>DAB2</i>	0.0297	-1.30	<i>LGALS12</i>	0.0468	-1.45
<i>PSMD7</i>	0.0138	-1.22	<i>RPS13P2</i>	0.0297	1.87	<i>C9orf16</i>	0.0468	-1.22
<i>TIMM17B</i>	0.0139	-1.29	<i>PNKD</i>	0.0298	-1.22	<i>CHMP4C</i>	0.0469	-1.52
<i>SMPD3</i>	0.0140	-1.41	<i>TECPR1</i>	0.0299	-1.23	<i>YDJC</i>	0.0470	-1.25
<i>MT-ATP8</i>	0.0140	-1.29	<i>AP2M1</i>	0.0299	-1.25	<i>KLHL35</i>	0.0470	-1.81
<i>RBM22P5</i>	0.0140	-1.50	<i>CERS2</i>	0.0299	-1.22	<i>ELMO1</i>	0.0471	-1.21
<i>NUDT3</i>	0.0141	-1.22	<i>CD93</i>	0.0300	-1.25	<i>ST8SIA6</i>	0.0473	-1.37
<i>SRPRA</i>	0.0141	-1.28	<i>MED18</i>	0.0301	-1.27	<i>VPS18</i>	0.0474	-1.27
<i>OR2AG1</i>	0.0141	-2.58	<i>PRR7</i>	0.0301	-1.36	<i>RPS14P5</i>	0.0474	-1.82
<i>PDLIM7</i>	0.0142	-1.33	<i>PLEKHG4B</i>	0.0302	-4.04	<i>HLA-C</i>	0.0476	1.38
<i>RAB8A</i>	0.0142	-1.21	<i>IL15RA</i>	0.0302	1.75	<i>ANKRD29</i>	0.0476	-2.70
<i>KPNA2</i>	0.0142	-1.39	<i>MAF1</i>	0.0303	-1.31	<i>WIPF3</i>	0.0476	-1.92
<i>LRFN3</i>	0.0142	-1.51	<i>DIPK1B</i>	0.0303	-1.52	<i>TERC</i>	0.0478	2.58
<i>NREP</i>	0.0143	-1.41	<i>ENKUR</i>	0.0304	-1.56	<i>DNAAF5</i>	0.0480	-1.32
<i>PRKACA</i>	0.0144	-1.21	<i>ROGDI</i>	0.0308	-1.27	<i>ZNF836</i>	0.0481	1.23
<i>PLEKHA6</i>	0.0145	-6.04	<i>CCDC86</i>	0.0308	-1.62	<i>KLHL5</i>	0.0483	-1.20
<i>MT-TC</i>	0.0147	-1.53	<i>EPSTI1</i>	0.0309	1.59	<i>PRG4</i>	0.0483	1.85
<i>ACER3</i>	0.0148	-1.26	<i>MT-ND5</i>	0.0310	-1.29	<i>BPHL</i>	0.0483	-1.56
<i>CD109</i>	0.0149	-2.12	<i>CD99L2</i>	0.0310	-1.23	<i>CMPK2</i>	0.0483	1.71
<i>ZFP69</i>	0.0150	1.64	<i>SCRIB</i>	0.0310	-1.24	<i>HECTD3</i>	0.0484	-1.23
<i>PSME3</i>	0.0150	-1.22	<i>RSAD2</i>	0.0310	2.22	<i>MSRB3</i>	0.0484	-1.43
<i>LIMS1</i>	0.0154	-1.23	<i>IFT80</i>	0.0311	1.34	<i>F12</i>	0.0487	1.40
<i>FAM209B</i>	0.0154	1.91	<i>MARCKS</i>	0.0313	-1.22	<i>TRIM22</i>	0.0487	1.24

<i>KNSTRN</i>	0.0155	-1.44	<i>METTL15P1</i>	0.0313	-2.06	<i>ZNF629</i>	0.0488	-1.38
<i>TAGLN2</i>	0.0155	-1.23	<i>ANP32BP1</i>	0.0315	-1.48	<i>PRKAA2</i>	0.0488	3.04
<i>TMTC4</i>	0.0155	1.40	<i>INO80</i>	0.0316	-1.23	<i>PDE6G</i>	0.0488	-1.59
<i>SLC35G1</i>	0.0158	-1.59	<i>AGAP3</i>	0.0317	-1.22	<i>HBA2</i>	0.0488	-1.46
<i>SKP1P1</i>	0.0159	-2.76	<i>SPNS3</i>	0.0317	-1.53	<i>FABP5</i>	0.0489	-1.32
<i>MZT2B</i>	0.0160	-1.25	<i>SUDS3P1</i>	0.0320	-1.25	<i>BLOC1S4</i>	0.0491	1.25
<i>DUBR</i>	0.0160	1.81	<i>AP2S1</i>	0.0322	-1.24	<i>IFIT1</i>	0.0491	1.72
<i>CORO7</i>	0.0160	-1.21	<i>TUBA3FP</i>	0.0323	-2.43	<i>DDX39A</i>	0.0493	-1.27
<i>KRT18P5</i>	0.0160	-2.51	<i>CLC</i>	0.0324	-1.41	<i>CHST13</i>	0.0498	-1.35
<i>TKT</i>	0.0160	-1.23	<i>TRAF3IP2</i>	0.0324	-1.27	<i>FAM30A</i>	0.0498	-1.44
<i>CHMP5</i>	0.0161	1.38	<i>BCAS3</i>	0.0324	-1.21	<i>SMCIA</i>	0.0498	-1.22
<i>ZNF630</i>	0.0161	1.84	<i>SLC35B4</i>	0.0324	-1.27	<i>PTPRK</i>	0.0500	-1.67
<i>PRMT7</i>	0.0163	-1.37	<i>PRKX</i>	0.0325	-1.25	<i>EPHA10</i>	0.0325	-2.25

**Table S2.1** Genes associated with cerebral amyloid angiopathy severity

<b>Gene</b>	<b>P-value</b>	<b>Partial Correlation</b>	<b>Gene</b>	<b>P-value</b>	<b>Partial Correlation</b>
<i>NUDT17</i>	0.00004	0.76	<i>USP2</i>	0.00974	0.54
<i>EBAG9P1</i>	0.00016	-0.72	<i>TMEM51</i>	0.00977	-0.54
<i>TRIM7</i>	0.00020	0.71	<i>SNORA1B</i>	0.00991	0.54
<i>SLC35G5</i>	0.00021	0.71	<i>KCNG2</i>	0.00998	0.54
<i>ZNF177</i>	0.00043	0.69	<i>RN7SL850P</i>	0.00999	-0.54
<i>WNT6</i>	0.00046	0.68	<i>SNX33</i>	0.01002	0.54
<i>PIP5K1B</i>	0.00050	-0.68	<i>PEBP1</i>	0.01009	0.54
<i>LZTS1</i>	0.00056	-0.68	<i>OR8B9P</i>	0.01012	0.54
<i>BET1L</i>	0.00063	0.67	<i>MIPOL1</i>	0.01014	-0.54
<i>C22orf39</i>	0.00071	0.67	<i>ZC2HC1C</i>	0.01015	0.54
<i>URM1</i>	0.00076	0.66	<i>ZNF12</i>	0.01018	0.54
<i>RTKN</i>	0.00080	-0.66	<i>CASC9</i>	0.01025	0.54
<i>WDR78</i>	0.00084	0.66	<i>CNIH1</i>	0.01026	0.54
<i>POLR1C</i>	0.00088	0.66	<i>MRPL20-AS1</i>	0.01028	0.54
<i>CFL1P1</i>	0.00118	0.65	<i>FANCG</i>	0.01030	0.54
<i>TLN2</i>	0.00130	-0.64	<i>MPG</i>	0.01034	0.53
<i>NUP107</i>	0.00133	0.64	<i>SELENOF</i>	0.01052	0.53
<i>CDK14</i>	0.00146	-0.64	<i>C5</i>	0.01054	0.53
<i>PLOD1</i>	0.00148	-0.64	<i>ATP8A2</i>	0.01055	0.53
<i>SH3BP4</i>	0.00152	0.63	<i>DIAPH3</i>	0.01061	-0.53
<i>HSPD1P10</i>	0.00154	-0.63	<i>TREH</i>	0.01064	0.53
<i>NECTIN2</i>	0.00154	-0.63	<i>CACNA2D3</i>	0.01078	0.53
<i>SORCS3</i>	0.00162	0.63	<i>PIP5KL1</i>	0.01079	0.53
<i>FXVD6</i>	0.00167	0.63	<i>ILVBL</i>	0.01081	0.53
<i>ZNF137P</i>	0.00174	-0.63	<i>CASR</i>	0.01081	0.53
<i>AMZ2P1</i>	0.00178	0.63	<i>TTC6</i>	0.01081	-0.53
<i>MTATP8P1</i>	0.00183	0.63	<i>NIFKP4</i>	0.01097	-0.53
<i>SPCS1</i>	0.00184	0.63	<i>CIDEB</i>	0.01100	0.53
<i>GNAQP1</i>	0.00185	-0.63	<i>ABCA9</i>	0.01101	0.53
<i>JOSD2</i>	0.00187	0.62	<i>NEXMIF</i>	0.01103	0.53
<i>SLITRK5</i>	0.00193	-0.62	<i>KCNAB3</i>	0.01114	0.53
<i>MFN2</i>	0.00193	-0.62	<i>ZNF670</i>	0.01116	0.53
<i>TMEM150B</i>	0.00197	0.62	<i>DPRXP4</i>	0.01117	-0.53
<i>DNAJA1P2</i>	0.00204	-0.62	<i>THEM6</i>	0.01117	0.53
<i>BCL2L2-</i>					
<i>PABPN1</i>	0.00207	0.62	<i>C11orf45</i>	0.01123	0.53



<i>MAST1</i>	0.00209	-0.62	<i>SHQ1</i>	0.01131	0.53
<i>TSHR</i>	0.00214	0.62	<i>NEUROD2</i>	0.01134	-0.53
<i>CFAP298</i>	0.00219	0.62	<i>ANXA13</i>	0.01139	-0.53
<i>ZDHHC7</i>	0.00219	0.62	<i>IL20RB</i>	0.01141	-0.53
<i>KLRC2</i>	0.00220	0.62	<i>FCHO1</i>	0.01143	0.53
<i>AARS2</i>	0.00220	0.62	<i>ABCB10</i>	0.01145	0.53
<i>TM6SF1</i>	0.00223	0.62	<i>STRAP</i>	0.01150	0.53
<i>PREP</i>	0.00235	0.61	<i>CLDN16</i>	0.01151	0.53
<i>GDPGP1</i>	0.00236	0.61	<i>GREM1</i>	0.01151	-0.53
<i>FDX2</i>	0.00241	0.61	<i>SCRG1</i>	0.01152	0.53
<i>ICAM1</i>	0.00241	-0.61	<i>TRAF7</i>	0.01154	0.53
<i>CD4</i>	0.00241	0.61	<i>CABLES1</i>	0.01160	0.53
<i>ACOT8</i>	0.00241	0.61	<i>TRIT1</i>	0.01175	0.53
<i>H4C14</i>	0.00252	-0.61	<i>SCN9A</i>	0.01178	-0.53
<i>SLC46A2</i>	0.00253	0.61	<i>SNHG18</i>	0.01182	0.53
<i>FAM89A</i>	0.00265	0.61	<i>XKR9</i>	0.01186	-0.53
<i>PROSER2</i>	0.00274	0.61	<i>AICF</i>	0.01190	0.53
<i>IL23A</i>	0.00279	0.61	<i>WDR11-AS1</i>	0.01191	-0.53
<i>SLC35A2</i>	0.00281	0.61	<i>Z97634.1</i>	0.01191	-0.53
<i>NUDT12</i>	0.00283	0.61	<i>MAN1B1</i>	0.01193	0.53
<i>ATP8A1</i>	0.00292	0.60	<i>H4C11</i>	0.01199	-0.53
<i>MUC6</i>	0.00294	-0.60	<i>CTNNA1</i>	0.01208	-0.53
<i>HAR1A</i>	0.00302	0.60	<i>PLAU</i>	0.01211	0.53
<i>RNASE4</i>	0.00334	0.60	<i>SERPINI1</i>	0.01214	-0.52
<i>IGFLR1</i>	0.00335	0.60	<i>TDRKH</i>	0.01218	0.52
<i>FTH1P11</i>	0.00338	-0.60	<i>ZNF543</i>	0.01218	-0.52
<i>PRR4</i>	0.00355	0.59	<i>PGLYRP2</i>	0.01222	0.52
<i>TNFRSF12A</i>	0.00356	0.59	<i>ST13P19</i>	0.01227	0.52
<i>WRAP73</i>	0.00364	0.59	<i>SNORD56</i>	0.01228	-0.52
<i>MIR646HG</i>	0.00364	-0.59	<i>OR4F15</i>	0.01251	-0.52
<i>METTL21A</i>	0.00368	0.59	<i>IL27</i>	0.01256	-0.52
<i>RPL13AP12</i>	0.00374	0.59	<i>ZNF781</i>	0.01259	0.52
<i>CEBPG</i>	0.00374	0.59	<i>OR3A1</i>	0.01269	0.52
<i>SNORA80E</i>	0.00375	0.59	<i>STX1A</i>	0.01272	0.52
<i>ALDH18A1</i>	0.00379	0.59	<i>GBP5</i>	0.01274	-0.52
<i>RNY1P9</i>	0.00383	0.59	<i>SLC35B1</i>	0.01277	0.52
<i>NOP16</i>	0.00386	0.59	<i>NBDY</i>	0.01278	0.52
<i>JAGN1</i>	0.00404	0.59	<i>FXYD3</i>	0.01278	-0.52
<i>SRGAP2C</i>	0.00407	0.59	<i>PPP1R13L</i>	0.01278	0.52
<i>NXT1</i>	0.00410	0.59	<i>BSPRY</i>	0.01279	-0.52
<i>TMEM115</i>	0.00411	0.59	<i>ZC3HC1</i>	0.01289	0.52
<i>KCP</i>	0.00413	-0.59	<i>F8A3</i>	0.01292	-0.52
<i>RNY4P23</i>	0.00414	0.59	<i>KCNG4</i>	0.01295	0.52
<i>TEX22</i>	0.00421	-0.59	<i>TUBA1B</i>	0.01297	-0.52
<i>RN7SL827P</i>	0.00432	0.58	<i>MZT1</i>	0.01298	0.52
<i>OR2AT4</i>	0.00438	0.58	<i>GSTA4</i>	0.01298	0.52
<i>RWDD4P1</i>	0.00444	0.58	<i>RN7SL589P</i>	0.01299	0.52
<i>CRTC3</i>	0.00446	0.58	<i>CENPF</i>	0.01305	0.52
<i>SRSF12</i>	0.00450	0.58	<i>OGG1</i>	0.01306	0.52
<i>SNORD19B</i>	0.00450	-0.58	<i>ZNF628</i>	0.01306	0.52
<i>DHX9P1</i>	0.00452	-0.58	<i>POMZP3</i>	0.01309	-0.52
<i>BEST2</i>	0.00456	0.58	<i>NDUFA3</i>	0.01318	0.52
<i>POLDIP2</i>	0.00466	0.58	<i>ZNF385A</i>	0.01335	0.52
<i>RN7SL448P</i>	0.00471	0.58	<i>ANKRD13A</i>	0.01345	-0.52
<i>ZNF469</i>	0.00485	0.58	<i>IRAK2</i>	0.01347	-0.52
<i>TMEM140</i>	0.00491	-0.58	<i>MYD88</i>	0.01347	0.52

<i>MLPH</i>	0.00492	0.58	<i>ROPN1B</i>	0.01365	-0.52
<i>GAS6</i>	0.00493	0.58	<i>PRMT9</i>	0.01366	0.52
<i>MN1</i>	0.00499	-0.58	<i>HAPLN1</i>	0.01369	0.52
<i>TUFT1</i>	0.00505	-0.58	<i>TXNRD3</i>	0.01370	0.52
<i>ZSWIM3</i>	0.00508	0.58	<i>DGCR6L</i>	0.01373	0.52
<i>C17orf99</i>	0.00528	-0.57	<i>PANTR1</i>	0.01374	0.52
<i>PSMA1</i>	0.00552	0.57	<i>SOD1P1</i>	0.01379	0.52
<i>LDHD</i>	0.00557	-0.57	<i>PPP1R2P6</i>	0.01381	0.52
<i>FCGR1A</i>	0.00557	-0.57	<i>NSG1</i>	0.01387	0.52
<i>SLC25A10</i>	0.00561	0.57	<i>PSMG2</i>	0.01389	0.52
<i>THAP11</i>	0.00563	0.57	<i>THOC3</i>	0.01401	0.52
<i>ANG</i>	0.00563	0.57	<i>RPS4X</i>	0.01404	0.52
<i>RPL23AP47</i>	0.00578	-0.57	<i>MAN1C1</i>	0.01405	0.52
<i>TAS2R14</i>	0.00585	0.57	<i>FAM107A</i>	0.01418	0.52
<i>ZNF816</i>	0.00585	0.57	<i>AIF1L</i>	0.01419	0.51
<i>PLIN4</i>	0.00587	-0.57	<i>SEMA6B</i>	0.01419	0.51
<i>EVC2</i>	0.00602	0.57	<i>TEAD1</i>	0.01420	-0.51
<i>SEMA5A</i>	0.00611	-0.57	<i>PSMB8</i>	0.01421	0.51
<i>THAP9</i>	0.00622	-0.56	<i>D2HGDH</i>	0.01422	0.51
<i>XYLT2</i>	0.00623	0.56	<i>AJAP1</i>	0.01423	-0.51
<i>ABCA8</i>	0.00628	-0.56	<i>SPATA6L</i>	0.01425	0.51
<i>SCARNA8</i>	0.00630	0.56	<i>TSFM</i>	0.01427	0.51
<i>HDAC11</i>	0.00644	-0.56	<i>KLHL12</i>	0.01431	0.51
<i>TYSND1</i>	0.00644	0.56	<i>CCDC9</i>	0.01435	-0.51
<i>ARHGAP42</i>	0.00648	0.56	<i>TMEM129</i>	0.01440	0.51
<i>WDR83OS</i>	0.00657	0.56	<i>B3GNT3</i>	0.01449	0.51
<i>DBF4B</i>	0.00660	-0.56	<i>CCR8</i>	0.01456	0.51
<i>ZNF138</i>	0.00663	0.56	<i>DNAJC4</i>	0.01471	0.51
<i>ARL1</i>	0.00667	0.56	<i>TRPT1</i>	0.01472	0.51
<i>PIAS3</i>	0.00668	-0.56	<i>TCF23</i>	0.01474	0.51
<i>FAM245B</i>	0.00676	0.56	<i>ABO</i>	0.01476	0.51
<i>UQCRRS1</i>	0.00679	0.56	<i>FAM83D</i>	0.01483	0.51
<i>COX8A</i>	0.00695	0.56	<i>DPY19L4P1</i>	0.01483	-0.51
<i>RPL23AP45</i>	0.00695	-0.56	<i>GOLGA2P1</i>	0.01485	-0.51
<i>EIF5AL1</i>	0.00696	0.56	<i>NT5E</i>	0.01489	0.51
<i>ALOX15</i>	0.00696	-0.56	<i>MTCO1P51</i>	0.01490	0.51
<i>NRIP3</i>	0.00699	-0.56	<i>CYP2A6</i>	0.01492	-0.51
<i>BUD23</i>	0.00703	0.56	<i>AS3MT</i>	0.01497	0.51
<i>DHRS9</i>	0.00706	-0.56	<i>RCE1</i>	0.01501	0.51
<i>TTC27</i>	0.00722	0.56	<i>LNCTAM34A</i>	0.01501	0.51
<i>PSMD11</i>	0.00726	0.56	<i>HSPD1P9</i>	0.01502	0.51
<i>RN7SL66P</i>	0.00731	0.56	<i>WDR77</i>	0.01510	0.51
<i>RPS26</i>	0.00735	0.55	<i>HHIPL2</i>	0.01511	0.51
<i>MTIF</i>	0.00739	0.55	<i>TNFRSF10B</i>	0.01519	0.51
<i>MUS81</i>	0.00741	0.55	<i>OR2AG1</i>	0.01521	-0.51
<i>CRYGS</i>	0.00741	0.55	<i>SLC12A5</i>	0.01524	-0.51
<i>CLDN10</i>	0.00742	0.55	<i>GP5</i>	0.01526	-0.51
<i>GPKOW</i>	0.00746	0.55	<i>ACSBG2</i>	0.01528	0.51
<i>CREG2</i>	0.00747	-0.55	<i>SARDH</i>	0.01532	0.51
<i>ERI2</i>	0.00752	0.55	<i>LRRIQ3</i>	0.01533	0.51
<i>SNORA64</i>	0.00755	-0.55	<i>RAB11FIP5</i>	0.01535	0.51
<i>INAVA</i>	0.00757	-0.55	<i>VMA21</i>	0.01536	0.51
<i>TCTA</i>	0.00758	-0.55	<i>RASGRP2</i>	0.01540	0.51
<i>SLC1A7</i>	0.00761	0.55	<i>ZNRF2P1</i>	0.01542	0.51
<i>PRMT5</i>	0.00764	0.55	<i>FAM8A3P</i>	0.01550	-0.51
<i>PDLIM4</i>	0.00768	-0.55	<i>SLC2A4RG</i>	0.01554	0.51

<i>NRN1</i>	0.00772	-0.55	<i>GTF2IP5</i>	0.01560	-0.51
<i>AGBL5</i>	0.00776	0.55	<i>OPRD1</i>	0.01561	-0.51
<i>MED16</i>	0.00777	0.55	<i>MSRA</i>	0.01566	-0.51
<i>GAPDH</i>	0.00778	0.55	<i>SMIM6</i>	0.01567	0.51
<i>SFT2D3</i>	0.00780	0.55	<i>ABITRAMP1</i>	0.01571	-0.51
<i>SNORA20</i>	0.00793	-0.55	<i>ARL9</i>	0.01576	0.51
<i>ULK3</i>	0.00794	0.55	<i>BIVM</i>	0.01576	0.51
<i>FBP1</i>	0.00794	0.55	<i>DNAI2</i>	0.01576	0.51
<i>EAF1</i>	0.00799	0.55	<i>DNASE2</i>	0.01595	-0.51
<i>CATSPER1</i>	0.00804	0.55	<i>PLA2G7</i>	0.01597	0.51
<i>C1orf162</i>	0.00810	0.55	<i>SLC36A3</i>	0.01602	-0.51
<i>PDE2A</i>	0.00819	-0.55	<i>SNORD1B</i>	0.01604	0.51
<i>FAM153A</i>	0.00837	0.55	<i>TSPAN32</i>	0.01615	0.51
<i>PITPNM3</i>	0.00840	-0.55	<i>TRIM71</i>	0.01617	-0.51
<i>IGFBP7</i>	0.00840	0.55	<i>OR2V2</i>	0.01624	0.51
<i>SLC6A15</i>	0.00840	0.55	<i>DDIAS</i>	0.01627	0.51
<i>KRT73</i>	0.00844	0.55	<i>GSK3A</i>	0.01627	-0.51
<i>GREM2</i>	0.00844	0.55	<i>MOCS2</i>	0.01630	0.51
<i>GDF7</i>	0.00845	0.55	<i>CCNYL6</i>	0.01631	-0.51
<i>ANKRD24</i>	0.00848	-0.55	<i>HNRNP KP3</i>	0.01633	-0.51
<i>SPATA2</i>	0.00849	0.55	<i>OR2A12</i>	0.01639	0.51
<i>FAM131B</i>	0.00856	0.55	<i>SNORA40B</i>	0.01639	0.51
<i>OR5AN1</i>	0.00858	-0.55	<i>ARL4AP5</i>	0.01642	-0.51
<i>UPF3AP1</i>	0.00859	0.55	<i>SPATA20</i>	0.01643	0.51
<i>MYO1B</i>	0.00862	0.55	<i>RXFP4</i>	0.01645	-0.51
<i>PMP22</i>	0.00863	0.55	<i>RPL37P6</i>	0.01650	0.51
<i>SUSD4</i>	0.00864	0.55	<i>PPP1R17</i>	0.01655	0.50
<i>NPIPB11</i>	0.00865	0.55	<i>RN7SL804P</i>	0.01659	0.50
<i>DTYMK</i>	0.00866	0.55	<i>ZNF517</i>	0.01662	0.50
<i>MED15P9</i>	0.00868	-0.55	<i>PPA1</i>	0.01664	0.50
<i>RNU6-638P</i>	0.00871	-0.55	<i>SNHG7</i>	0.01665	0.50
<i>APOL4</i>	0.00873	-0.54	<i>DGCR9</i>	0.01666	0.50
<i>EDDM13</i>	0.00876	0.54	<i>IQANK1</i>	0.01666	-0.50
<i>SIRPD</i>	0.00880	-0.54	<i>OVCA2</i>	0.01667	0.50
<i>EPDR1</i>	0.00890	0.54	<i>ZNF493</i>	0.01670	0.50
<i>OR7E46P</i>	0.00895	-0.54	<i>MRPL21</i>	0.01680	0.50
<i>MED6P1</i>	0.00895	-0.54	<i>MTND5P14</i>	0.01682	-0.50
<i>C2orf81</i>	0.00915	-0.54	<i>NHLH1</i>	0.01687	-0.50
<i>ZNF304</i>	0.00924	0.54	<i>GABRA2</i>	0.01691	0.50
<i>FBXO28</i>	0.00924	0.54	<i>TRPV3</i>	0.01694	0.50
<i>TPTEP2-</i>					
<i>CSNK1E</i>	0.00925	-0.54	<i>GRK4</i>	0.01694	0.50
<i>ATP1A4</i>	0.00926	0.54	<i>RNF40</i>	0.01696	-0.50
<i>CCDC39</i>	0.00926	-0.54	<i>SPINK1</i>	0.01696	-0.50
<i>PKD2L1</i>	0.00928	0.54	<i>LYPLA1</i>	0.01697	0.50
<i>FUCA2</i>	0.00930	0.54	<i>FAM167B</i>	0.01707	0.50
<i>RALGPS1</i>	0.00932	0.54	<i>ORC6</i>	0.01708	0.50
<i>KRT86</i>	0.00933	0.54	<i>RPS4XP2</i>	0.01709	0.50
<i>RNA5SP242</i>	0.00935	0.54	<i>APOL2</i>	0.01727	-0.50
<i>DOCK6</i>	0.00935	-0.54	<i>IL15RA</i>	0.01729	0.50
<i>TMOD4</i>	0.00936	0.54	<i>KDEL R2</i>	0.01729	0.50
<i>CHST6</i>	0.00936	0.54	<i>OR10H5</i>	0.01738	-0.50
<i>EDA</i>	0.00941	0.54	<i>ADSS1</i>	0.01740	-0.50
<i>OR56A1</i>	0.00941	-0.54	<i>MAP2K1</i>	0.01742	0.50
<i>AXIN1</i>	0.00949	0.54	<i>MIR205HG</i>	0.01743	-0.50
<i>GDNF</i>	0.00958	0.54	<i>HAUS4</i>	0.01749	0.50

<i>FADS6</i>	0.00958	0.54	<i>AAAS</i>	0.01759	0.50
<i>FRMPD3</i>	0.00964	-0.54	<i>ZCCHC3</i>	0.01760	0.50
<i>PLP2</i>	0.00968	0.54	<i>E2F3P2</i>	0.01772	-0.50
<i>RELB</i>	0.00969	-0.54	<i>PEG10</i>	0.01777	-0.50
<i>GALNT2</i>	0.00971	0.54	<i>MAGEE1</i>	0.01781	0.50
<i>NUDT17</i>	0.00004	0.76	<i>USP2</i>	0.00974	0.54
<i>EBAG9P1</i>	0.00016	-0.72	<i>TMEM51</i>	0.00977	-0.54
<i>TRIM7</i>	0.00020	0.71	<i>SNORA1B</i>	0.00991	0.54
<i>SLC35G5</i>	0.00021	0.71	<i>KCNG2</i>	0.00998	0.54
<i>ZNF177</i>	0.00043	0.69	<i>RN7SL850P</i>	0.00999	-0.54